MASTER´S THESIS
DIPLOMARBEIT

Geosynthetics in Landfill Design
Geokunststoffe im Deponiebau

carried out at the
ausgeführt am

Institute for Ground Engineering and Soil Mechanics
Vienna University of Technology

Institut für Grundbau und Bodenmechanik
der Technischen Universität Wien

Univ.Doz. Dipl.-Ing. Dr.techn. Dietmar Adam, Associate Prof.

Monash University
Department of Civil Engineering
Melbourne, Australia

Dr. Abdelmalek Bouazza, Associate Prof.

University of Colorado at Boulder
Department of Civil, Environmental and Architectural Engineering
Boulder, USA

Jorge Zornberg, Ph.D., P.E., Assistant Prof.

written by
verfasst von

Christian Pfneisl
A. Baumgartnerstraße 44/C3/063
A-1230 Wien

Wien, im Mai 2003

To my

FAMILY

Acknowledgements

Writing main parts of this thesis in Australia and the USA and crossing the ways of so many interesting people is the thing I consider as the main personal development during my study. Of course, it has not always been fun but at the whole I would recommend such experiences to all my student colleagues. Sometimes you have to go a step away from all the things you take for granted to see the true value of them and to discover the importance of each of them to yourself. All this would not be possible without the support of some people I would like to thank for:

First of all thank my family for all they are to me. Thank you to my parents who made this family a place of love, security, fun and respect towards each other. Thank you for giving the same love and support to all of us three sons, no matter how different our situations might have been. Thank you to my brothers Andreas and Stephan, who I spent so many great years with. I truly hope this close tie of our family will develop more and more in the future.

The combination of going abroad and finishing my degree would not have been possible without the help of Dietmar Adam, my Austrian supervisor. Not only that he opened me the door to new experiences I also got to know him as a friend. Dietmar helped me to open my mind to see many different things beyond the technical part of this thesis. Thank you for guiding me towards these human values.

Furthermore, I thank Malek Bouazza and Jorge Zornberg, my supervisors in Melbourne and Boulder for their excellent support during the work on my thesis.

Last but not least thank you to all my friends from home and all the friends and colleagues who accompanied me on the way this thesis took me. Thank you for all the support, motivation, discussions and different thoughts you gave me.

Preface

The first idea about writing my thesis about geosynthetics arose while attending basic courses in geotechnics. Geosynthetics are considered a technical new and highly economical supplement or alternative to conventional materials and methods used in geotechnical applications. The fact that in landfill design a large variety of geosynthetic products is used and that environmental applications will be a highly demanded future issue created the idea of writing a thesis about geosynthetics in landfill design. Furthermore this topic gave me the opportunity to write parts of my thesis abroad (Australia, USA). Soon after starting to work on that topic I had to realize that my primary intention to present a state of the art report about all different kinds of geosynthetics used in landfills would be far beyond the scope of this thesis. Finally I decided to write a general introduction about geosynthetics in landfill design and to concentrate my work on three selected landfill applications with a relevance to current topics. It should be noticed that my work on this thesis was always closely related to the paper “Geosynthetics in waste containment facilities: recent advances” (Bouazza *et al.*, 2002) because I spent some months with each author and assisted them by working on various sections of their paper.

Abstract

During the last decades geosynthetics have become a technical and economical alternative or supplement to various well-tried materials and technologies in the field of geotechnical engineering. This thesis focuses on the use of geosynthetics in landfill design.

The introduction (chapter 1) explains the development of landfills from open dumps towards highly engineered constructions. Furthermore the different types of geosynthetics and their functions are presented. Finally an overview of possible applications of geosynthetics in landfills is given.

Chapter 2 (Geosynthetics for cut-off walls) presents the use of geosynthetics in geomembrane barrier walls, in composite cut-off walls (diaphragm walls with incorporated liners) and in other barrier systems such as permeable reactive barriers. Topics discussed include used materials, containment transport through the wall, possible wall failures, their prevention and detection as well as construction issues such as installation methods and panel connection.

Chapter 3 (Tension in geomembranes placed on steep slopes) focuses on the development of tension at the anchorage of geomembranes placed on steep slopes. Results of an analytical solution and a numerical one are compared. Difficulties during the modeling of the numerical model as well as its sensitiveness towards certain parameters are shown. Furthermore, areas future work on this topic could concentrate on are pointed out.

Chapter 4 (Stability of steep cover systems) provides an analytical framework to analyze the stability of steep landfill cover slopes. Solutions for unreinforced, slope-parallel-, horizontally- and fiber-reinforced veneers are presented. Expressions for the required reinforcement of a slope are derived as a function of material parameters and the veneer configuration. Finally other design concepts for additional slope stability such as reinforced soil structures at the bottom of the slope, a module-based cover system and a geocell-reinforced cover system are presented.

Kurzfassung

Geokunststoffe, eine im Bauingenieurwesen relativ junge Technologie, stellen eine technisch und wirtschaftlich sehr interessante Alternative bzw. Ergänzung zu vielen „altbewährten“ Materialien und Technologien in der Geotechnik dar. Die Verwendung im Deponiebau ist ein großes Anwendungsgebiet für Geokunststoffe im Bauwesen. Die vorliegende Diplomarbeit befasst sich, nach einer allgemeinen Einleitung über Deponien sowie Geokunststoffe (Kapitel 1), mit drei ausgewählten Anwendungsgebieten der Geokunststoffe im Deponiebau.

Das Kapitel 2 („Geokunststoffe in Dichtwänden“) beschäftigt sich mit dem Einsatz von Geokunststoffen in Geomembranwänden, Kombinationsdichtwänden (Schlitzwände mit zusätzlichem Dichtkern) sowie anderen Barrieresystemen, wie zum Beispiel in durchlässigen, reaktiven Wänden. Ergänzend zur Diskussion zahlreicher planungs- und ausführungsrelevanter Themen werden Fallbeispiele zur Erläuterung präsentiert

Kapitel 3 („Spannung in Geomembranen auf steilen Hängen“) befasst sich mit der Entstehung von Spannungen am Ankerpunkt einer hangparallelen Geomembrane. Ergebnisse einer frühren analytischen Lösung und einer im Zuge dieser Arbeit modellierten numerischen Lösung werden verglichen. Schwierigkeiten während des Modellierungsprozesses und die Anfälligkeit des Modells auf eine Änderung bestimmter Eingangsparameter werden aufgezeigt.

Die Stabilisierung steiler Oberflächenabdichtungen stellt ein weiteres Anwendungsgebiet für Geokunststoffe im Deponiebau dar. Im Kapitel 4 („Stabilität steiler Oberflächenabdichtungen“) wird eine analytische Methode zur Analyse der Stabilität steiler Deponiehänge präsentiert. Lösungen für Hänge ohne Geokunststoffe, mit hangparallelen Geokunstoffen, mit Schichten horizontaler Geokunststoffe und mit Geofaserverstärkung werden herausgearbeitet. Mit Hilfe dieser Lösungen ist es möglich, Ausdrücke für die erforderliche „Hangbewehrung“ (durch Geokunststoffe) als Funktion von Bodenkennwerten und Hanggeometrie herzuleiten. Abschließend werden andere Konzepte zur Stabilisierung steiler Oberflächenabdichtungen, wie zum Beispiel Wände aus bewehrter Erde am Fuße eines Hanges, eine modulare Oberflächenabdichtung oder die Erhöhung der Stabilität durch Geozellen, vorgestellt.

Contents

1 Introduction

1.1 Landfills

According to the Concise Oxford Dictionary, a landfill is defined as follows:

> **Landfill**, *n*.
>
> 1 waste material etc. used to landscape or reclaim areas of ground.
> 2 the process of disposing of rubbish in this way
> 3 an area filled in by this process.

For the purposes of this thesis, the third definition is the operable one used herein. Landfills, in various forms, have been used for many years. The first recorded regulations to control municipal waste were implemented during the Minoan civilization, which flourished in Crete (Greece) from 3000 to 1000 B.C. Solid wastes from the capital, Knossos, were placed in large pits and covered with layers of earth at intervals (Tammemagi, 1999). This basic method of landfilling has remained relatively unchanged right up to the present day. Landfill design evolved as a series of responses to problems. Only when a problem was identified or reached a sufficient level of concern were corrective steps taken. These improvements were invariably driven by regulatory requirements. In Athens (Greece), by 500 B.C. it was required that garbage be disposed of at least 1,5 kilometers from the city walls. Each household was responsible for collecting its own waste and taking it to the disposal site. The first garbage collection service was established in the Roman Empire. People tossed their garbage into the streets, and it was shoveled into a horse drawn wagon by appointed garbageman who then took the garbage to an open pit, often centrally located in the community. The semi-organized system of garbage collection lasted only as long as the Roman Empire. As industrialization of nations occurred, many containment facilities were constructed to retain various types of raw materials and/or waste products. Most of these containment facilities were not designed and almost none were lined to prevent leakage of wastes into the surrounding environment.

Until the late 1970s there was little engineering input into landfilling practice and little consideration given to the impact of landfilled wastes on land and groundwater. By the end of the 1970's, the problems in managing landfill sites had

arisen from the contamination of soil and groundwater (with, for example, heavy metals, arsenic, pesticides, halogenated organic compounds and solvents) and the potential risks to exposed populations. From the 1970's through the 1990s landfill design philosophy moved towards the objective of containment and isolation of wastes. This has resulted in a major upsurge in the development of engineered waste disposal systems, which included extensive use of geosynthetics. In the United States and Europe, the evolution of municipal landfill design philosophy since the 1970's has been relatively simple and has involved three significant phases through the 1990s and is entering a fourth phase as we enter the 21st century. These phases of municipal landfill development are summarized in Table 1.1. In Australia this evolutionary process has followed the same steps with the exception that the development of policy, regulation and guidance for landfill design was given more attention only in the mid-1990s (Bouazza and Parker, 1997). The focus in this decade is anticipated to be on mechanical and biological waste treatment, either in ground or prior to deposition, including increased use of leachate recirculation and bioreactor technology, as owners, regulators, and engineers become more familiar with these concepts and their benefits with respect to decreasing long term costs and liabilities. While waste reduction and reuse efforts may diminish the per capita quantity of waste generated in industrialized nations, there is no doubt that landfills will remain an important method of waste disposal for the foreseeable future due to their simplicity and cost-effectiveness. In this respect, geosynthetics will certainly continue to play a key role in landfill design, construction and operation. Obviously in less developed countries, this evolutionary process is taking place at a much slower pace since their priorities are on providing housing, education and health to their population.

Date	Development	Problems	Improvements
1970s	Sanitary landfills	Health/nuisance, i.e odour, fires, litter	Daily cover, better compaction, engineered approach to containment
Late 1980s-early 1990s	Engineered landfills, recycling	Ground and groundwater contamination	Engineered liners, covers, leachate and gas collection systems, increasing regulation, financial assurance
Late 1980's, 1990s	Improved siting and containment, waste diversion and re-use	Stability, gas migration	Incorporation of technical, socio-political factors into siting process, development of new lining materials, new cover concepts, increased post-closure use
2000s	Improved waste treatment	?	Increasing emphasis on mechanical and biological waste pre-treatment, leachate recirculation and bioreactors, "smart landfills"

Tab. 1.1: Summary of municipal landfill evolution
(modified from Bouazza and Kavazanjian, 2001).

1.2 Geosynthetics

Geosynthetics are natural or synthetic polymeric materials that are specially manufactured to be used in civil engineering, especially in geotechnical engineering applications. Other major fields of applications are transportation engineering, hydraulics engineering and environmental engineering. That rock and soil are closely related to the use of geosynthetics can be seen by the given name for this product group. The second part of the name – *synthetics* – signals that the majority of the products are man-made, however some applications may also include natural products.

The two main reasons why geosynthetics are used and regarded as an emerging future market are: They are either more economical (e.g.: lower construction costs and/or lower life-time cost) or perform a specified function in a better way, eventually also fulfilling more than one function. These functions are defined by the International Geosynthetic Society (IGS) as follows (IGS, 2000):

- **Barrier:** The use of geosynthetic material to prevent the migration of liquids or gases.
- **Containment:** The use of a geosynthetic material to contain soil or sediments to specific geometry and prevent its loss. The contained fill takes the shape of the inflated at-rest geometry of the geosynthetic container.[1]
- **Drainage (a.k.a. transmission):** The use of geosynthetic material to collect and transport fluids.[2]
- **Filtration:** The use of geosynthetic material to allow passage of fluids from a soil while preventing the uncontrolled passage of soil particles.
- **Protection:** The use of a geosynthetic material as a localised stress reduction layer to prevent or reduce damage to a given surface or layer.

[1] This definition should be more general in terms of the materials which are contained (e.g.: in landfill applications encapsulation is also used to contain lechate).

[2] This definition should also include the collection and transport of gases.

- **Reinforcement:** The use of the tensile properties of a geosynthetic material to resist stresses or contain deformations in geotechnical structures.
- **Separation:** The use of geosynthetic material between two dissimilar geotechnical materials to prevent intermixing.
- **Surficial erosion control:** The use of geosynthetic material to prevent the surface erosion of soil particles due to surface water run-off and/or wind forces.

It should be emphasized that there are various other definitions of this functions (e.g.: TC 5 – Task Force 1).Other ways of categorizing this functions often reduce the ones mentioned above to six major categories by regarding containment as part of the barrier function and surficial erosion control as part of the separation function.

Talking about the historical development earth reinforcement is considered the mother of all geosynthetics. A well know example for an ancient reinforced earth structure similar to modern highly engineered ones is the Chinese Wall. Although the materials have changed from bamboo to polymers the design concept of reinforcing an earth structure with layers that are able to work in tension is still the same. It seems that this old field of interaction between soil and other materials was forgotten for a long time and had to be reinvented during the last century to open the way for the new technology of geosynthetics. During the last decades geosynthetics have become an integral part of civil engineering, with a well organized community of manufactures, constructors, designers and researchers. This helped to creat special knowledge in all these different areas which will lead to better and new products, improved installation methods and new design tools to incorporate these developments into the field of engineering.

Within geosynthetics there are different product groups. The main groups of geosynthetics and their definitions are shown in Table 1.2. The following summary of characteristics of the main geosynthetic product groups is mainly based on the book *“Designing with Geosynthetics”* by R. Koerner (1998). This book will furthermore provide detailed information to all readers which are interested in getting deeper into the topic of geosynthetics.

	ASTM D 4439 (2001)	IGS (2000)	TC 5 –TF 1
GEOSYNTHETIC	A planar product manufactured from polymeric material, which are used with soil, rock or other geotechnical engineering material as an integral part of man-made project, structure or system.	A planar, polymeric (synthetic or natural) material used in contact with soil/rock and/or any other geotechnical material in civil engineering applications.	see ASTM D 4439
GEOTEXTILE	A permeable geosynthetic comprised solely of textile.	A planar permeable, polymeric (synthetic or natural) textile material, which may be nonwoven, knitted or woven, used in contact with soil/rock and/or any other geotechnical material in civil engineering applications.	Any permeable textile used with foundation, soil, rock earth, or any other geotechnical engineering related material as an integral part of human-made project, structure, or system.
GEOMEMBRANE	An essentially impermeable geosynthetic composed of one or more synthetic sheets	A planar, relatively impermeable, polymeric (synthetic or natural) sheet used in contact with soil/rock and/or any other geotechnical material in civil engineering applications.	Very low hydraulic conductivity synthetic membrane liners or barriers used with any geotechnical engineering related material so as to control fluid migration in a man-made project, structure or system.
GEOGRID	A geosynthetic formed by a regular network of integrally connected elements with apertures greater than 6,35 (1/4 in.) to allow interlocking with surrounding soil, rock, earth and other surrounding materials to function primarily as reinforcement.	A planar polymeric structure consisting of a regular open network of integrally connected tensile elements, which may be linked by extrusion, bonding or interlacing, whose openings are lager than the constituents, used in contact with soil/rock and/or any other geotechnical material in civil engineering applications.	Open grid structure of orthogonal filaments and strands of polymeric material used primarily for tensile reinforcement.
GEOSYNTHETIC CLAY LINER (GCL)	A manufactured hydraulic barrier consisting of clay bonded to a layer or layers of geosynthetic materials.	Geocomposite Clay Liner: An assembled structure of geosynthetic materials and low hydraulic conductivity earth materials (clay or bentonite), in the form of a manufactured sheet, used in contact with soil/rock and/or any other geotechnical material in civil engineering applications.	Factory-manufactured hydraulic barriers consisting of a layer of bentonite clay or other low permeability material supported by geotextiles and/or geomembranes, and mechanically held together by needling, stitching, or chemical adhesives.
GEONET	A geosynthetic consisting of integrally connected parallel sets of ribs overlying similar sets at various angles for planar drainage of liquid or gases.	A planer, polymeric structure consisting of a regular dense network, whose constituent elements are linked by knots or extrusions and whose openings are much larger than the constituents, used in contact with soil/rock and/or any other geotechnical material in civil engineering applications.	see ASTM D 4439
GEOCOM-POSITE	A product composed of two or more materials, at least one of which is a geosynthetic.	A manufactured or assembled material using at least one geosynthetic product among the components, used in contact with soil/rock and/or any other geotechnical material in civil engineering applications.	A manufactured material using geotextiles, geogrids and/or geomembranes in laminated or composite form. May or may not include natural materials.

Tab. 1.2: Main groups of geosynthetics and their definitions

Geotextiles are the group with the widest range of applications. Their fabric like appearance and the permeability of the structure are their common characteristics. The main reason why there are more than 100 applications geotextiles are used in, is that they can fulfill all different geosynthetic functions.

Geomembranes are the second major group of geosynthetics. In terms of sales market the probably might be ranked above geotextiles. Geomembranes are thin impermeable sheets of polymeric materials with the objective to act as a barrier to liquid and vapor migration. Environmental applications (e.g.: landfills, mining) are the main market of geomembranes, however, applications in hydraulic, geotechnical and transportation engineering are growing.

Geogrids provide reinforcement to earth structures. Their appearance is grid like with apertures big enough to interact with the surrounding soil matrix. Depending on their use geogrids might be uniaxial (providing the required tensile strength only in one direction) or biaxial products. Major fields of applications are foundations, reinforced soil structures, embankments and veneer slopes.

Geosynthetic Clay Liners (GCLs) represented the newest product group within the geosynthetic family. They are manufactured of two sheets of geotextiles and/or geomembranes with a layer of bentonite clay between these sheets. A composite is formed through needle punching, stitching or physical bonding. Areas of applications are similar to those of geomembranes; consequently they are either used in combination with geomembranes to form a composite liner or by themselves as an alternative to geomembranes or conventional compacted clay liners.

Geonets are three-dimensional structures of polymeric ribs used for in-plane drainage. They are always accompanied by a filter product or geomembrane below and above themselves which prevent soil intrusion and clogging of the geonet. Applications can be found wherever drainage products are required.

Geocomposites are composite products including one or more geosynthetics. The idea is to combine the advantages of each individual product to form a composite which provides the required function(s) for a special application. Geocomposites are able to fulfill all geosynthetic functions and are therefore part of various applications in civil engineering.

A summary of the functions the main geosynthetic groups can provide is given in Table.1.3. Generally it should be pointed out that there is a difference between the primary function, which is required by design and one or more secondary functions which might have additional benefits for the construction.

	Barrier	Containment	Drainage	Filtration	Protection	Reinforcement	Separation	Erosion Control
Geotextile	x	x	x	x	x	x	x	x
Geomembrane	x							
Geogrid						x		
Geosynthetic Clay Liner (GCL)	x				x			
Geonet			x					
Geocomposite	x	x	x	x	x	x	x	x

Tab. 1.3: Functions of different geosynthetics

Besides this products geosynthetics also include geopipes, geocells, geospacers, geomats, geoarmours, geobars, geoblankets, geofoams, geoforms, geostrips, geofibers and other related products which include a variety of polymeric (synthetic or natural) materials in the form of single, composite or assembled strands, filaments, mats, tubes, pipes and other shapes used in geotechnical and civil engineering applications (Brandl, 2002).

1.3 Geosynthetics in landfills

The multiple use of geosynthetics in the design of modern municipal solid waste landfills is a good illustration of an application in which the different geosynthetics can be and have been used to perform all the functions discussed previously. Virtually all the different types of geosynthetics discussed previously have been used in the design of both base and cover liner systems of landfill facilities. Figure 1.1 illustrates the extensive multiple uses of geosynthetics in both the cover and the base liner systems of a modern landfill facility. The base liner system illustrated in Figure 1.1 is a double composite liner system. Double composite liner systems are used in some instances for containment of municipal solid waste and are frequently used for landfills designed to contain hazardous waste. The base liner system shown in the figure includes a geomembrane/GCL composite as the primary liner system and a geomembrane/compacted clay liner composite as the secondary

system. The leak detection system, located between the primary and secondary liners, is a geotextile/geonet composite. The leachate collection system overlying the primary liner on the bottom of the liner system consists of gravel with a network of perforated pipes. A geotextile protection layer beneath the gravel provides a cushion to protect the primary geomembrane from puncture by stones in the overlying gravel. The leachate collection system overlying the primary liner on the side slopes of the liner system is a geocomposite sheet drain (geotextile/geonet composite) merging into the gravel on the base. A geotextile filter covers the entire footprint of the landfill and prevents clogging of the leachate collection and removal system. The groundwater level may be controlled at the bottom of the landfill by gradient control drains built using geotextile filters. Moreover, the foundation soil below the bottom of the landfill may be stabilized as shown in Figure 1.1 using randomly distributed fiber reinforcements, while the steep side soil slopes beneath the liner could also be reinforced using geogrids. Different types of geosynthetics (e.g. geogrids, geotextiles, fibers) could have been selected for stabilization of the foundation soils.

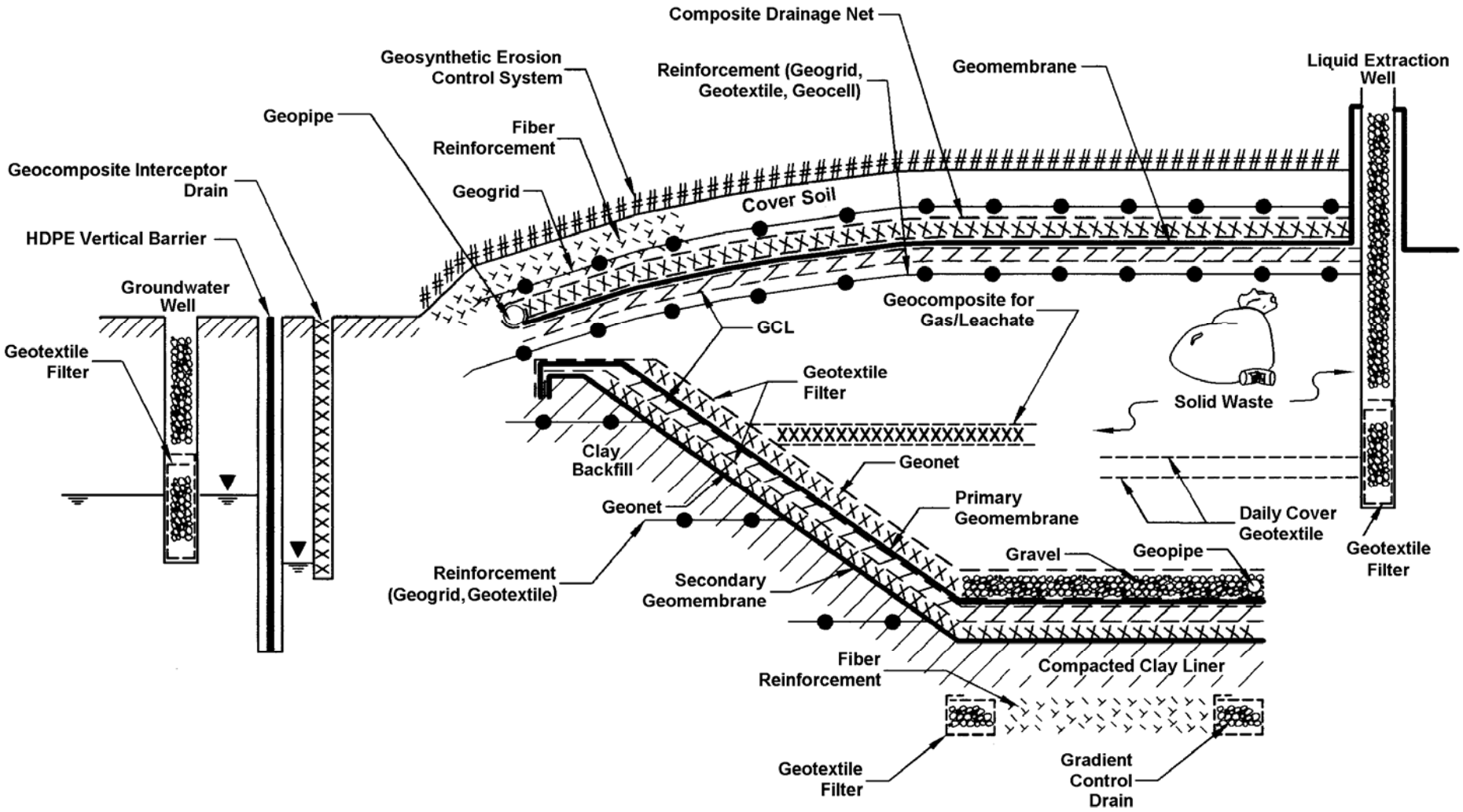

Fig. 1.1: Multiple use of geosynthetics in landfill design
(from Zornberg and Christopher, 1999)

The cover system of the landfill illustrated in Figure 1.1 contains a composite geomembrane/GCL barrier layer. The drainage layer overlying the geomembrane is a geocomposite sheet drain (composite geotextile/geonet). In addition, the soil cover system may include geogrid, geotextile, or geocell reinforcements below the infiltration barrier system. This layer of reinforcements may be used to minimize the strains that could be induced in the barrier layers by differential settlements of the refuse or by a future vertical expansion of the landfill. In addition, the cover system could include geogrid or geotextile reinforcement above the infiltration barrier to provide stability to the vegetative cover soil. Fiber reinforcement may also be used for stabilization of the steep portion of the vegetative cover soil. A geocomposite erosion control system above the vegetative cover soil is indicated in the figure and provides protection against sheet and gully erosion. Figure 1.1 also illustrates the use of geosynthetics within the waste mass, which are used to facilitate waste placement during landfilling. Specifically, the figure illustrates the use of geotextiles as daily cover layers and of geocomposites within the waste mass for collection of gas and leachate. Geosynthetics can also be used as part of the groundwater and leachate collection well system. The use of geotextiles as filters in groundwater and leachate extraction wells is illustrated in the figure. Finally, the figure shows the use of an HDPE vertical barrier system and a geocomposite interceptor drain along the perimeter of the landfill facility. Although not all of the components shown in Figure 1.1 would normally be needed at any one landfill facility, the figure illustrates the many geosynthetic applications that can be considered in landfill design.

2 Geosynthetics for cut-off walls

2.1 Overview

The construction of cut-off walls, especially in geotechnical and hydraulic engineering, has been a traditional field for civil engineers for decades. Encapsulation of contaminated ground or contaminated sources (abandoned landfill, special industrial plants etc.) and landfill containment increase the demand on vertical barriers in environmental engineering. The principle of Encapsulation (Figure 2.1) is to embed cut-off walls in an artificial base or in a natural low permeable or aquitard stratum.

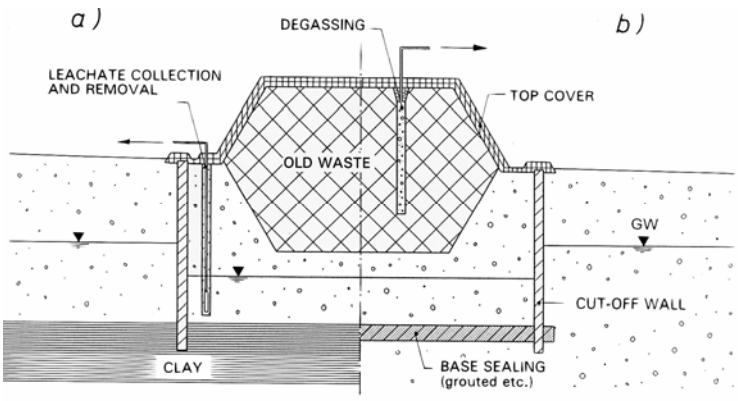

Fig. 2.1:
Encapsulation of a waste deposit and groundwater lowering within the cut-off walls
(from Brandl 1994).
a) embedment of the cut-off walls in a natural in a natural low-permeable stratum
b) embedment of the cut-off walls in a natural in a grouted base sealing

According to Brandl and Adam (2000) and Manassero *et al*. (2000) general design aspects of a vertical barrier are a function of various parameters, including the shape, extension and pollutants of the contaminated site, the geometry of the vertical wall as well as the required function(s) the cut-off wall has to fulfill.

TECHNOLOGY	CUT-OFF SYSTEM	GROUND PLAN (schematical)	DIMENSIONS d (m)	DIMENSIONS t_{max} (m)
permeability reduction of in-situ soil	compaction wall		0,4-1,0 [1]	10-20
	grouting wall		1,0-2,5	20-80
	soil freezing wall		≥ 0,7	50-100
	jet grouting wall		0,4-2,5	30-70
		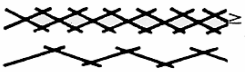	≥ 0,15-0,3 [2] (lamella)	20-30
	soil mix wall	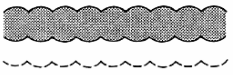	0,8-1,5	30-60
	cut-mix-grout wall		≥ 0,7	10
soil displacement methods	geomembrane wall	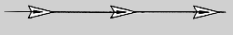	≥ 0,005 (0,002) [6]	20-40
	sheet pile wall		≈ 0,02	20-30
	vibrating beam -slurry wall "thin (diaphragm) wall"		≥ 0,05-0,2 [3]	10-35
	earth concrete driven-sheet pile wall		≥ 0,4	15-25
excavation methods	secant bored pile wall		0,4-1,5	20-40
	diaphragm wall (with hydrofraise)		0,4-1,6 [4]	100-170
	diaphragm wall (with grab)		0,4-1,0	40-70
	diaphragm wall with incorporated liner(s)		0,6-1,0 (0,4-1,6) [5]	20-50

Tab. 2.1:
Overview of Methods for cut-off wall construction.
Approximate values for common with d (m) and currently maximum wall depth t_{max} (m) (from Brandl and Adam, 2000).

1) vibrocompaction, vibroflotation (vibrodisplacement, vibroreplacement)
2) total width of lozenge-shaped jet grouting walls: ≥ 0,5m
3) near the flanges of the vibrating beam significantly wider
4) up to 3,0 m in special cases
5) in special cases
6) in the case of twin walls

Table 2.1 gives an overview of various methods for cut off wall construction. In the area of encapsulation diaphragm walls and vibrating beam slurry walls (“thin diaphragm walls”) predominate (Brandl and Adam, 2000). Diaphragm walls with incorporated liner(s) (“composite cut-off walls”) and single geomembrane walls are the two main types of cut-off walls using geosynthetics. Koerner and Guglielmetti (1995) describe five common installation methods (Table 2.2). Geomembrane cut-off walls are installed with the trenching machine-, the vibrated insertion plate-, the segment trench box- or the slurry supported installation method. The vibrating beam- and the slurry supported installation method are suitable to construct composite cut-off walls. In the following chapters each technique will be discussed detailed.

Method or Technique	**Geomembrane Configuration**	**Trench Support**	**Typ. Trench Width mm (in)**	**Typ. Trench Depth m (ft)**	**Typical Backfill**	**Some Advantages**	**Some Disadvantages**
Trenching machine	Continuous	None	300-600 (12-14)	1,5-4,5 (5-15)	Sand or native soil	• No Seams • Rapid installation • No slurry	• Depth limitations • Soil type limitations • Trench stability necessary
Vibrated insertion plate	Panels	None	100-150 (4-6)	1,5-6,0 (5-20)	Native Soil	• Rapid installation • Narrow trench • No material spoils	• Soil type limitations • possible panel stressing • Bottom key is a concern
Slurry supported	Panels	Slurry	600-900 (24-36)	No limit, except for trench stability	SB, SC, CB, SCB, sand or native soil	• No stress on panels • Conventional method • Choice of backfill	• Requires slurry • Buoyancy concerns • Slow process
Segment trench box	Panels or continuous	None	900-1200 (36-48)	3,0-9,0 (10-30)	Sand or native soil	• Can weld seams • Visual inspection • No stress on panels • No slurry	• Depth limitations • Slow incremental process
Vibrating beam	Panels	Slurry	150-220 (6-9)	No Limit	SB, SC, CB, SCB slurry	• Narrow trench • No material spoils • No stress on panels • Usually CB slurry	• Requires slurry • Slow incremental process • Soil type limitations

Tab. 2.2: Installation methods for geomembranes
(adapted from Koerner and Guglielmetti, 1995)
SB…soil-bentonite SC…soil-cement CB…cement-bentonite SCB…soil-cement-bentonite

The main function of geosynthetics used in cut-off walls is to build a low permeable barrier against containment transport. For standard applications including geosynthetics HDPE geomembranes are utilized because they increase the effectiveness of such a barrier wall by orders of magnitude. Tachavises and Benson (1997a, 1997b) compare the flux of water and organic solvent through the geomembrane barrier wall with the performance of the soil-bentonite (SB) slurry trench wall, the predominating type of wall in the U.S.A. It is shown that in the case, when geomembranes have fair joints, a geomembrane wall offers the same resistance against migration as a conventional soil-bentonite wall does. Carefully jointed geomembrane walls outperform the standard type. Effectiveness is increased further if both technologies are combined to build a composite cut-off wall.

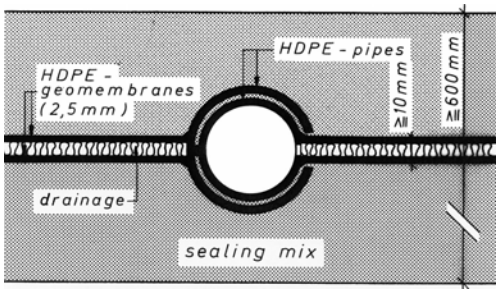

Fig. 2.2:
Composite cut-off wall with integrated geomembrane. Central geomembrane lining system with two geomembranes and a drainage core as a lechate collection and removal system (from Brandl 1994).

For special applications geocomposites are used instead of single geomembranes. The geocomposite shown in Figure 2.2 consists of two geomembranes with a drainage core as a leachate collection and removal system. With this lining system leak detection is possible. Furthermore, hazardous constituents, migrating by diffusion can be removed by the drainage system and the monitoring pipe (Brandl, 1994). Another alternative is the insertion of sandwich-like composite panels into the slurry trench wall (diaphragm wall). In this case a metal foil (usually aluminum) is placed between two HDPE-geomembranes. This method is theoretically promising if seepage or groundwater is heavily contaminated by chlorinated hydrocarbons, and also protects against certain vapor migration. Comprehensive practical experience does not yet exist (Brandl and Adam, 2000).

Although cut-off walls using geosynthetics have proved to be an adequate barrier in many cases designers should always open their minds to other possible solutions or additive measures of great effectiveness. Brandl and Adam (2000) emphasize that an inverse hydraulic gradient, created by lowering the groundwater within the containment, has a higher and more reliable barrier effect against containment migration than the installation of geomembrane liners in slurry trench walls. This measure has also proved to be very cost-effective, and furthermore it facilitates leak detection.

2.2 Geomembranes as cut-off wall systems

2.2.1 Materials

Geomembranes are “very low permeability synthetic membrane liners or barriers used with any geotechnical engineering related material so as to control fluid migration in a human made project, structure or system” (ASTM D4439). Most geomembranes are made of thin sheets of polymeric materials, however they can also be made from the impregnation of geotextiles with asphalt or elastomer sprays.

Currently used materials for geomembranes and properties of geomembranes are listed in Table 2.3 and Table 2.4. Further details are given by Koerner (1998).

Most widely used	Somewhat less widely used
High density polyethylene (HDPE)	Flexible polypropylene (fPP)
Very flexible polyethylene (VFPE)	Flexible polypropylene – reinforced (fPP-R)
Very low density polyethylene (VLDPE)	Chlorosulfonated polyethylene – reinforced (CSPE-R)
Linear low density polyethylene (LLDPE)	Ethylene interpolymere alloy – reinforced (EIA-R)
Low density linear polyethylene (LDLPE)	
Polyvinyl chloride (PVC)	

Tab. 2.3: Geomembranes in current use (Koerner 1998)

Physical	Mechanical	Chemical	Biological	Thermal
• Thickness • Density • Melt (Flow) Index • Mass per Unit Area • Water - Vapor Transmission • Solvent - Vapor Transmission	• Tensile Behaviour • Seam behaviour • Tear Resistance • Impact Resistance • Puncture Resistance • Interface Share • Anchorage • Stress Cracking	• Resistance against: • Chemicals • Ultraviolet light • Radioactive Degradation • Oxidation	• Resistance against: • Animals • Fungi • Bacteria	• Various properties of geomembranes are sensitive to changes in temperature. Therefore, these properties should always consider field temperatures.

Tab. 2.4: Geomembranes´ properties (adapted from Koerner 1998)

According to Koerner (1998) the chemical resistance to the contained liquid is the most important aspect for the selection of a material as liner. General chemical resistance guidelines of some geomembranes are given in Table 2.5. This makes it easy to understand why, although there a lot polymers which might be used for geomembrane cut-off wall, high density polyethylene (HDPE) is currently the preferred product to construct vertical barriers. Other reasons for its dominating status include availability, cost and ease of installation compared to other polymers (Thomas and Koerner, 1996). Furthermore good seams can be achieved with good skills and a high level of Quality assurance (Privett *et al*., 1996). There are also some disadvantages, such as low friction surfaces and that it is relatively easily punctured. Due to its predominating use in cut-off walls this chapter will completely be focused on HDPE.

According to Thomas and Koerner (1996) future advances might include stiff sheets that can be driven directly into the ground which would reduce installation costs. Materials with higher resistance to chemicals might be useful in some critical

applications. Such materials are available, but normally to expensive to challenge with HDPE.

	Geomembrane Type							
	PE		PVC		CSPE		EPDM	
Chemical	38°C	70°C	38°C	70°C	38°C	70°C	38°C	70°C
General:								
Aliphatic	x	x						
Aromatic	x	x						
Chlorinated solvents	x	x					x	
Oxygenated solvents	x	x					x	x
Crude petroleum	x	x						
Alcohols	x	x	x	x			x	x
Acids:								
Organic	x	x	x	x	x		x	x
Inorganic	x	x	x	x	x		x	x
Heavy Metals	x	x	x	x	x		x	x
Salts	x	x	x	x	x		x	x

x = general good resistance

Tab. 2.5: General chemical resistance guidelines of some commonly used geomembranes (from Koerner, 1998)

2.2.2 Lifetime for HDPE geomembranes

In the field of environmental geotechnics the in-service lifetime of materials is very important to protect next generations from irreparable harm to their environment. HDPE has been used as lining material during the last 20 years. This time represents just a small part of its estimated lifetime, which is probably some hundred years or more. Consequently not enough field data exist yet. Nevertheless the long term performance of HDPE in buried applications is well established, due to thousands of EPA 9090 compatibility tests (Koerner and Guglielmetti, 1995).

The common mechanism for long term degradation is chemical oxidation. It is generally considered that HDPE passes through the following three different stages during its service lifetime:

- depletion of anti-oxidants
- an induction time proceeding the onset of degradation, and
- time for degradation of 50% of relevant engineering property, such as strength or elongation.

As a result of laboratory simulation studies, in-service lifetimes for buried HDPE could approach 1000 years (Koerner and Guglielmetti, 1995). However, Koerner (1998) has real concerns about the proper installation of geomembranes. The

surviving of the initial installation process is considered as the key issue to achieve this long lifetimes for geomembranes.

Thomas and Koerner (1996) point out that there are just a few factors that could decrease the lifetime of HDPE geomembranes, however non of them should, under regular circumstances, harm the geomembrane seriously. Besides stress that can lead to slow crack growth, the exposure to chemicals, especially to concentrated hydrocarbons, might lower the tensile yield strength up to 30% and might result in a extraction of some anti-oxidants or other stabilizers. The need for stabilizers in buried geomembranes is minimal. Due the reversibility of the process of losing strength there should be now problems as long as the reduced strength is above the design strength.

2.2.3 Contaminates transport through geomembrane cut-off walls

The main purpose of geomembranes in cut-off walls is to minimize the hydraulic flow, so that transport trough the intact system is dominated by means of diffusion. Transport rates caused by diffusion are several orders of magnitude less than the ones for hydraulic permeation. For intact geomembrane cut-off walls these rates are usually so low that the focus is placed on the performance of the joints (Koerner and Guglielmetti, 1995).

In conventional cut-off walls main contaminates transport occurs in the liquid phase. Thus, the hydraulic conductivity or even better the permittivity, which is the quotient of the hydraulic conductivity and the walls thickness, should be seen as the predominating parameter. However, in the case of intact geomembrane cut-off walls, contaminates can pass through the barrier mainly by diffusion. Hydraulic permeability is related to a hydraulic gradient, whereas diffusion needs different solvent concentration to occur. Upon absorption of the liquid phase into the geomembrane as a vapor, it enters the polymer structure and defuses through the amorphous phase. After diffusing through the geomembrane, the vapors condense to liquid on the opposite side of the geomembrane (Koerner and Guglielmetti, 1995).

Thomas and Koerner (1996) emphasize that among the variety of factors, including thickness, concentration and temperature, which affect the rate of permeation through a HDPE-geomembrane the thickness of the sheet and the

concentration of the solvent play a fundamental role. They compared data from different other authors to come to the conclusion that a decrease in concentration on the one hand, and an increase in the geomembranes thickness on the other hand contribute overlinear to the reduction of transport rates trough geomembrane cut-off walls (Figure 2.3, 2.4). Consequently, Brandl (1998) recommends 2 or more millimeter thick geomembrane sheets for applications in environmental geotechnics, especially if there is a high risk potential (abandoned landfills) thickness of more than 2,5 mm should be achieved.

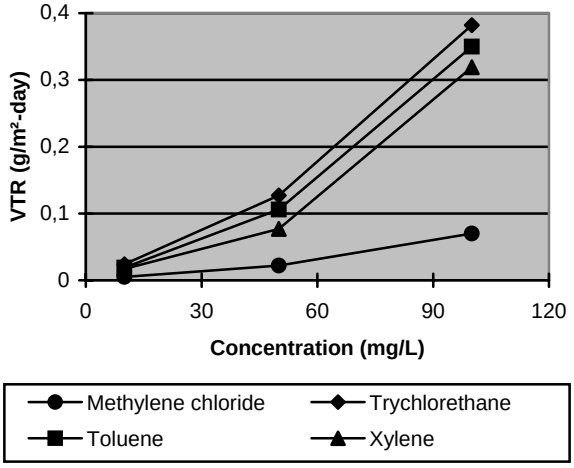

Fig. 2.3: The effect of concentration on the vapor transmission rate.
(from Thomas and Koerner, 1996)

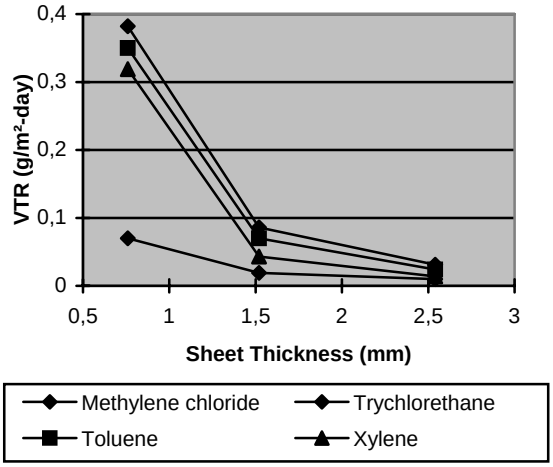

Fig. 2.4: The effect of sheet thickness on the vapor transmission rate.
(from Thomas and Koerner, 1996)

Foose and Vonderemebse (2001) point out that beside the migration of contaminates through the geomembrane sheets two other pathways exist. Contaminate transport can also occur through defects in the geomembrane panels or poor joints and beneath the cut-off wall. Diffusion through geomembranes is mainly an issue for volatile organic compounds, whereas geomembranes are a good diffusion barrier to inorganic contaminates. The relative amount of each pathway compared to the total contaminant transport rate is a function of several parameters including hydraulic conductivity of the aquifer, the aquitard and the presence of windows (defects or poor joints) in the wall.

Talking about gas containment, Daniel and Koerner (2000) point out that no comparative information between different barrier walls and there ability to contain gas have been published. Vapor transport through porous material is closely related to unsaturated zones of the medium. Because in most cases parts of the cut-off walls

are above the water table high gas transport rates can occur through this parts of the wall. Furthermore earthen walls types are likely to crack due to desiccation and differential settlements. Geomembranes are much more flexible and can withstand these problems in a better way. Consequently geomembrane cut-off walls are considered to offer better gas containment than most porous barriers.

2.2.4 Flow rates through geomembrane cut-off walls-sensitiveness to leaks

To create a geomembrane cut-off wall without or just with a small area of defects is one of the key issues for its function as vertical barrier. Among various factors that that influence the flow through the cut-off wall, defects of joints have the worst impact on transport rates.

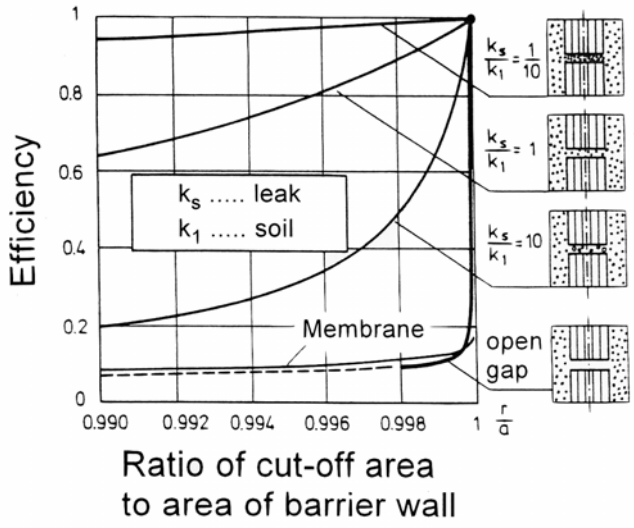

Fig. 2.5: Barrier effect of cut-off walls with a leak (joint). Comparison of geomembrane and thick wall, influence of partial clogging of joints (after Brauns,1978). Example for a soil with effective grain size d_{w1} = 0,2mm.
a = axial spacing of cut off panels (= axial distance of joints)
r = effective length of cut-off panels
k_s = hydraulic conductivity of leak filling (due to clogging)
k_1 = hydraulic conductivity of surrounding soil

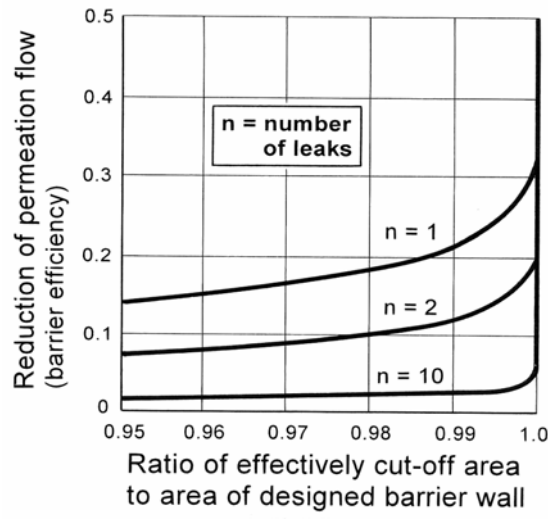

Fig. 2.6: Barrier effect of cut-off walls with one or more leaks of the same total (cumulative) area. Behaviour of a geomembrane for comparison (after Dachler, 1936)

For an intact geomembrane permeability is typical between 10-12 m/s and 10-15 m/s (Koerner, 1998). Several papers (Koerner and Guglielmetti, 1995; Thomas and Koerner, 1996; Daniel and Koerner 2000) mention 0,006g/m²-day as typical value for the water vapor transmission test according to ASTM E96. This value is negligible, however if only a small area of leaks occurs a significant discharge of seepage is

possible (Figure 2.5). Brandl and Adam (2000) have pointed out that for a leak of only 1% of the screen area the barrier efficiency is only 10 to 20 % (depending on theoretical hydraulic assumptions), and it drops further if there are more leaks which in total exhibit the same area as one large (Figure 2.6)

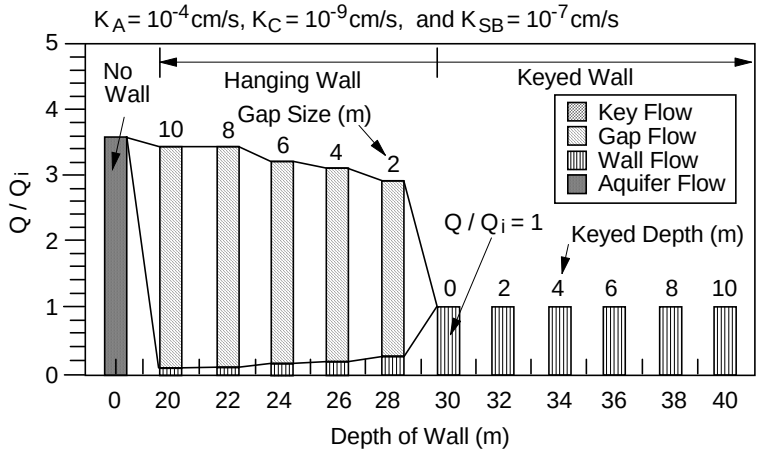

Fig. 2.7: Normalized flow rates past a SB wall as a function of wall depth (from Tachavises and Benson, 1997b)
Q_i = flow rate through intact wall in intimate contact
K_A = hydraulic conductivity of the aquifer
K_C = hydraulic conductivity of the aquitard
KSB = hydraulic conductivity of the backfill

Tachavises and Benson (1997a, 1997b) investigated the hydraulic importance of defects in vertical cut-off walls using a three-dimensional numerical model of groundwater flow. They compared flow rates through soil-bentonite (SB), geomembrane (GM) and composite geomembrane-soil cut-off (CGS) walls. The focus was put on the influence of location, size, hydraulic conductivity and penetration (that means whether the defect is as thick as the wall or just influences a part of the walls thickness) of the leak area on the flow through the barrier wall. All materials (also geomembranes and joints) were modeled as porous, thus having different hydraulic conductivities. Figure 2.7 shows the importance of a good key to reduce the flow rate. Hanging walls with a gap between the bottom of the wall and the aquitard layer don't increase effectiveness seriously, whereas, if there is good key flow rates are reduced significantly. Constructing deeper walls doesn't lead to a further increase in the effectiveness of the barrier wall. Due to results of simulations for soil-bentonite walls, partially penetrating defects (defects which are not as thick as the wall is) were also considered hydraulically insignificant to geomembrane walls. Furthermore it is shown that defective joints have a dramatic impact on flow rates past geomembrane walls. The joints where modeled poor, semi-pervious and perfect.

Although semi-pervious joints have a less dramatic impact on flow rates past the wall, they render a geomembrane wall far less effective. Variation of the joints width and position did not change the results significantly, thus these two parameters can be considered unimportant.

Composite cut-off walls are far less sensitive to leaks than single geomembranes. However, if the “windows” in the soil bentonite wall and the defects in the geomembrane are lined up (having the same position in the wall) only a small area of leaks renders the wall practically ineffective (similar results as for soil-bentonite walls). It is much more probable that defects in the geomembrane and windows in the soil-bentonite shell do not line up. In this case the flow rates past composite cut-off walls are between those past intact geomembrane and intact soil-bentonite walls (Figure 2.8). It is also shows that poor shells can reduce the effectiveness of such measures. This fact can also be seen in Figure 2.5, where clogging of leaks, maybe cause by a good shell, leads to a significant improvement of the barrier effect (Brandl and Adam, 2000). Consequently, single geomembrane walls should be used rather for secondary purposes, in the case of low contaminant potential and for temporary measures. For the permanent containment of polluted areas with an excessively high contaminant potential slurry trench walls or geosynthetic twin-walls, as well as systems with leak detection and leakage removal are recommended (Brandl and Adam, 2000).

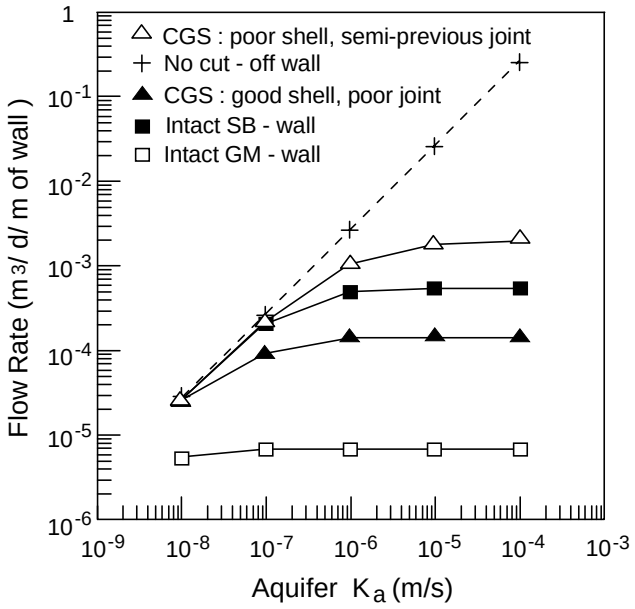

Fig. 2.8: Flow rates trough soil bentonite, geomembrane and composite soil bentonite cut-off walls (adapted from Tachavises and Benson, 1997a)

Tachavises and Benson (1997b) conclude that defects in any type of wall can potentially render the wall ineffective. Consequently, future research should be directed at developing methods to identify and repairs defects in situ. Furthermore, test methods used to asses walls should provide a direct measure of quality (i.e. a leakage or pressure test should be used, such as those used to evaluate lining systems).

2.2.5 Interlocks

This sensitiveness to leaks leads to a demand of high quality interlocks, the main problem in the construction of geomembrane cut-off walls. The objective of the interlocking connections is to perform as good as the geomembrane panels. To reach this goal the focus should be placed on proper installation and especially on testing the integrity of the joints.

All interlocking connections are complicated shapes that are made by a continuous extrusion process, then cut to length and fusion welded to geomembrane panels (Thomas and Koerner, 1996). Basically four main connection types can be distinguished (Table 2.6.):

- Plug-in connections
- Grouted connections
- Welded connections
- Interlocks using hydrophilic sealings

Welding or grouting leads to a significant higher barrier effect than a mere plug-in connection. Consequently, homogeneous extrusion welding is used increasingly, but also interlocks with hydrophilic seals. This method uses primarily neoprene based rubber material as gasket. In contact with water the sealing material can swell up to 8 times its original diameter, thus creating a high sealing pressure. Additionally the lock can be grouted. For this technology sealing materials, which swell after coming into contact with hydrocarbons, are still evolving (Brandl, 1998).

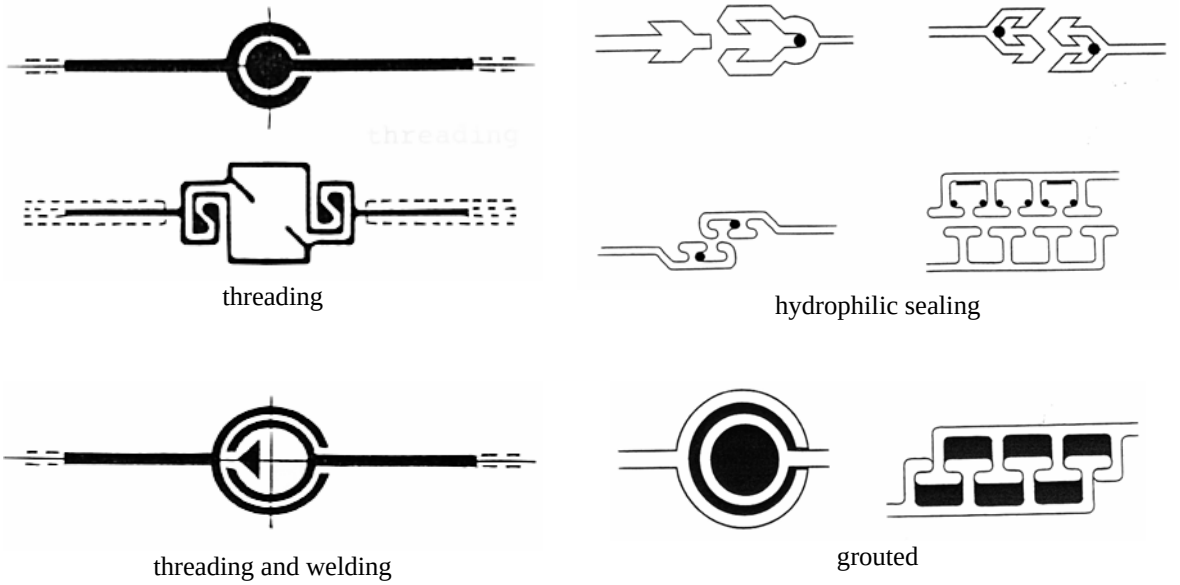

Tab. 2.6: Locks of vertical geomembrane liners

According to Thomas and Koerner (1996) the installation process, some settlement or lateral deformation might stress the connections. Therefore, it is important to evaluate the strength and the permeation resistance of the interlocks. Usually indirect methods are used: To maintain the proper performance of the construction, even in a highly deformed condition, the tensile strength of the lock section exceeds that of the liner material itself. Koerner and Guglielmetti (1995) describe several methods to test the continuity of the different connection types. The installation of a contact element to the bottom and conductive wires up to the top of each side of the connection is an appropriate method to test the integrity of the interlocks. Measuring the resistance in the open versus the closed circuit verifies the continuity of the interlock at the intended depth. For grouted interlocks a visual way to inspect the joints is to observe the flow of grout coming out of the adjacent channel our outer pipe, respectively. Volumetric checks to provide a mass balance could be developed. Testing the liquid tightness of interlocks in the field is very difficult. Figure 2.9 shows a laboratory test setup to measure the flow through an interlock. Pressures up to 700 kPa have lead only to a small amount of seepage passing through this hydrophilic gasket interlock.

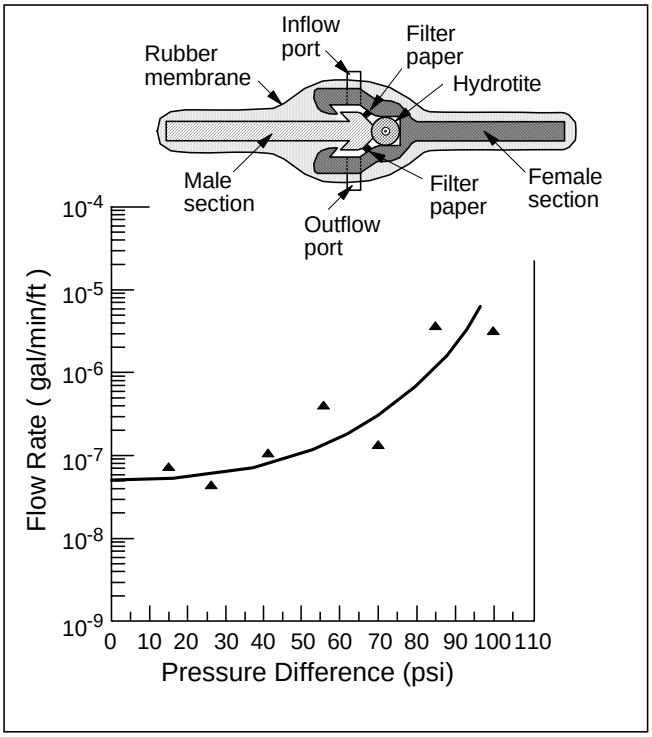

Fig. 2.9: Hydraulic gasket interlock test
(from Gundle Lining Systems, Inc 1993, after Koerner and Guglielmetti, 1995)

Due to its special importance for the whole cut-off wall further advances for interlocks will develop soon. Full fusion welding is evolving, thus probably leading to welded connections even in the slurry supported trench. Other developments include grouts that a more chemically resistant and sealing materials that swell after getting into contact with hydrocarbons. Another advance would be to make the connection profile on the sheet at the site or just before installation. This would reduce the cost of the materials because the profiled edge is currently made separately and welded on in a secondary operation (Thomas and Koerner, 1996).

2.2.6 Leak detection techniques

Post-construction monitoring is necessary to ensure the proper function of the cut-off wall and to detect occurring leaks. There are a various methods, including geophysical, electrochemical, mechanical and electric ones. All these techniques are under different stages of research and development, however none have been used with unconditional success and some are experimental (Koerner, 1998). This chapter is not considered to go into detail, mainly the readers attention should be drawn on the importance of leak detection. Inyang (1995) distinguishes between

- barrier integrity monitoring, where changes within the barrier are monitored,
- barrier permeation monitoring, where developments within the components of a containment system are measured, and
- external monitoring, which is based on measurements outside the containment system.

Generally external monitoring (i.e. net off wells) is most often used. Barrier permeation monitoring systems (i.e. electrodes on both sides of the geomembrane) have to be designed before and installed with the vertical barrier. Nevertheless, for critical applications the tendency should go towards leak detection and removal systems in the barrier itself (i.e. Figure 2.24).

A network of downgradient monitoring wells is the most often used method to provide leak detections. Especially for geomembrane cut-off walls the number of wells to install is a very difficult question. The leakage would probably be from one or only a few sources. As a consequence a system of widespread monitoring wells would perhaps fail because the plume is likely to concentrate on some narrow pathways (Koerner and Guglielmetti, 1995). However, Koerner (1998) points out that if there are enough wells and the same pollutant can be measured in different wells concentration gradient can be drawn and might lead to the detection of the leaks position in the wall.

For critical applications, however, a different strategy for leak detection should be considered when using geomembranes as vertical walls. A central drainage core consisting either of sand or a geonet should be put between two parallel geomembrane sheets (Figure 2.24). Such double liner systems can be the most secure of the various alternatives within the vertical wall category (Koerner and Guglielmetti, 1995). More details about the construction are given in chapter 2.3.

2.2.7 Installation methods

Installation methods for geomembrane cut-off walls and composite cut-off walls are under constant development. The major advance is that existing techniques became faster, better, cheaper and deeper. Koerner and Guglielmetti (1995) distinguish between five common methods for installing a geomembrane cut-off wall, however there might be some methods representing a mixture of these. Not to need

slurry is the main advantage of all the methods described in this chapter. Most of the information about the installation of geomembranes in cut-off walls given herein are based on the papers by Koerner and Guglielmetti (1995) and Daniel and Koerner (2000).

In the trenching machine method (Figure 2.10) a geomembrane is unrolled in a self-supporting trench. The trench is excavated backhoe or with a trenching machine. At the same time the geomembrane is progressively unrolled from a box mounted on the trenching machine or from a trailer at the ground surface (Thomas and Koerner, 1996). After the installation of the geomembrane sand, native soil or drainage material or a combination, e.g. low permeable soil on one side and drainage gravel on the other, are possible backfills. The main advantage of this technique is that no seams are needed. If a deep vertical barrier is required (generally the depth of the cut-off wall is limited by the geomembranes width - maximum 10 meters) some stripes are welded together to form a new prefabricated panel of greater width. The walls depth is limited by the stability of the unsupported trench. Discussing cut-off walls with a variation in depth it might be more suitable to use vertical panels. In the vertical direction the panels are welded together at the end of each roll.

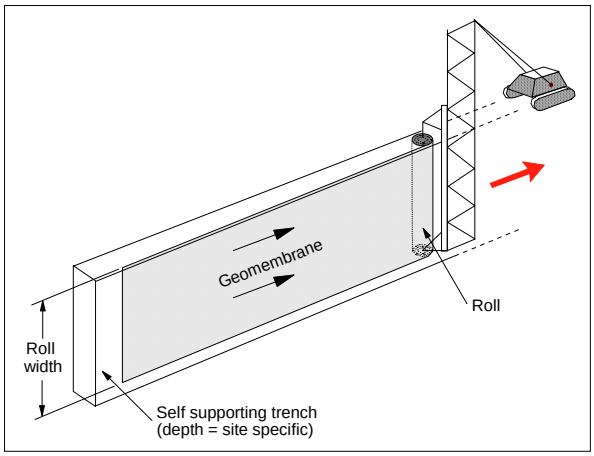

Fig. 2.10: Trenching machine method
(from Koerner and Guglielmetti, 1995)

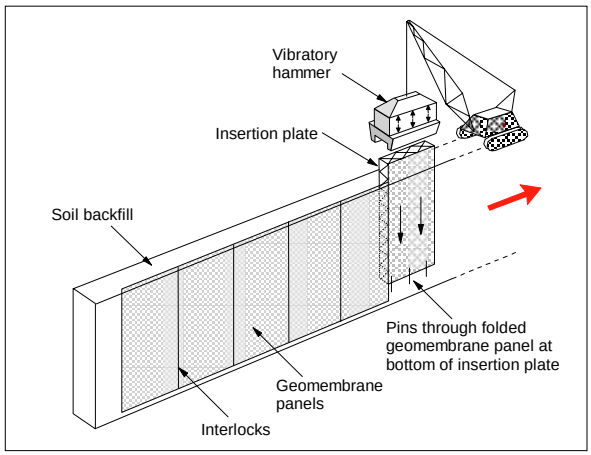

Fig. 2.11: Vibrated insertion plate method
(from Koerner and Guglielmetti, 1995)

The vibrated insertion plate method consists of steel plate, supporting the geomembrane on the way down to its required depth, and a vibratory hammer. The geomembrane is pinned to the bottom of the frame by means of dowels and then inserted into native soil or a backfilled narrow trench with the aid of a vibratory hammer (Figure 2.11). If the desired depth is reached the insertion plate is withdrawn, leaving the geomembrane in the trench. Interlock connections are

required between panels to seal joints. This technique is limited to certain types of soil. It is best suited for relatively weak fine-grained soils that are reasonable uniform in their strength properties. Loose sands can also receive a vibrated plate without excessive resistance to penetration initially, although densification of sand may make the insertion of the vibrated beam difficult to job progress. Any soil with stones or cobbles would be suspect because of the potential to tear the geomembrane during insertion.

In the segmented trench box method (Figure 2.12) both sides of the trench are, immediately after excavation, supported by a modified steel trench box. The trench box is advanced along the length of the trench, and geomembrane panels are inserted in the gap between respective halves of the trench box Installation of a geomembrane cut-off wall with this method is a slow incremental process with limitations in depth but on the other hand, there is hardly any restriction on soil conditions and, because of the supported trench, seams can be welded and a visual inspection of the geomembrane is possible.

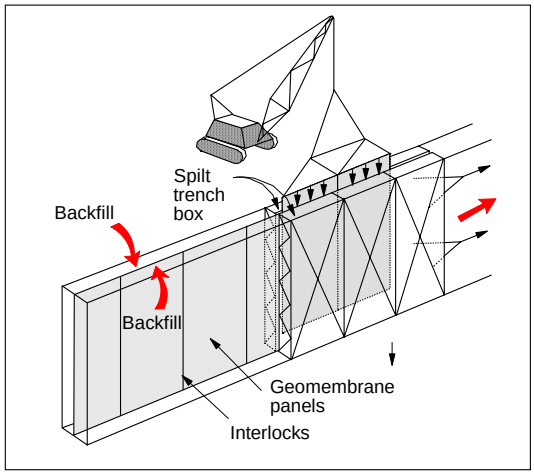

Fig. 2.12: Segmented trench box method
(from Koerner and Guglielmetti, 1995)

2.2.8 Comparison to other vertical barriers

Most of the current methods for encapsulation and containment of waste have been adapted from other applications such as in-ground structural walls and groundwater cut-off walls. Therefore, cut-off walls are very similar to theses structures in terms of installation techniques used, but have likely to fulfill other performance criteria than the walls in other applications (Privett *et al*., 1996).

Among the various possibilities to construct a cut-off wall, soil- and cement based barriers form the biggest group. These types include soil-bentonite-, cement-bentonite-, plastic concrete cut-off walls, cut-off walls backfilled with mixtures of cement, bentonite, fly ash, ground granulated blast furnace slag, and/or natural clay and walls constructed by deep mixing or jet grouting. Steel sheet piling and chemical grouts are other possible methods for vertical barriers, however these methods had had limited applications in the past due to several disadvantages they have. Both have in common that it is difficult to achieve the required sealing against contaminates. Reasons are the excessive leakage through the sheet pile interlocks and the natural heterogeneity of most soil strata, which might lead to discontinuities in grouted walls (Mitchell and Rumer, 1997). The following discussion will be focused on wall types constructed by the “cut and fill” method, such as soil-bentonite (SB), cement-bentonite (CB) cut-off walls. Table 2.7 gives an overview of potential advantages and disadvantages for these two types compared to geomembrane cut-off walls. Further details are given by Rumer and Ryan (1995), Rumer and Mitchell (1995) and Privett *et al*. (1996).

Type	Potential advantages	Potential disadvantages
Cement-bentonite	• one of the most straightforward techniques • the most flexible technique • capable of withstand high hydraulic gradients • can be used as single phase or double phase system	• cannot be constructed in areas where vertical or lateral space is limited • cannot be constructed easily across buried services • more expensive than soil-bentonite walls
Soil-bentonite	• the most inexpensive form of barrier construction • capable of forming walls with permeabilities of 10-9 m/s or less • environmental friendly component materials	• need suitable graded soil • very large operation space required • only suitable for flat lying areas • cannot be constructed easily across buried services • settlement of wall can cause settlement of surrounding ground • need hydraulic gradient of less than about 10
Geomembrane	• not vulnerable to damage by desiccation or freeze-thaw • flexible and can withstand much more strain than any other vertical barrier material • can only transmit liquids by diffusion, which results in transport rates for many chemicals that are orders of magnitude lower than for porous material • practically impermeable to gas under nearly all conditions • high resistance to chemicals	• vulnerability to damage caused by puncture • potential for leakage at the joints between the panels • potential for concentrated volatile organic fluids to diffuse through the HDPE geomembrane • little or no retardation/attenuation capacity compared to soil-bentonite backfill

Tab. 2.7: Potential advantages and disadvantages of some vertical barriers (adapted from Privett *et al*., 1996 and Daniel and Koerner, 2000)

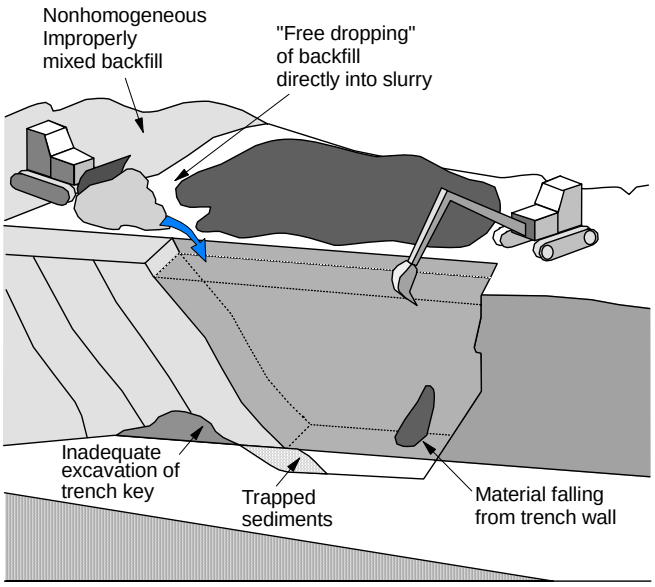

Fig. 2.13: Potential defects in slurry trench cut-off walls (from Rumer and Ryan, 1995)

The essential reason for using a geomembranes as a cut-off wall is to assure complete continuity by means of an extremely low permeable material. Such integrity and low permeability might be compromised in soil- and cement- based vertical walls due to aspects in Figure 2.13 and other factors, such as (Koerner and Guglielmetti, 1995; Thomas, and Koerner, 1996):

- changes in the quality of backfill material during field mixing
- sand deposits , discontinuities at joints and locations of work stoppage during the backfilling process,
- backfill material drying below its initially placed water content
- drying and desiccation above the water level or during water table fluctations
- freeze and thaw circles in upper portions of the wall,
- chemical incompatibility with the lechate that the site contains, and
- diffusive transport through the final backfilled wall.

These technical advantages of geomembrane walls and the competitive costs, which will drop further when geomembrane cut-off walls are used more often and new installation techniques will be developed, are the main reasons for the use of geomembranes in vertical barriers. Table 2.8 shows an overview of estimated cost for conventional cut-off walls and vertical barriers including geomembranes. Although prices may vary due to project specific circumstances geomembrane cut-off walls

may challenge with the conventional ones. However, Koerner and Guglielmetti (1995) point out that one reason for not using geomembranes in vertical cut-off walls more often is the increase of costs between 10% and 30% compared to conventional backfilled walls without a geomembrane liner.

According to Koerner and Guglielmetti (1995) the use of geomembrane vertical barriers could be increased further by publications of performance case studies focusing on solutions to special challenges of a project and by pointing out the possible advantages and disadvantages of the technology used in that project. This could maybe lead to a methodology of performance based design becoming a mayor factor in decision-making by owners, designers and regulators.

	Wall Type	Typical Cost ($/m²)		Method	Typical Cost ($/m²)
conventional cut-off walls	Soil bentonite	20 - 80	geomembrane cut-off walls	Trenching machine	20 - 50
	Cement bentonite	50 - 180		Vibrated insertion plate	30 - 70
	Deep mixing	60 - 150		Slurry supported	50 - 150
	Jet grouting	300 – 800		Segment trench box	160 - 180
	Grout courtain	400 - 1000		Vibrating beam	180 - 250

Tab. 2.8: Construction costs for vertical cut-off walls (adapted from Mitchell and Rumer, 1997)

2.3 Composite cut-off wall systems

2.3.1 Introduction

Composite cut of walls have been developed to encapsulate abandoned landfills with a high chemical risk potential (Brandl, 1998). They increase the effectiveness of vertical barriers by combining the advantages of two systems: the diaphragm wall technique and the single liner (geomembrane) method. Geomembranes and geocomposites are only two possibilities for the integrated second sealing screen. Sheet piling walls, special metal liners, special glass liners and reinforced prefabricated concrete elements are also suitable for the incorporated

liner (Brandl 1998). Although there are many different liner types, composite cut-off walls with a geomembrane/geocomposite core are the most reliable passive vertical flow barriers. Tachavises and Benson (1997b) point out that low permeable backfill material adjacent to the geomembrane mitigates leakage defects in the geomembrane or its joints. Despite all this advantages the use of composite cut-off walls should, because of the high effort during the installation process, be reduced to cases where conventional cut-off walls would be permeable to substance which are harmful for the environment (Brandl, 1998).

2.3.2 Installation methods

To install a composite cut-off wall two methods are utilized: the vibrating beam method and the slurry supported method. Both of them use slurry, either to support the trench (slurry supported method) or to create a thin slurry wall (vibrating beam method). The slurry-supported method is the one of all five techniques that has been most frequently used whereas the vibrating beam method is theoretically possible but not common.

The slurry supported installation method (Figure 2.14) begins by excavating a trench and supporting it with slurry. The geomembrane panels are then inserted directly into the fresh suspension using a steel frame for support. The density of HDPE is lower than of water so that the panels must be held in their final position with weights to prevent them from floating. After the geomembrane is installed the backfill can be self hardened slurry (one phase cut-off wall-usual case) or some other separate backfill (two phase method-unusual case). Like all other techniques using vertical panels the interlocks are considered to have a high potential for leaks.

The vibrating beam method combines (Figure 2.15) the vibrating beam slurry wall technique (“thin diaphragm wall”) with the vibrated insertion plate method. First a thin wall of slurry is created as a beam is vibrated into the ground. After a section of slurry filled “trench” has been constructed, geomembrane panels are inserted in a manner similar to the vibrated insertion method.

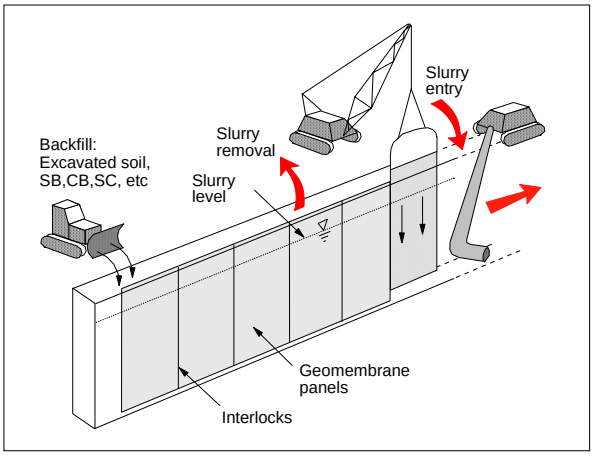

Fig. 2.14: Slurry supported installation method
(from Koerner and Guglielmetti, 1995)

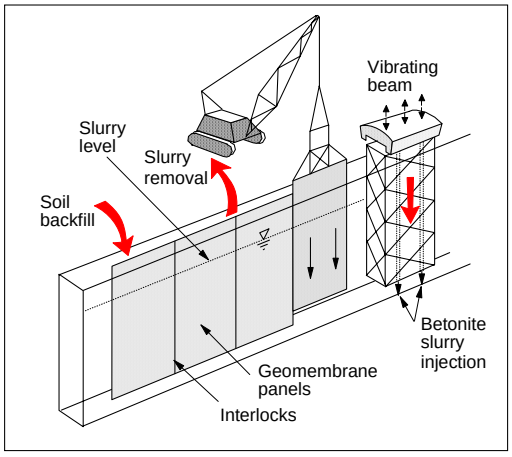

Fig. 2.15: Vibrated beam method
(from Koerner and Guglielmetti, 1995)

2.3.3 Case histories

Three case histories of successful application of composite cut-off wall as part of remediation strategies for contaminates areas are presented. In all applications composite cut-off walls were considered to be the most feasible and cost effective solution among various alternatives. The installation of the high safety containment barriers was always accompanied by a special testing program prior, during and after construction.

Cortilever (1999) describes the geo-hydrological isolation of the former landfill Schoteroog in Harleem, the Netherlands. A significant part of the landfill had to be cut off from open water locations. Furthermore, a near water treatment plant extracts ground water. Therefore the landfill was surrounded by a cement-bentonite composite cut-off wall. A main object of this project was to control the contamination of the ground water. 21 extraction filter wells where installed to lower the groundwater table within the wall thus creating an inward hydraulic gradient. Furthermore a special monitoring tube (Figure 2.16.) was welded on numerous joints to measure the permeability of the interlocks.

A cement-bentonite composite cut-off wall was chosen to be installed around the landfill Schoteroog. Due to calculation the permeability of the wall was estimated to be a factor 36 lower than for a cement-bentonite wall without a geomembrane liner. At the beginning of the construction process two main problems occurred:

- Over-consumption of the cement-bentonite mixture due caused by flow of the mixture in sand layers and shell banks
- Instability of the wall in the sand layers caused by liquifaction of the sand layers due to the vibration technique used to install the panels

After adjustment of the cement-bentonite mixture the wall could be successfully keyed into the sandy clay layer situated approximately 11 to 12 meters under the surface. Further details about the subsoil and the installed geomembrane are given in Table 2.9.

Subsoil	
depth	soil
0 - 3 m	sand
3 – 4/4,5 m	thick peat
4/4,5 – 11/12m	permeable sand with shell banks
> 12 m	low permeable sandy clay

Geomembrane	
wall length:	2.415 m
wall area:	29.103 m²
installed panels:	1.180
average panel length:	12,1 m
installed lock length:	14.278 m

Tab. 2.9: Landfill Schoteroog: Subsoil conditions and data of the installed geomembrane (adapted from Cortilever 1999)

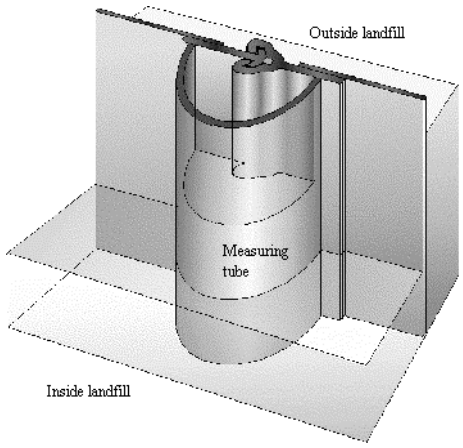

Fig. 2.16: Landfill Schoteroog: Monitoring tube (Cortilever 1999)

To determine the permeability of the interlocks a geomembrane tube was welded onto the panels (Figure 2.16). The water table within the wall was lowered one meter under the outside one, thus creating an inward hydraulic flow. Measuring the water table within the tube over a certain period and comparing it to the ground water table outside the wall makes it possible to calculate the flow through the interlock. The calculated average leakage through the joints was 3,21 cm³/day per meter lock at 1 meter water head. During the summer (May to September) of 1996 17.742 m³ of leakage where discharged from the wells inside the landfill, whereas only 6,6 m³ passed through the joints during the same period. For this project the amount of leakage passing through the joints is negligible.

In 1992 special government founding was given to Derby City in England for the reclamation of the Pride Park site, a 96 ha area parts of which were earlier used as landfill, gas works site, heavy engineering and gravel pits sites (Barker *et al*., 1997). Part of the remediation work included the construction of composite cut-off

wall around the abandoned landfill and the gas works site which occupy approximately two third of the whole area. Surrounding the contaminated soil with a vertical barrier prevented the migration of contaminates into the adjacent river and had the advantage of minimizing the off-site disposal of contaminated soils. Additional safety was achieved through a system of groundwater wells, installed on both sides of the wall creating an inward hydraulic gradient and serving as monitoring system.

A 600 mm cement bentonite cut-off wall with an incorporated 2 mm HDPE geomembrane was chosen as containment barrier because site investigations had shown that the soil was contaminated heavily. The wall was constructed with the slurry trench method using 5.7 m wide HDPE panels which were connected by means of hydrophilic joints. To ensure a sufficient cut-off wall durability results from chemical testing of approximately 800 soil samples were used to asses the durability of slurry mix. Although average contaminates concentrations where below the limits, some local spots with a high maximum concentration of pollutants were considered to eventually harm the mixture. The majority of these areas were far enough away from the line of the cut-off wall so that no special treatment was needed. Harmful spots near the wall were generally shallow, such that the contaminated soil could be excavated and replaced by new material.

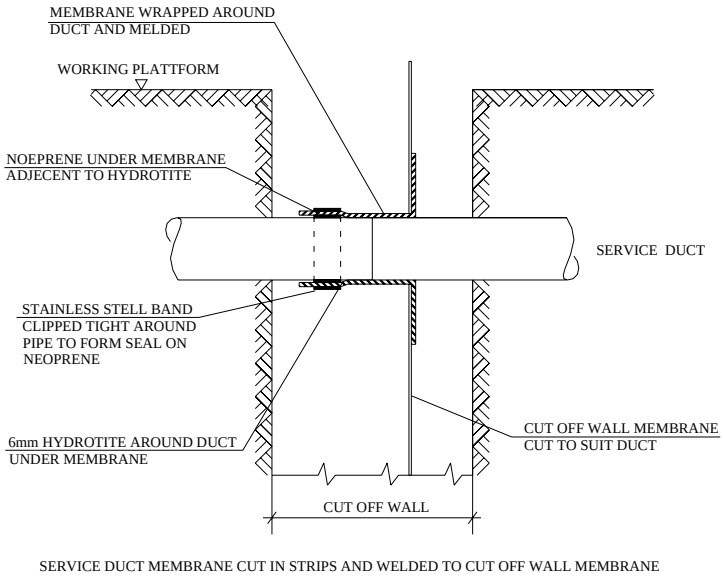

Fig. 2.17: Construction of the geomembrane cut-off wall around a service crossing (from Barker et al., 1997)

One of the major challenges of this project was the construction of the geomembrane cut-off wall around 36 service crossings (Figure 2.17). Generally, the cut-off wall around the services was constructed in advance of the main run, with temporary stopends attached to the joints for later connection to the adjacent geomembrane panels. Two services crossings were at such depths that sheet pile cofferdams and a local dewatering was installed to make work possible.

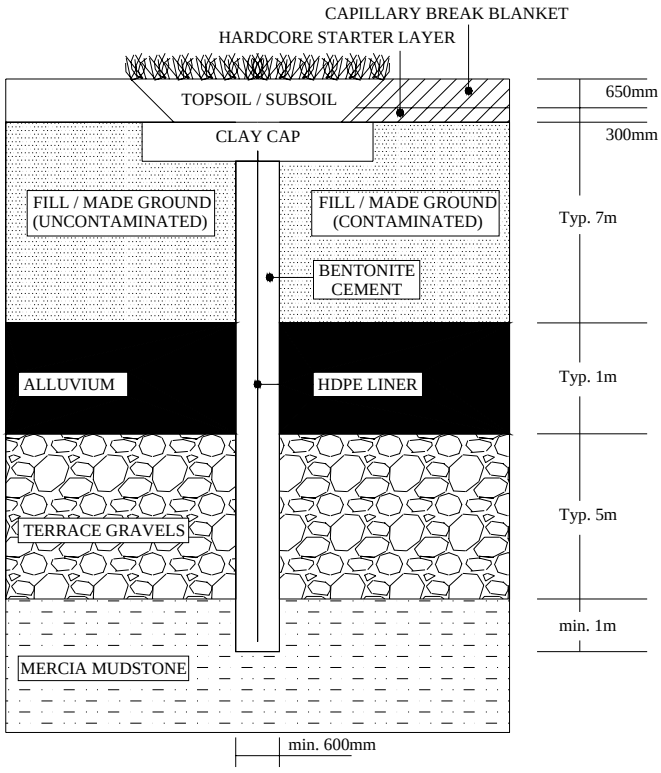

Fig. 2.18: Cross section through the cut-off wall
(from Barker et al., 1997)

After construction of the main parts of the wall had finished a special capping was installed. The upper 0.5 m of the slurry was removed and the geomembrane was trimmed to the required level. Furthermore an area of 2.5 m on each side of the centreline of the cut-off wall was excavated and refilled with clay to protect the wall from damage and desiccation. The capping of the whole site was finished with a 300 mm layer of uncontaminated soil and a 650 mm permeable capillary break blanket to ensure that during dry periods the capillary rise of any pollutant would not reach the surface of the cover. A typical cross section trough the composite cut-off wall is given in Figure 2.18. Finally the construction of the 3 km long vertical barrier could be finished within 26 weeks, gaining around 60 ha of vulnerable land for development.

Constructing a composite cut-off wall between the contaminated subsoil under the areal of a chemical plant in northern Italy and the adjacent river shows another successful application of the vertical barrier technique for remediation works (Manassero and Viola, 1992).

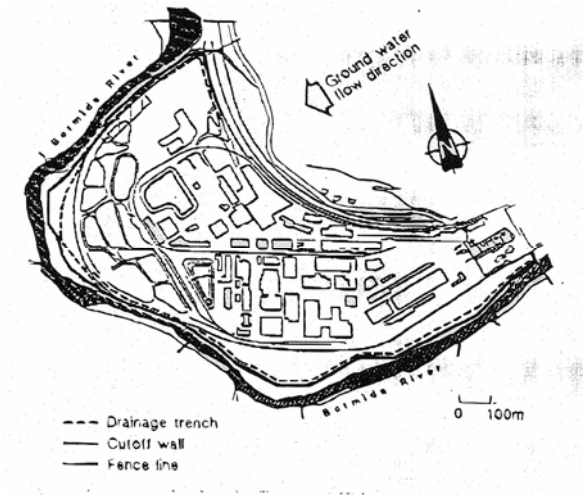

Fig. 2.19: Plan view of the alignment of the slurry wall (adapted from Manassero and Viola, 1992)

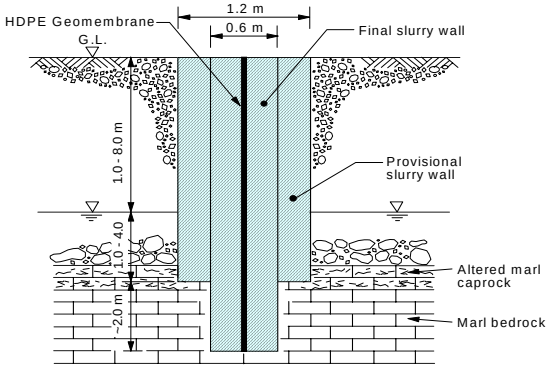

Fig. 2.20: Schematic cross section trough the composite cut-off wall (from Manassero and Viola, 1992)

After a sudden closing down of the “ACNA” chemical plant due to the serious pollution of the adjacent Bormida River a fast and safe remediation strategy was required to reopen the site as soon as possible. Site investigations had shown that the pollution of the river was caused by a groundwater flow from the contaminated subsoil under the chemical plant towards the river (Figure 2.19). The geological profile of this site was nearly ideal for the construction of a cut-off wall as a barrier to protect the river from future pollution. A high permeable polluted layer of sand and gravel was underlaid by a low permeable, unpolluted layer of marl bedrock at depths between 3 –12 m. The final design emphasized on a precise constructed, high safety barrier (Figure 2.20). Therefore, a 120 cm thick cement bentonite slurry wall was constructed prior the actual composite barrier. The outer wall was built to the base of the permeable sand and gravel layer with the aim to remove large boulders and to allow a precise installation of the inner wall. Afterwards the final barrier was constructed as a 60 cm composite cut-off wall reaching 2 m into the marl bedrock. Additional safety was added to the system by lowering the water table inside the contaminated area, thus creating an inward hydraulic gradient. The whole design and construction process was accompanied by a testing program including chemical compatibility testing of the cement bentonite slurry mixture, quality control of the

slurry during construction and in-situ permeability tests inside trial panels which were constructed close to and under the same conditions as the actual cut-off wall but without a geomembrane core. Data collected from the groundwater monitoring wells during the first time after finishing the construction showed a decrease of the pollutant concentration outside the vertical barrier of about one order of magnitude per year, thus proving the effectiveness of this chosen solution.

2.4 Unconventional cut-off walls

2.4.1 Introduction

Geosynthetics are also used in some other fields, where people would not expect to deal with them. In permeable reactive barriers geosynthetics are utilized as exchangeable filter panels, or to hold special (granular) material in shape. Further advances might include geosynthetic panels filled with reactive material. A better know application is the system of to parallel walls with a drainage and removal zone in between. A leak detection and drainage layer (i.e. sand, geonet, grout) is surrounded by two parallel geomembrane sheets (Figure 2.25). Putting a geomembrane/goenet/geomembrane composite to on side of the wall and backfilling the other side with low permeable material can be the most secure vertical barrier (Koerner and Guglielmetti, 1995).

2.4.2 Permeable reactive barriers

Commonly, barrier walls are tight cut-off walls thus forming a passive containment. However, for in-situ containment groundwater cleaning, permeable walls are also utilised, designed as reactive walls or funnel and gate systems (Figure 2.21). The contaminant plume is then flowing through a straight or curved wall or is directed to a gate. Groundwater cleaning in the reactive wall or gate is performed site-specifically, whereby physical, chemical and/or microbiological measures are possible. Several systems contain exchangeable geosynthetic filter panels, but also geotextiles to encapsulate special (granular) reactive material. A barrier wall may also consist of a row of consecutive wells for groundwater cleaning (Figure 2.22) or of an alternating sequence of cut-off wall elements and reactive walls (Brandl and Adam 2000).

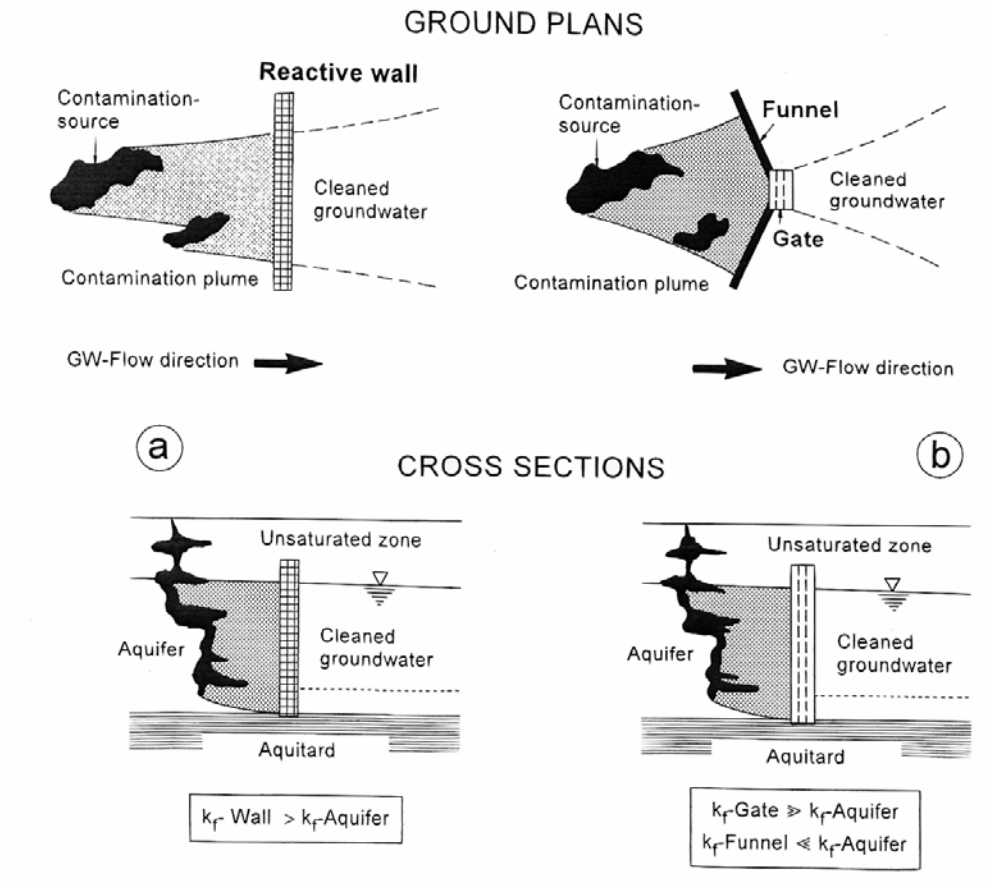

Fig. 2.21: In-situ groundwater cleaning with permeable reactive (a) walls or “funnel and gate” system (b). (from Brandl and Adam, 2000)

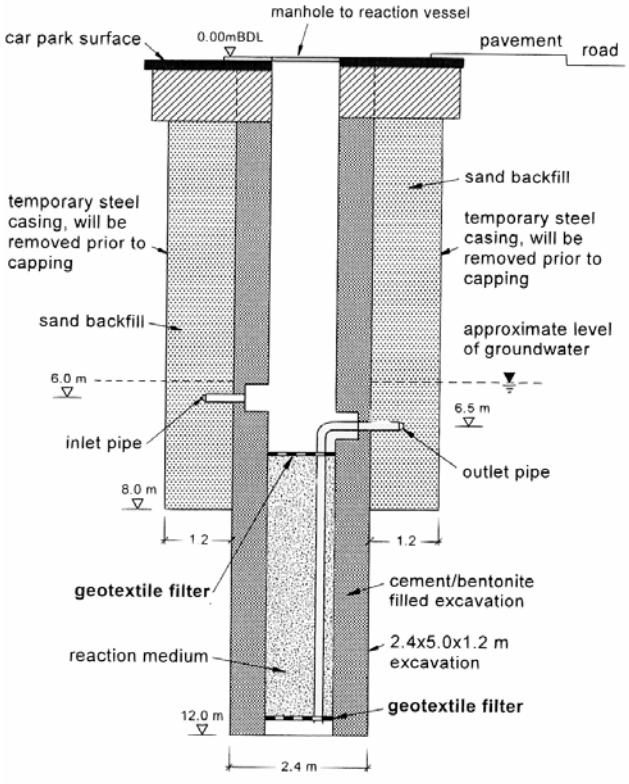

Fig. 2.22: In-situ groundwater cleaning in a reactor vessel installed within a slurry trench cut-off wall (from Soudain, 1997).

Low costs, the in-situ treatment of contaminants and the low influence on the local groundwater regime make permeable reactive barriers a real alternative to common treatment procedures (Hermanns Stengele, 1999). At the present time the major limitation, especially talking about landfills, of this new treatment method is the relatively narrow range of contaminates that can be treated and the complications introduced by mixed contaminates (Jefferis et al., 1997).

2.4.3 Cellular cut-off walls

Conventional geomembrane cut-off walls have two main problems:

- they are sensitive to leaks, thus a leak area of only 1-2% of the whole wall leads to a significant water flux through the barrier
- the detection of possible leaks is very difficult

In 1985 a new barrier wall system, the cellular cut-off wall, was first installed to deal with these problems. The central Vienna waste deposit, an area of approximately 60 ha, was surrounded by two parallel walls being connected by cross walls at certain longitudinal intervals to form a ring of consecutive cells around the deposit (Figure 2.23, 2.24). In each chamber the water was reduced to a level lower than outside but higher than inside the waste deposit. In combination with installed piezometer and wells in each cell the detection of leaks and an easy repair of the wall before pollutants may spread outside, is possible. Furthermore an inward seepage pressure, with counter effects towards an eventual diffusion through the wall, is created. Usually diaphragm walls and vibrating beam slurry walls are utilized, although for special applications, e.g. to high permeation trough the conventional system, composite cut-off walls are installed. This technique is not only suitable for abandoned landfills but also for the construction of hazardous waste deposits (Brandl, 1990).

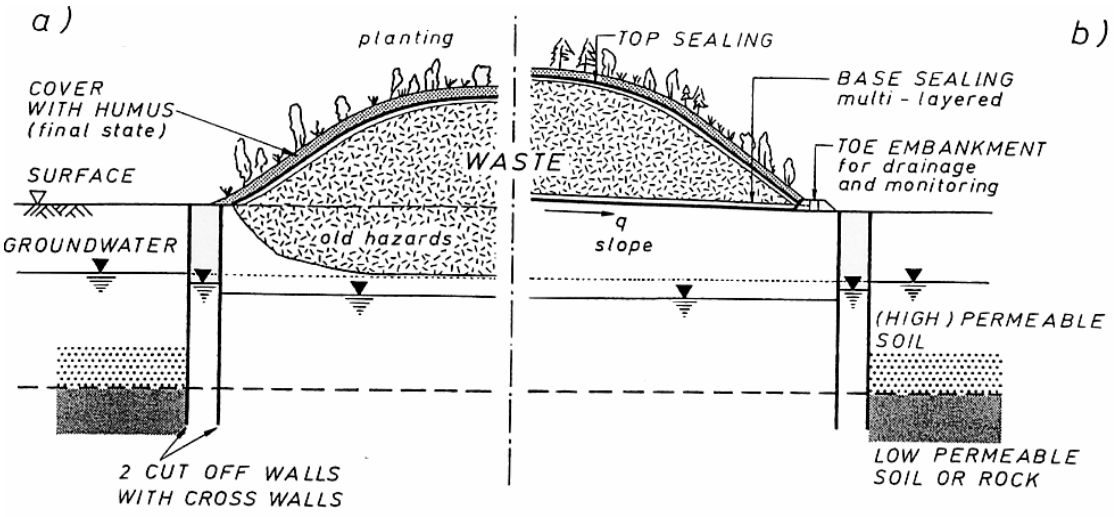

Fig. 2.23: High-safety encapsulation of waste deposits.
Schematical sketch (from Brandl, 1994):
a) cut-off and top sealing of old waste deposits (or critical sites which might cause environmental pollution)
b) scheme for designing new waste deposits with multi-barrier sealings

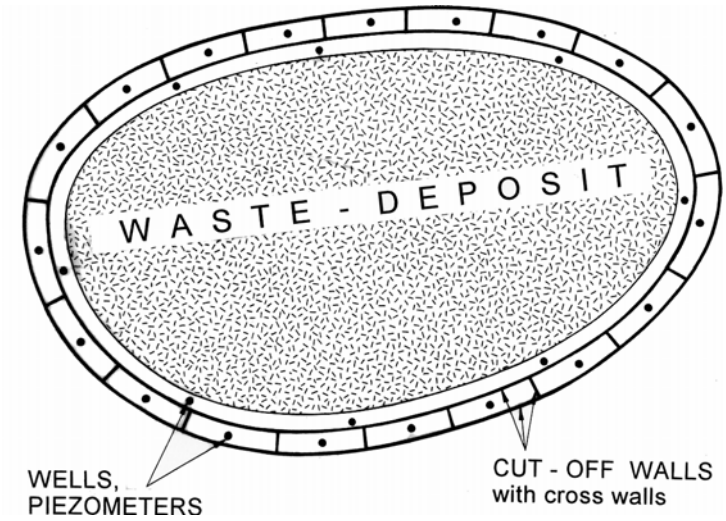

Fig. 2.24: "Vienna cut-off double wall system" with a cellular screen a around waste deposit site.
Schematical ground plan to Fig. 2.23 (from Brandl, 1994)

Another vertical barrier, using the same principal – two parallel walls with a central monitoring and leak detection core - as the cellular cut-off wall is shown in Figure 2.25. This system, two parallel HDPE geomembranes with a central core (sand, grout mass, geosynthetics etc.) serving as monitoring and leak detection system, is used to encapsulate areas with high contaminate potential (Brandl, 1998). The technology is also available with a geonet leak detection layer between two geomembrane sheets or with a geonet between two geomembrane sheets backfilled with soil-bentonite, soil-cement, cement-bentonite or soil-cement bentonite. With sand as leak detection drainage layer, the geomembrane would be placed on each

side of the excavated trench. With a geonet as the drainage layer , the composite system is placed against one side of the trench and the remainder backfilled as desired. For such a double liner system placed against the side of the trench facing the waste and the opposite side backfilled with a low hydraulic conductivity soil, cement or grouted material, one has the vertical equivalent of hazardous waste liner system type (Koerner and Guglielmetti, 1995).

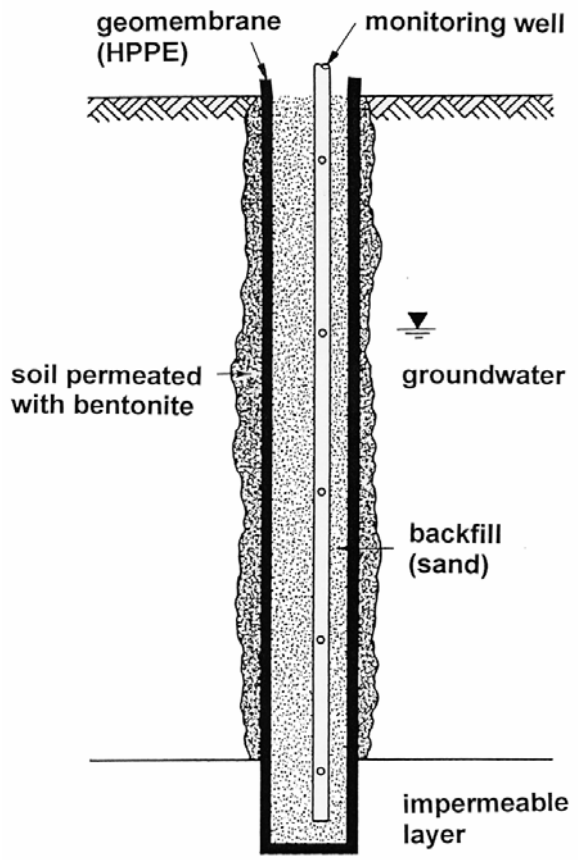

Fig. 2.25: Geosynthetic – double wall system with monitoring and leak-detection system. Schematically (from Brandl, 1998

2.5 Conclusion

Containment of landfills has increases the demand for vertical barriers. Using geomembrane cut-off walls to encapsulate landfills offers several advantages (e.g.: high chemical resistance, contaminate transport mainly by means of diffusion) over conventional soil- and cement- based barriers. Nevertheless more effort should be put on future research and publication of existing case history to increase the use of this relatively new technique.

The following statements about geomembranes as vertical barriers can be made:

- HDPE is the preferred material used in geomembrane cut-off walls. This is mainly because of its high resistance to various types of chemicals, but also because of availability, cost and ease of installation.
- Although there are a few factors, especially the exposure to chemicals, that might reduce the geomembranes lifetime none of them is considered to seriously harm the geomembrane. The lack of enough field data has lead to laboratory simulations with estimated lifetimes up to 1000 years. However, these lifetimes could only be achieved if the geomembrane is installed without being damaged.
- Due to its main function to minimize the hydraulic permeability, for geomembrane cut-off walls diffusions becomes the dominating transport process for contaminates. Sheet thickness and solvent concentration are the two parameters that have the biggest influence on the contaminant flow trough HDPE cut-off walls. Consequently HDPE sheets used in vertical barriers should at least be 2 mm thick. Intact geomembranes cut-off walls usually have such low transport rates that the emphasis should be put on the integrity of the interlocks.
- Geomembrane cut-off walls are very sensitive to leaks. A leak area of only 1% reduces the barrier effect of geomembrane cut-off walls up to 80 - 90%. On the other hand composite cut-off walls, which perform even with defects similar to intact geomembrane and soil-bentonite walls, are an adequate measure to increase the effectiveness of a vertical barrier. Therefore, for applications with a high risk potential geomembranes should be used as liners in slurry-trench walls or as geosynthetic twin-walls. Furthermore applications with leak detection and removal systems should be preferred.
- To ensure the function of a geomembrane cut-off wall the interlocks, the most sensitive parts to leaks, have to be installed and tested properly. There are four different connection types (plug-in -, grouted -, welded and hydrophilic sealant connections) available; however interlocks with hydrophilic sealants dominate. Full fusion welding, which is under development, would be a step forward to guarantee high quality connections even under difficult installation circumstances. Monitoring the continuity of the joint is an important part of the installation process. Indirect methods including measuring the electric resistance through a circuit closed by two contact elements on the bottom of

each sheet or watching the outflow of grout trough the adjacent channel are well established, whereas it is very difficult to test the liquid tightness of the interlocks in the field.

- Among the various methods for post-construction monitoring a net of downgradient wells is most common. This technique is widespread however it does not guarantee success in detecting an occurring leak. For critical application, such as hazardous wastes another leak detection and removal system should be preferred. Two parallel geomembrane sheets with a central leak detection drainage layer (sand, geonet), eventually backfilled with low permeable material are considered as the most secure vertical barrier.
- Installation methods for geomembrane cut-off walls are under constant development. The trenching machine-, the vibrated insertion plate-, the segment trench box-, the vibrating beam- and the slurry supported installation method are the five common installation methods. Primarily the established techniques will become faster, deeper, better and cheaper.
- Most of the current methods for encapsulation and containment are, in terms of installation techniques, very similar to other applications such as in-ground structural walls and groundwater cut-off walls, due to the fact that they have been adapted from these techniques. However, considering the performance they are likely to fulfil other criteria. Geomembrane cut-off walls offer several advantages, such as that contaminates transport occurs mainly by means of diffusions, they have a high resistance to chemicals and that they are not vulnerable to damage by desiccation or freeze-thaw, over soil- and cement-based barriers. On the other hand geomembranes are very are likely to fail at the joints and are easily damaged by puncture during the installation process. Talking about costs, geomembranes acting alone are likely to compete with other walls whereas when included as an additive liner in a conventional wall costs may rise for another 10% to 30%. Publications of case histories and a few full scale demonstration projects may help to increase the use of geomembrane cut-off walls.

Furthermore geosynthetics are also used in other barrier systems. This include permeable reactive barriers, where geosynthetics are used as exchangeable filter panels or to contain material in the required shape as well as systems of two parallel geomembrane sheets with a drainage and removal zone in between.

3 Tension in geomembranes placed on steep slopes

3.1 Introduction

On landfill slopes several types of geosynthetics (e.g. geomembranes, geotextiles, GCLs) are used as a lining system to protect the environment from harmful impacts created by the waste stored above the slope liner. Interface slipping, pulling out of the anchorage and rupture at the top of the geomembrane are typical failure mechanisms. To prevent such failures it is important to have models representing the reality as close as possible. This chapter will focus on the tension at the top of a barrier lining element placed on a slope.

Work carried out to date on this issue involves predominately the employment of two solutions. Results are either based on the limit equilibrium method or on the load-displacement analysis such as finite element method. The first approach ignores the stress strain-laws of the slope system and is therefore not suitable for such a system including materials with different stress-strain behaviour. Furthermore the slope system is assumed to be at the verge of failure, thus leading to no results for cases where the system is not failing. The second method is more general, but requires detailed knowledge of the parameters for the slope, the waste and the materials between them, and is furthermore very time consuming. Kodikara (2000) and Krishna Prasad *et al.* (2001) have presented a simplified analytic solution to calculate the tension and the displacement developed in a geomembrane slope liner.

The aim of this project is to model Kodikara's (2000) assumptions with FLAC (Fast Lagrangian Analysis of Continua). Special effort is put on the sensitiveness of the model towards various parameters. Similar results for both methods would help to save a lot of time, using the analytic solution instead of the numerical one.

The nomenclature used in this thesis is the same as in Kodikara's (2000) paper:

c_l	Adhesion at the geomembrane-clay interface
D	Thickness of the clay layer
E	Young's modulus of the geomembrane
G	Shear modulus of the clay liner
H	Overburden height at the top of the geomembrane or bench
h_x	Overburden height at distance x along the geomembrane
K_x	The ratio of horizontal to vertical stress developed in the overburden

k_s	Shear stiffness of the geomembrane and underlying clay
L	Length of the geomembrane on the slope
L_p	Distance to elastic-plastic boundary from *x=0* position
p_l	Liquid pressure below the geomembrane
T	Tension in the geomembrane at distance *x*
T_{max}	Maximum tension in the geomembrane
t	Thickness of the geomembrane
u	Displacement of the geomembrane at distance *x*
u_p	Displacement of the geomembrane at τ_l^p
x	Distance measured along the geomembrane from top of the bench
β	Slope of the overburden surface as shown in Figure 3.1(a)
ϕ_l	Friction angle at the lower interface of the geomembrane
ϕ_u	Friction angle at the upper interface of the geomembrane
γ	Unit weight of the overburden
η	Ratio of residual to peak shear strength in geomembrane-clay interface
θ	Slope angle to the horizontal level
σ_h	Horizontal stress on the geomembrane at distance *x*
σ_n	Normal stress on the geomembrane at distance *x*
σ_v	Vertical stress on the geomembrane at distance *x*
τ_l	Shear stress at the lower side of the geomembrane (geomembrane-clay interface)
τ_l^p	Peak shear stress at the lower side of the geomembrane
τ_u	Shear stress at the upper side of the geomembrane

3.2 Previous work – analytic solution

Kodikara (2000) presented a simplified analytic solution to calculate the tension at the anchorage and the displacement of the free end of a geomembrane based on a slope (Figure 3.1). Previous work on this topic was either based on the limit equilibrium method or on the load-displacement analysis such as finite element method. Compared to the solutions presented in his paper the limit equilibrium method ignores the stress-strain laws of the slope. The load-displacement analysis is more general, but requires exact knowledge of the input data and is very time consuming.

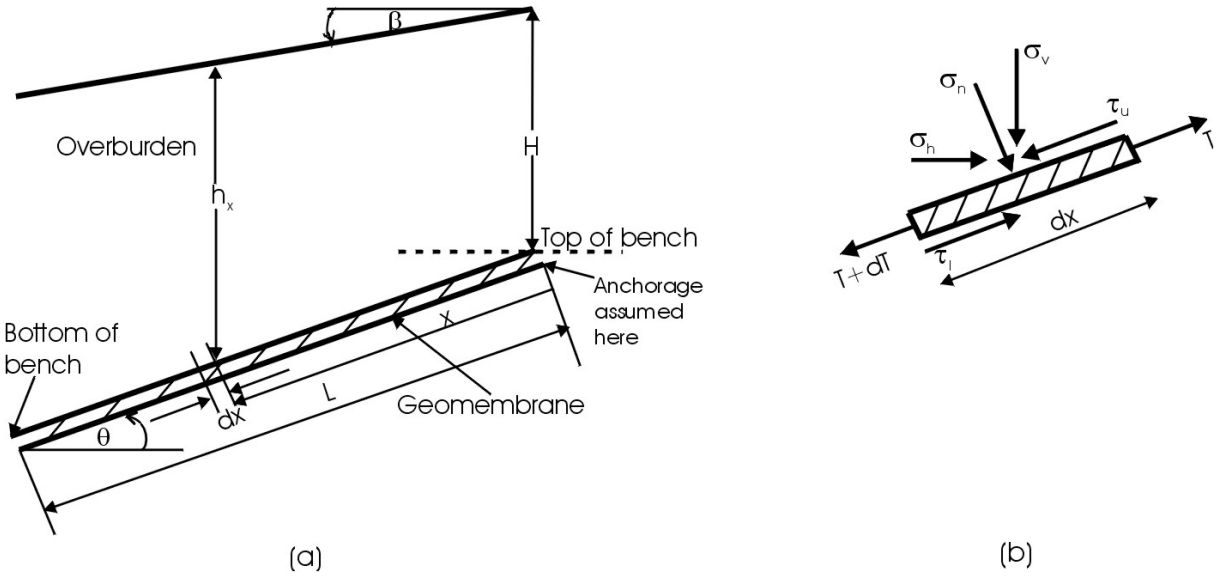

Fig. 3.1: Analytic solution - General idealisation of the problem
(a) variables and definitions; (b) stresses on a small geomembrane element (from Kodikara, 2000)

The material above the geomembrane was modeled as a single mass with no slipping at any interfaces and no significant liquid pressure. This leads to the governing differential equations (1)[3], (2) an (3) for a small element of the geomembrane.

$$\frac{dT}{dx} = \tau_l - \tau_u \tag{1}$$

$$\frac{du}{dx} = \frac{T}{tE} \tag{2}$$

$$\frac{d^2u}{dx^2} = \frac{1}{tE}(\tau_l - \tau_u) \tag{3}$$

Numerous parameters including geomembrane (Young's modulus E) and slope (shear modulus G) elasticity, interface characteristics (shear stiffness k_s) and the ratio of horizontal to vertical stresses (K_x) have been considered. The geomembrane stress-strain behavior was assumed to be elastic-ideal plastic. These assumptions leaded to two equations, one for the geomembrane being in the elastic state (9) and another for being in the plastic state (11). These dimensional equations

[3] The numbers of the equations in this chapter refer to the number of the equations in the paper by Kodikara (2000)

were than transformed into a form with non-dimensional variables to make the solutions more general.

$$\frac{d^2u}{dx^2} - \frac{k_s}{tE}u = -\frac{\gamma \sin 2\theta}{2tE}(1-K_x)(H + x\sin\theta - x\cos\theta\tan\beta) \qquad (9)$$

$$\frac{d^2u}{dx^2} = \frac{1}{tE}\left[\eta\left\{\left(K_x\cos^2\theta + \sin^2\theta\right)(H + x\sin\theta - x\cos\theta\tan\beta)\gamma - p_l\right\}\tan\phi_l\right.$$

$$\left. + \eta c_l - \frac{1}{2}(1-K_x)(H + x\sin\theta - x\cos\theta\tan\beta)\gamma\sin 2\theta\right] \qquad (11)$$

Although Kodikara (2000) presented the exact solution for both cases (geomembrane total in the elastic state / geomembrane partly in the elastic state and partly in the plastic state) he emphasized on the design purpose. The objective was to create simple solutions for maximum strength (T_{max}) at the anchorage and the maximum displacement (u) at the free end of the geomembrane. Therefore terms of the solution containing the term e^{-x}, which is close to zero were ignored. Furthermore it was shown that under these assumptions the geomembrane behaves either elastic or fully plastic. The results were satisfying due to parametric studies which have proved that the differences between the exact and the approximate solutions are less than 5%. Further research could concentrate on verifying the appropriateness of the modeling of shear stiffness k_s and to provide better data for the earth pressure coefficient (K_x).

Parametric studies for elastic conditions have shown:

- T_{max} increases with the slope angel and the stiffness of the geomembrane.
- However, the influence of the slope angel decreases for steeper slopes because the change of the shear stress is not as big as for flatter slopes.
- T_{max} decreases with increasing K_x
- T_{max} increases with more waste overlying the geomembrane
- The displacement u at the bottom of the geomembrane does not increases significantly for longer geomembranes, because most of the displacement occurs at the top of the geomembrane

When reducing the interface friction between the geomembrane and the clay fully plastic conditions occurred. In this state the maximum tension at the anchorage was independent from the geomembrane's stiffness, thus developing due to the

difference between the limiting shear stress acting on the upper and lower surface of the geomembrane. However the tension on the anchorage needed some strain to occur. Consequently the maximum stress is directly proportional to the displacement (which is dependent on the stiffness of the geomembrane) at the end of the geomembrane.

Another paper dealing with the same problem was presented by Krishna Prasad *et al.* in 2001. Most of the assumptions for the model were similar to those presented by Kodikara (1996, 2000). The main difference is that the response of the interface between the geomembrane and the subsoil was considered to be hyperbolic. The resulting non-dimensional governing equation was solved with the finite difference approach.

Results showed that the maximum tension occurred at the anchorage and is decreasing very fast with increasing distance from the anchor point. Correlating to this results large initial displacements are calculated near the anchorage then following a linear increase. Numerous parametric studies have been done leading to design charts for the maximum tension. The tension at the anchorage increases with the length of the liner, the unit weight of the overburden, the height of the overburden and for angles up to 35°, with the slope angle. For higher values the tension decreases. Decreasing tension also occurs for increasing lateral support of the waste body and for a higher initial shear stiffness of the interface.

Supplementary two comments should be made on Kodikara's (2000) paper. In equation (6) sinus and cosines have been mixed up accidentally. The correction of equation (6) leads to equation:

$$\sigma_n = \sigma_v \cos^2\theta + \sigma_h \sin^2\theta =$$

$$\left(K_x \sin^2\theta + \cos^2\theta\right)\left(H + x\sin\theta - x\cos\theta\tan\beta\right)\gamma \qquad (6^*)$$

Sinus and cosines should also be change against each other in Eqs. (11), (19), (20) and (A.12). As long as the interface is in the elastic state this change has no influence on the results. Through this change the boundary between elastic and plastic state (τ_l^p in Eq. 10) changes and also the results for the plastic state are different. All comparison between the analytic solution and FLAC are made with the corrected equations.

Although for most of the cases the results of the exact solution and the simplified one are within 5% difference, the simplified solutions has a singularity. This happens at the change from the elastic to the plastic state. For the exact solution the tension and the displacement changes continuously from one state to the other, whereas for the simplified one these values drop to zero. The reason for this discontinuity is that for the simplified solution the interface behaves either elastic or fully plastic. For approximate solution it is possible that τ_u and τ_l^p are equal. This can be express by the following equation:

$$\frac{1}{2}(1 - K_x)(H + x\sin\theta - x\cos\theta\tan\beta)\gamma\sin 2\theta = \left[(K_x\sin^2\theta + \cos^2\theta)(H + x\sin\theta - x\cos\theta\tan\beta)\gamma - p_l\right]\tan\phi_l + c_l \quad (3.1)$$

Knowing all except one parameter the equation can be solved for the missing parameter, thus finding the discontinuity. An example where this is done through varying the K_x value is shown in Figure 3.2. Although it's very unlikely to calculate results close to that point, very small values for the tension in the geomembrane should be checked with the exact solution. With this one it's also possible to calculate cases where parts of the interface are slipping and others are still in the elastic state.

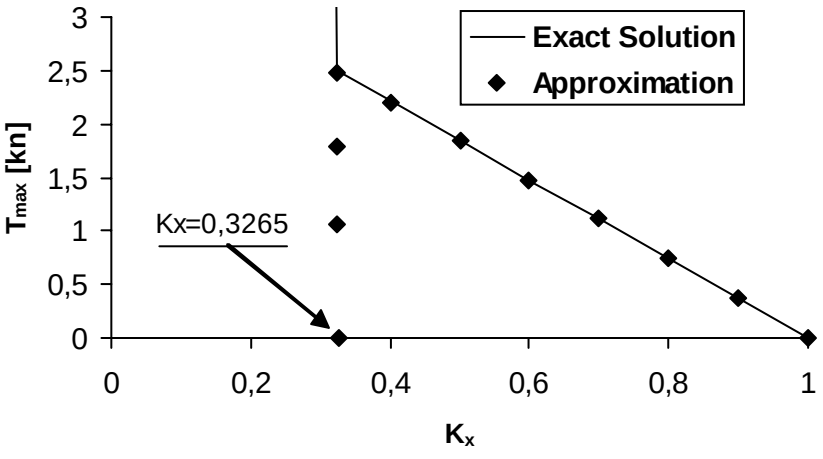

Fig. 3.2: Approximate Solution - Discontinuity at the change from elastic to plastic state

3.3 The numerical model

3.3.1 Introduction

The aim of modeling the analytic solution presented by Kodikara (2000) with FLAC, a finite difference program is to see how close the assumptions of the analytic solution fit to the results carried out with a numerical model. Furthermore the sensitiveness of the results to several parameters such as grid size, stiffness of the interface or waste parameters should be evaluated.

3.3.2 The model

Figure 3.3 shows a general first set up of the grid. As expected from the analytic solution the area around the anchorage at the top of the slope is the one where the strain of the geomembrane is a maximum, hence the tension in the geomembrane is built up. This high tension occurs due to the fixation (= zero displacement) of the geomembrane and the maximum displacement of the waste body above the geomembrane leading to a high relative shear displacement at the upper interface. Therefore it is very important to provide a fine mash size at the top of the slope. Running some calculations has shown that, for equal lengths of the top element of the geomembrane, it is less time consuming to use a model with a grid that becomes finer towards the top of the slope (Figure 3.4) than using one with equal distances between the grid points. The boundary conditions for the subsoil can be seen in Figure 3.5. All grid points around the soil are fixed in both directions thus forming a rigid body. These assumptions are comparable with the analytic solution, where the shear modulus (G) and the thickness (D) of the subsoil clay layer are used to determine the shear stiffness $\left(k_s = \frac{G}{D} \right)$ of the interface between the subsoil and the geomembrane. In FLAC this shear stiffness is a parameter of the interface, consequently for a model with rigid subsoil independent of the subsoil.

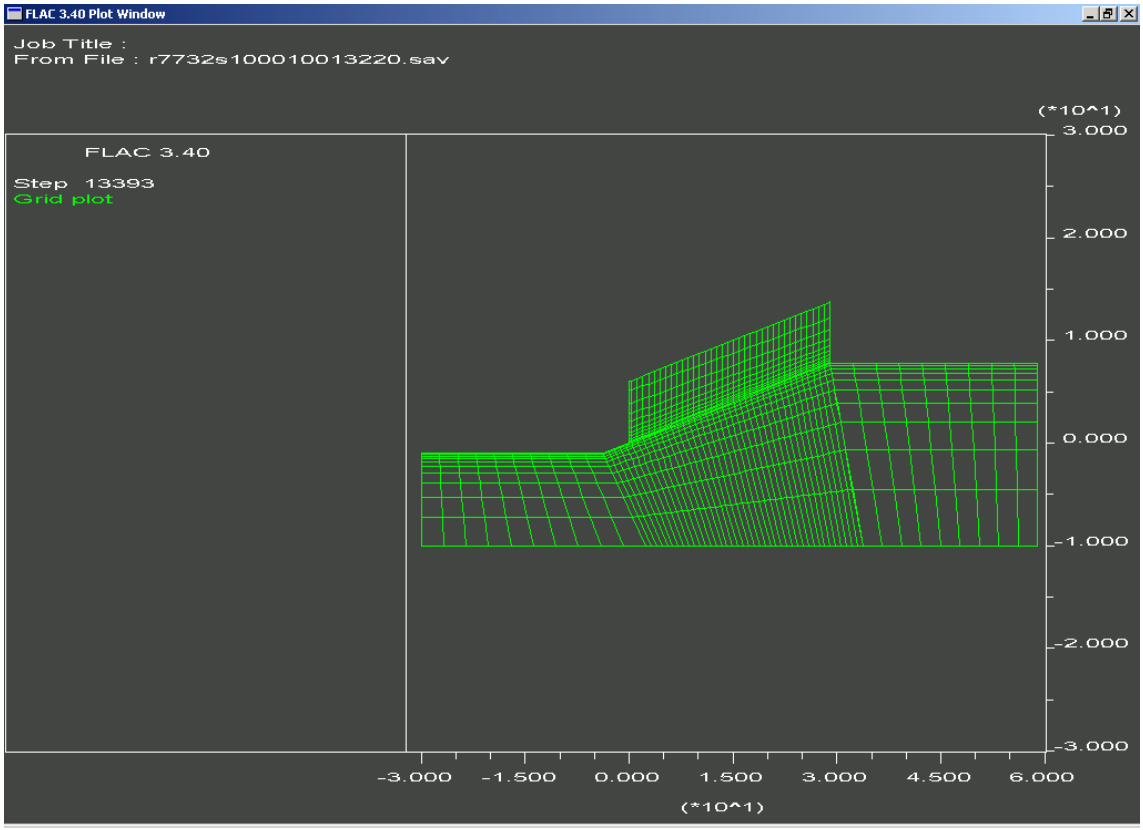

Fig. 3.3: FLAC - The grid

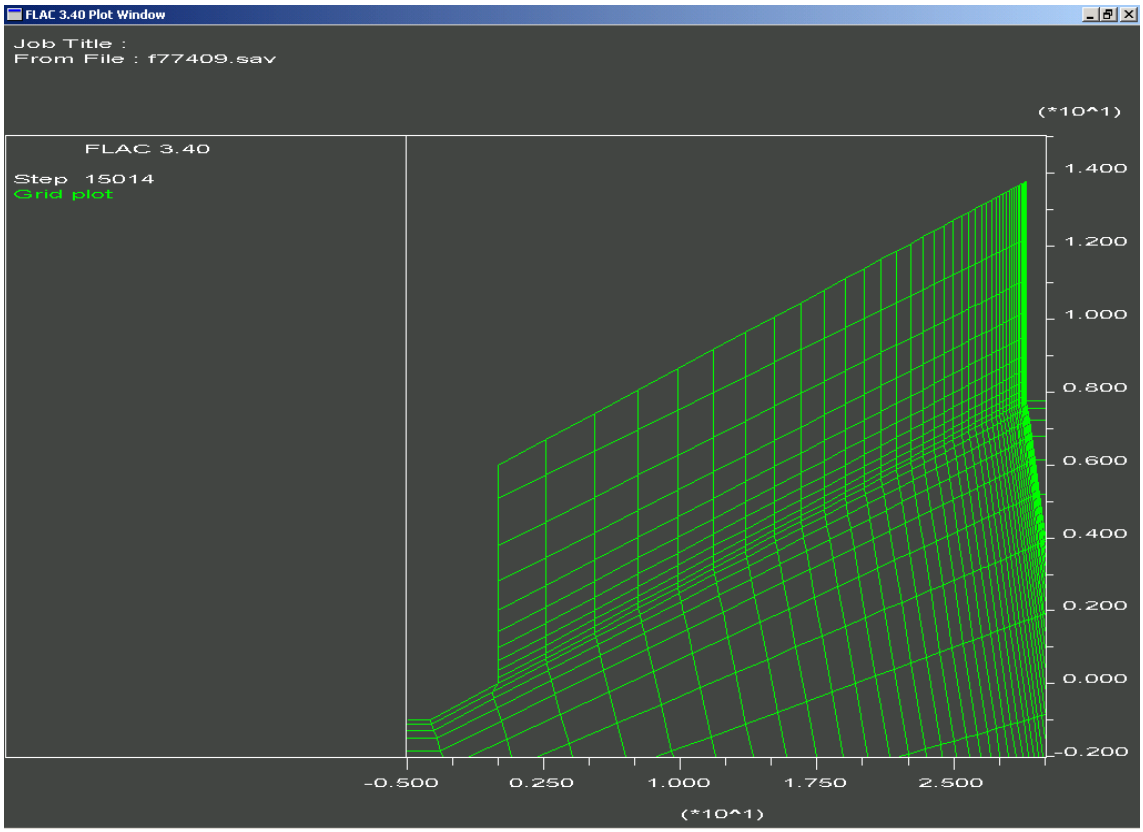

Fig. 3.4: FLAC – Refinement of the grid

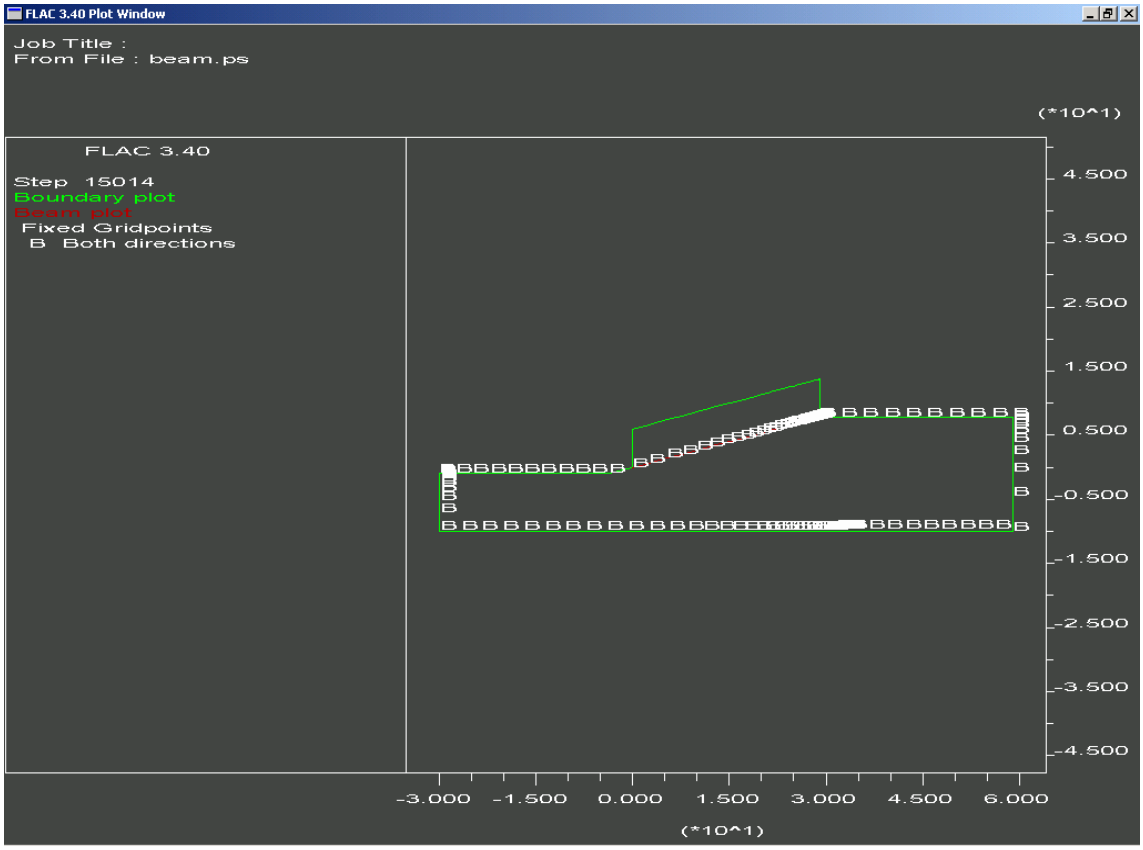

Fig. 3.5: FLAC - Boundary Conditions

Both, the waste body and the subsoil are modeled as elastic and isotropic. Bulk modulus K, shear modulus G and the density γ are the required input parameters for this model. It should be highlighted that in the analytic model the waste stresses do not depend on the modulus of the waste material because stresses are approximated for an infinite element. The elastic isotropic model is chosen, although some others (e.g. Drucker – Prager or Mohr – Coulomb) are more likely to represent the reality in a closer way, because it runs faster than the other models and furthermore it is easier to understand the behavior of the systems than it would be for a more complex material model. If there are comparable results between the elastic-isotropic FLAC model and the analytic model, a next steep could be to run FLAC with another material model such as Mohr-Coulomb to verify the accuracy of the simplification made by using elastic parameters.

Due to the fact that it is important for geomechanical applications to use structural support elements FLAC provides 4 different types of structural elements. Among these (beam-, cable-, pile element and support members) the beam element is chosen to represent the geomembrane between the waste and the sub soil. A main advantage of the beam to all other structural elements is that interfaces can be

connected to both sides of the beam. This simulates a realistic stress-displacement behavior of the waste – geomembrane – subsoil system. Width, height, Young's modulus, density and plastic moment have to be specified for the beam. By setting the plastic moment zero it is guaranteed that no bending resistance is built up, hence enabling free deformation normal to the main direction of the beam/geomembrane. According to the analytic solution the following boundary conditions have to be fulfilled:

(a) no displacement at the top of the geomembrane (x = 0, u = 0)

(b) no tension at the bottom of the geomembrane (x = L, T = 0)

In the numerical model these boundary conditions are modeled by fixing the displacement of the top node of the geomembrane and by creating a free end at the bottom. Although the boundary conditions are for both cases the same it will be shown in this chapter that these limitations are the reasons for some problems with the numerical model.

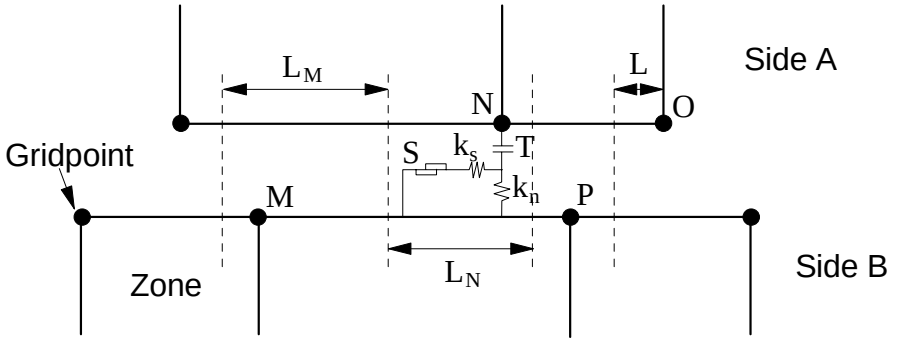

S = slider T = tensile strength kn = normal stiffness ks = shear stiffness
LN = length associated with gridpoint N LM = length associated with gridpoint N
---- denotes limits for joint segments (placed halfway between adjacent gridpoints

Fig. 3.6: FLAC – interface model
(from Itasca, 1998)

The shear stress on both sides of the geomembrane will depend on the shear-displacement characteristic of the waste-geomembrane and geomembrane-subsoil interface. This is a difference to the analytic solution, where the shear stresses on the upper side of the geomembrane were determined by the height of the overburden and $K_{x,}$ the ratio of horizontal to vertical stresses. This leads to direct impact of these stresses on the geomembrane, whereas different shear stress above the geomembrane might develop for the numerical model due to the shear-displacement characteristic of the upper interface. Figure 3.6 shows the way interfaces are

represented in FLAC. For this application matching points of both sides of the interface were situated exactly opposite each other to create a simple geometry of the interface. The shear stiffness k_s and the normal stiffness k_n are the main parameters which control the stress – displacement behavior of the interface. Similar to the analytic solution an elastic – ideal plastic shear displacement response (Figure 3.7) is assumed for both interfaces. The limiting shear stress is defined by the Mohr – Coulomb parameters c (cohesion) and ϕ (friction angle). In contrast to the analytic solution a strain softening interface response for the plastic state is not included at this stage of the model , because it's not straightforward in FLAC to apply strain-softening interface properties. Modeling the subsoil as a rigid body leads to direct comparability for the shear stiffness for both, the analytic and numerical solution. For possible future models with settlements in the subsoil special care should be taken when comparing results for cases with the same shear stiffness k_s of the lower interface. The results of the analytic and numerical model might differ because if the subsoil is allowed to move this might soften the stiffness of the geomembrane – subsoil system.

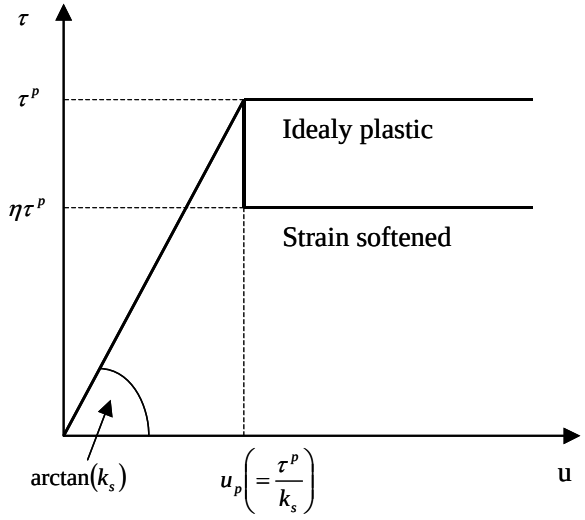

Fig. 3.7: Elastic – ideal plastic interface response

Before talking about the general procedure for running the model it is important to know how equilibrium is defined in FLAC. A numerical model will never reach total equilibrium. During each timestep FLAC calculates for each gridpoint the sum of all forces acting on this gridpoint, the so called unbalanced force. For total equilibrium the maximum unbalanced force should be zero. One way to donate equilibrium is if the maximum unbalanced force is below a certain limit, chosen by the

user. Another way to denote equilibrium is through the equilibrium ratio. The equilibrium ratio is the ratio of maximum unbalanced force to the representative internal force acting in the grid. Running different cases has shown that for this model suitable results are provided by controlling the model through the maximum unbalanced force. The accuracy of the results does not improve significantly if the ratio of maximum unbalanced force to expected tension at the top of the geomembrane decreases under a value of 0,01. The steps until equilibrium of the system are as follows (with equilibrium after each step):

- The subsoil with the fixed boundary conditions is brought to equilibrium.
- The geomembrane and a first layer of waste is put on the slope.
- Waste is stored layer after layer until the full height of the overburden is reached.

Due to the fact that there is no lateral support for the waste body this model represents a worst case scenario. This cases is characterized by $K_x = 0$ in the analytic model. Furthermore it should be emphasized that only cases with a constant thickness of the waste body are modeled because this makes it easier to find problems of the model and to perform parametric studies.

3.3.3 Modelling issues

One of the first problems which occurred can be seen in Figure 3.8. With a higher relative shear stiffness k_s^u of the upper interface to the shear stiffness k_s^l of the lower interface the tension at the top of the geomembrane increases rapidly. This effect can be explained by the spring interface model in FLAC. The higher shear spring stiffness of the upper interface has a similar effect as if the rigid waste body would hang on to the geomembrane. This would not be a problem if the geomembrane could move down the slope with a similar displacement as the waste body, thus creating no bigger relative shear displacement between the geomembrane and the waste. Whereas in this model the geomembrane is fixed at the top while the waste body moves down the slope as a rigid block creating the shear displacement situation of the upper interface shown in Figure 3.9. The high shear displacement gradient at the top of the upper interface leads also to a high shear stresses in this part of the interface (Figure 3.10). In comparison to that the

upper shear stress τ_u in the analytic solution is constant (assuming a constant thickness of the overburden) for the whole slope.

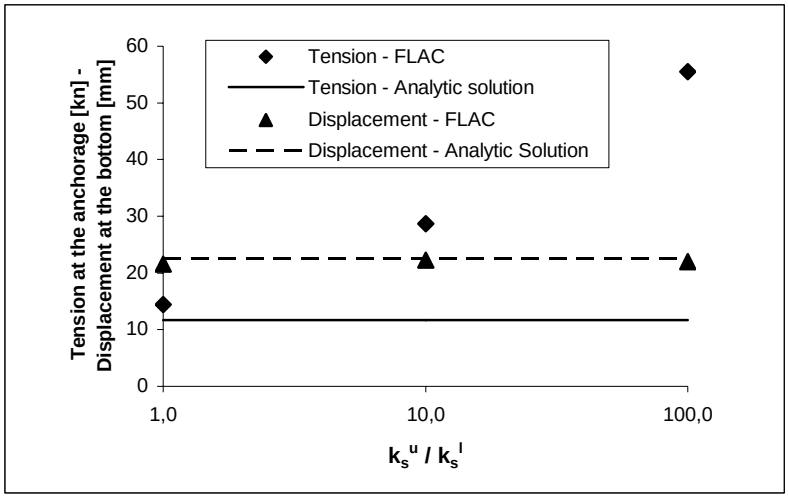

(a) k_s^l = 1e6 Pa/m

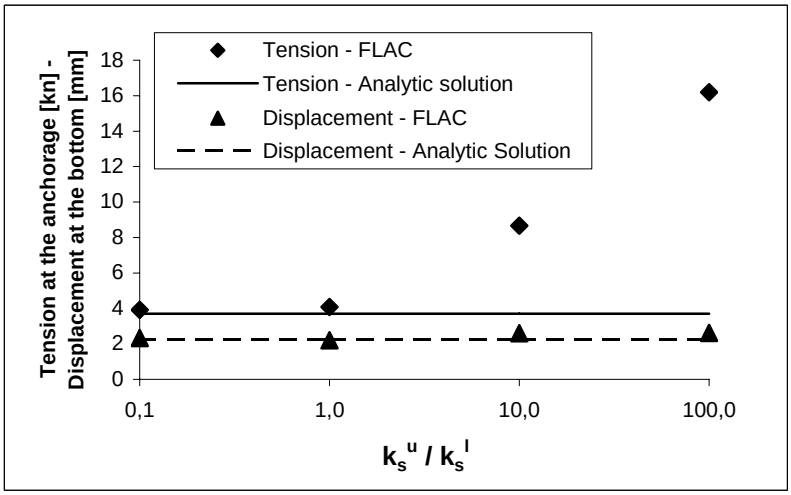

(b) k_s^l = 1e7 Pa/m

Fig. 3.8: Influence of the shear stiffness ratio of the upper tot he lower interface on the tension at the anchorage and the displacement at the bottom of the geomembrane
k_s^u = shear stiffness of the upper interface k_s^l = shear stiffness of the lower interface

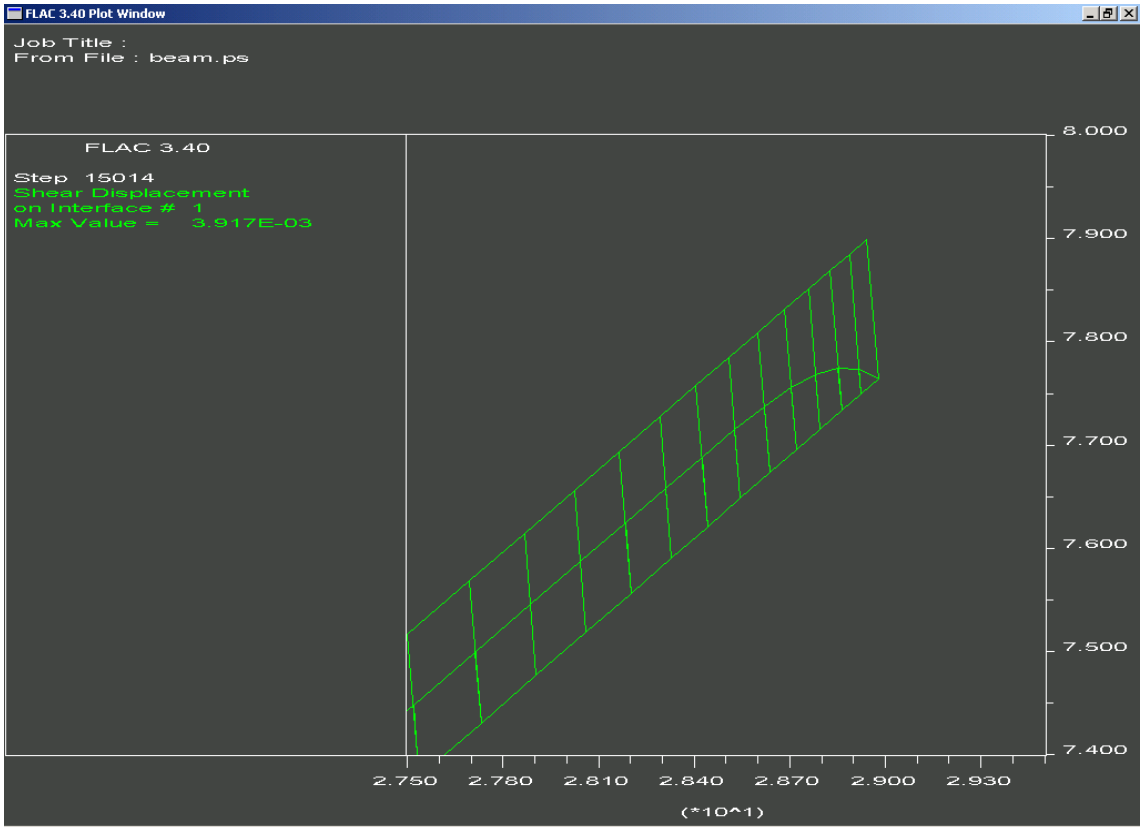

Fig. 3.9: Upper interface: - Shear displacement

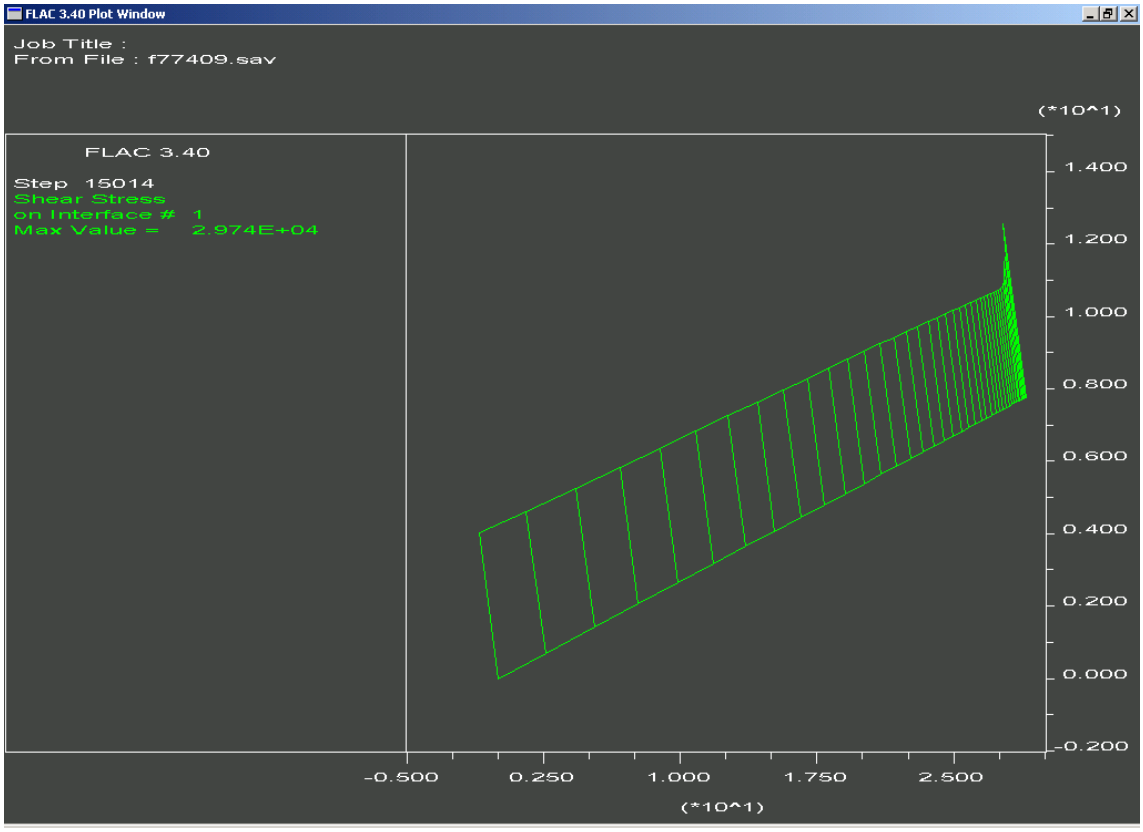

Fig. 3.10: Upper interface: - Shear stress

To become similar shear stress distributions above the geomembrane it was necessary to consider a limit of shear resistance of the upper interface to control stresses at the interface. This provides that the peak at the top of the upper interface is cut off. The maximum shear stress, τ_{max} acting at one interface element is limited by the following relation:

$$\tau_{\max} = c * L + \tan\phi * \sigma_n \qquad (3.2)$$

where c = cohesion along the interface, L = effective contact length, ϕ = friction angle of the interface surface and σ_n = the normal stress acting on the interface. Setting c = 0 and the friction angle a little higher than the angle of the driving force of the waste body allows the top elements of the upper interface to slip, whereas all other interface elements are staying in the elastic state. This model is a more realistic assumption than the one where the whole waste body is attached to the geomembrane with a stiff spring. Figure 3.11 highlights the importance of finding a friction angle for the upper interface which is not to low (slipping for many or all elements will occur) and not to high (too high shear stresses can develop).

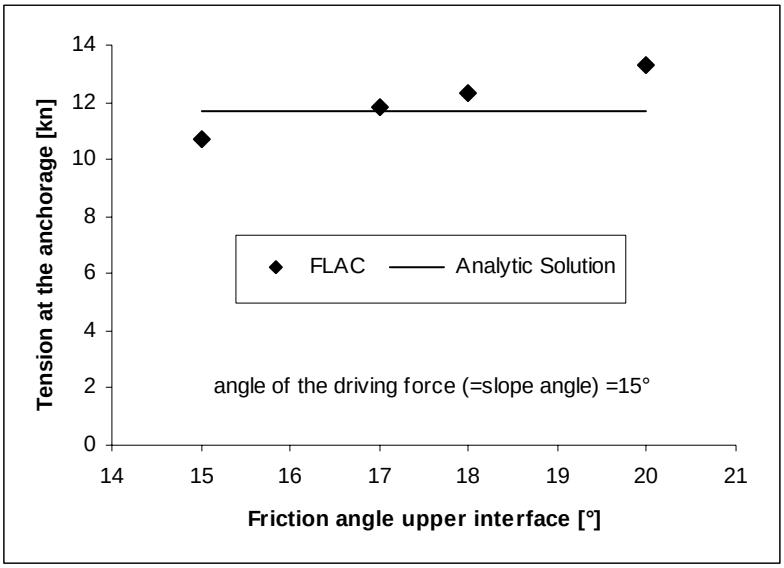

Fig. 3.11: Finding a suitable friction angle for the upper interface

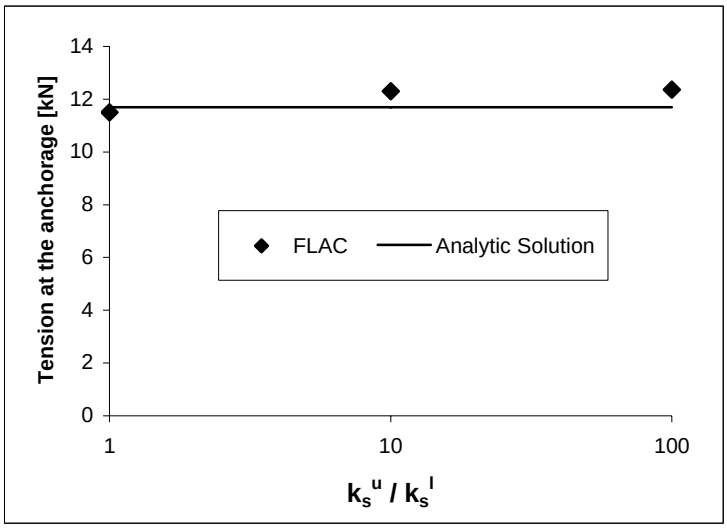

Fig. 3.12: Influence of the shear stiffness ratio of the upper to the lower interface on the tension at the anchorage

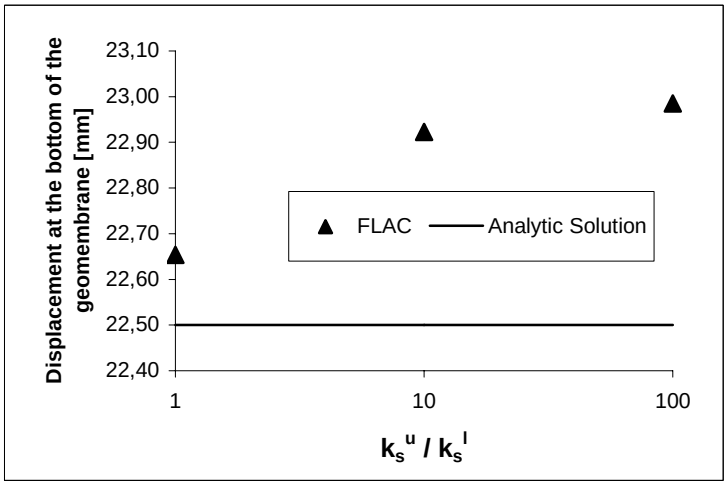

Fig. 3.13 Influence of the shear stiffness ratio of the upper to the lower interface on the displacement at the bottom of the geomembrane

The influence of the ratio of both interface stiffnesses does not disappear fully (Figure 3.12), but is far less significant than for the other model. That this influence is still there has two main reasons. First the shear stresses at the top will always be a little bit higher than for the analytic solution because it is not possible to cut the peak exact at the shear stress level of the analytic solution (Figure 3.14). Trying to do so with a low friction angle leads to slipping for many or all elements of the interface. Second there is always an increase of the normal stress for the last element of the interface. This high normal stress leads directly to a higher limiting shear stress τ_{max}. The reason is again the fixation of the geomembrane at the top which creates a high relative normal displacement between the waste and the geomembrane (Figure 3.15). The effect of a higher stiffness ratio on the displacement at the bottom of the geomembrane is shown in Figure 3.13. The displacement is slightly increasing with a

higher stiffness ratio because the top elements of the upper interface are slipping. To minimize the influence of the interface stiffness on the results, all parametric studies presented in this chapter are performed with equal shear stiffness for both interfaces. Future models could concentrate on modeling the anchorage in a different way. The results might not be directly comparable with the analytic solution, but maybe less sensitive to parametric changes of the interfaces.

As mentioned above it is very important to define a suitable grid to represent the high stress/strain gradient at the top of the geomembrane. If the mash size is too big these effects can not be seen, whereas if the grid is too fine numerical errors might occur (Figure 3.16) and the runtime of the model will increase. These numerical errors might be due to the fact that with decreasing length of the top element, waste and subsoil elements around the anchorage become longer and thinner. Generally it is recommended to avoid thin zones with an aspect ratio greater than 5:1. The optimal length for the top element of the geomembrane is also depending on the stiffness of the interfaces. Therefore, before looking at other parameters, the optimal length was carried out for several different interface stiffnesses.

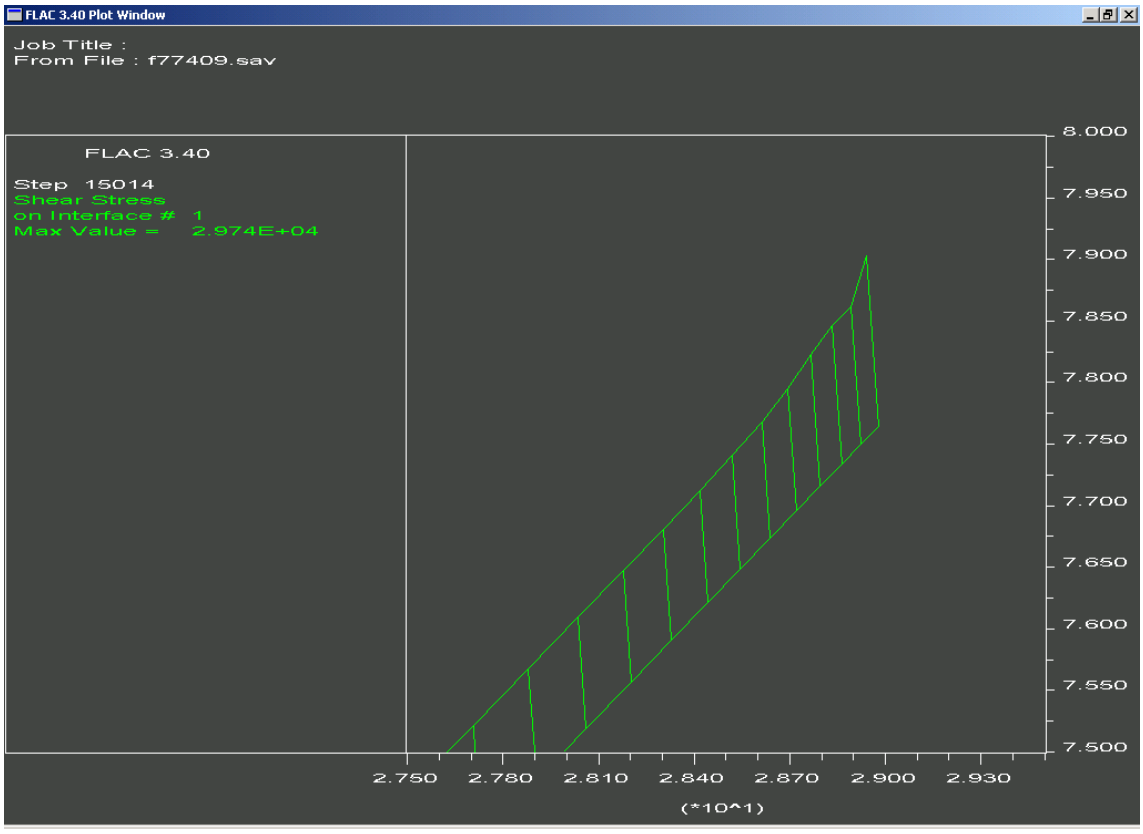

Fig. 3.14: Top of the upper interface - Shear stiffness

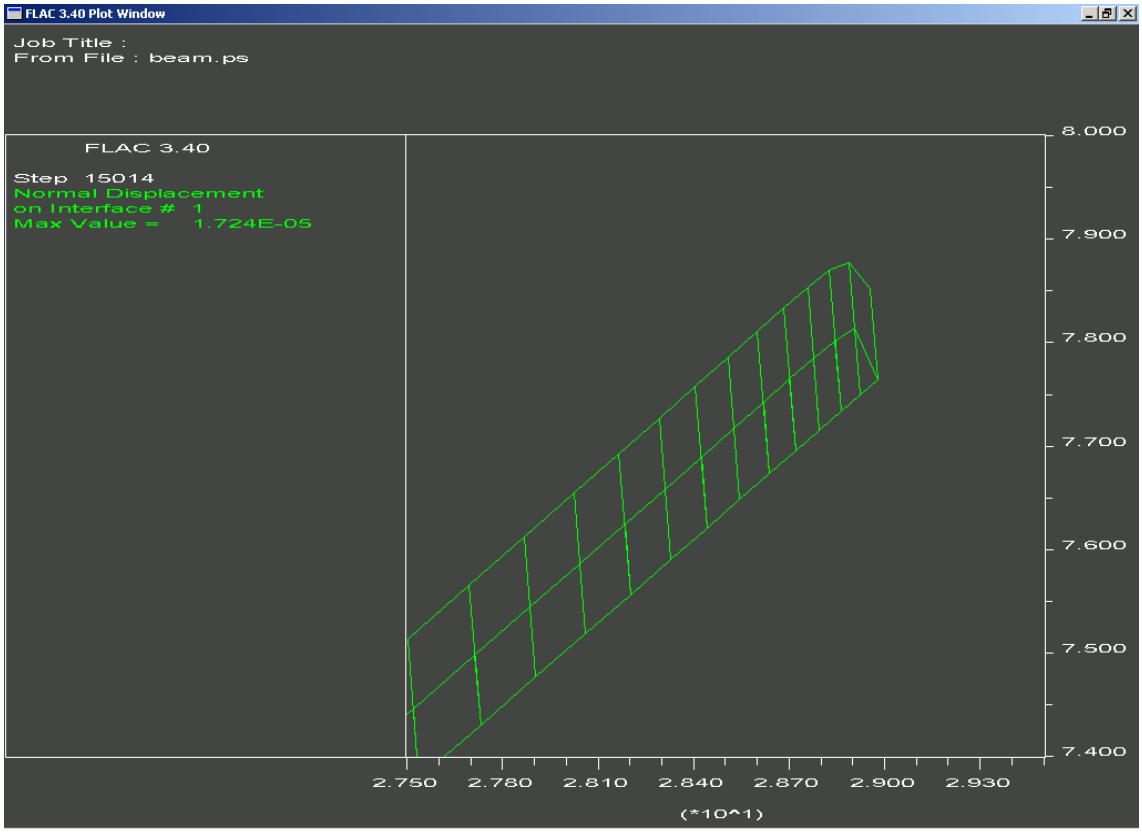

Fig. 3.15: Upper interface – Normal displacement

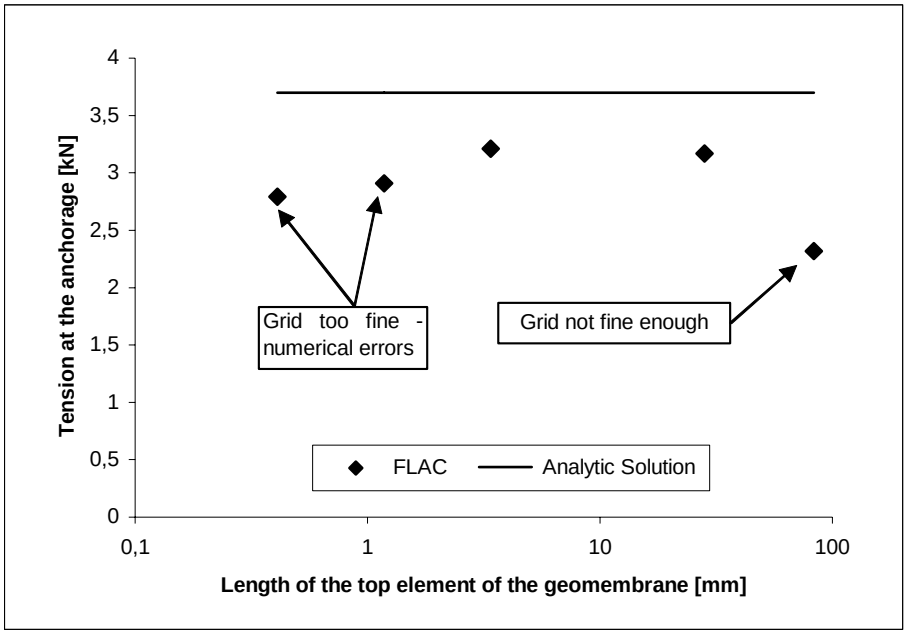

Fig. 3.16: Influence of the grid refinement on the tension at the top of the geomembrane

The next point to look at is the shear modulus G of the waste body. So far all models mentioned above have been run with a shear modulus of 100 MPa to create a rigid waste body with small deformations. Manassero *et al.* (1997) presented values between 0,3 and 5 MPa as realistic boundaries for the stiffness modulus E_S of

municipal solid waste. Depending on the poisons ratio of waste, comparable boundaries for the shear modulus G are 0,1 and 2,5 MPa. Reducing the shear modulus for the FLAC model to these values causes increasing displacements and decreasing tension (Figure 3.17). To get comparable results with the analytic solution a shear modulus of 100 MPa is chosen to run further models, well knowing that this value does not represent real conditions.

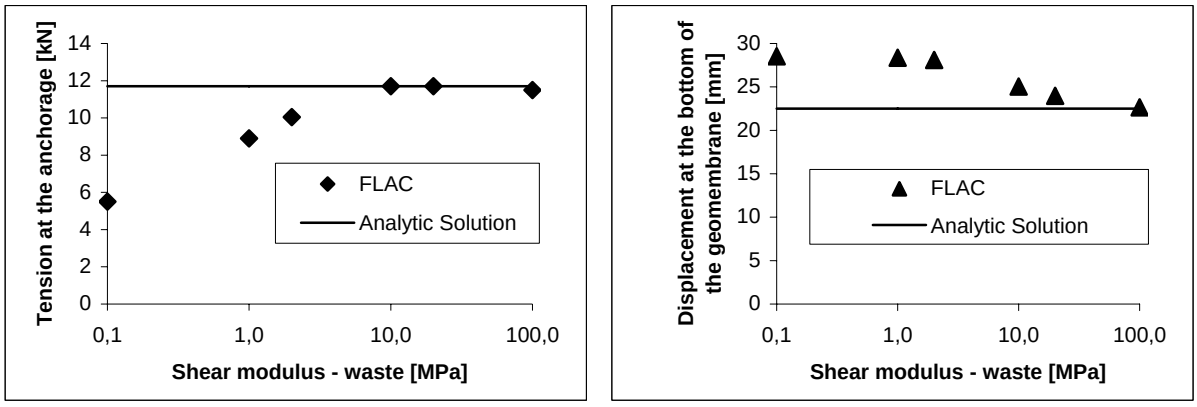

(a) $k_s^l = k_s^u$ = 1e6 Pa/m

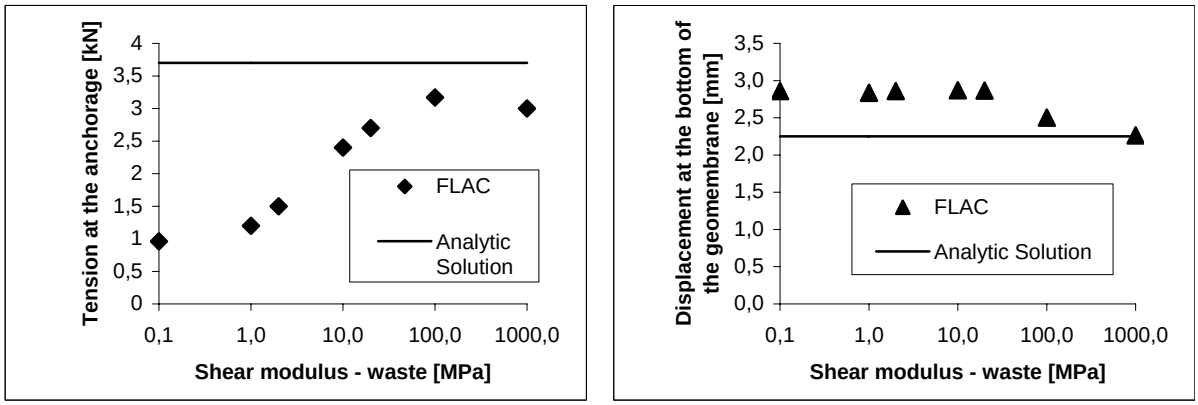

(b) $k_s^l = k_s^u$ = 1e7 Pa/m

Fig. 3.17: Influence of the shear modulus G on the tension at the anchorage and the displacement at the bottom of the geomembrane

The next step is to compare results of this adapted model with the analytic solution. All parameter studies (different slope angle, height of the overburden, unit weight of the waste and length of the slope) are run for both interface being in the elastic state and for k_s-values of 1, 10 and 100 MPa/m. This is done because it is very hard to estimate the shear stiffness of an interface. Results from previous work (Mitchell *et al*., 1990) on this topic have shown values between 10 and 40 MPa/m as characteristic for a HDPE/Clay interface. The influence of the shear stiffness on the

results can be seen in Figure 3.18. For a shear stiffness of 1 MPa/m the results are within a 5% difference to the analytic solution, whereas for stiffer interfaces the results can vary up to 35%. On reason for that might be the shear stress distribution of the upper interface. For softer interface it is nearly constant, thus similar to that of the analytic solution. Stiffer interface show decreasing shear stresses towards the top of the slope (Figure 3.19). A reason for this might be that for a higher interface shear stiffness the waste body is not stiff enough, thus deforming to much to get comparable results with the analytic solution. Consequently the shear modulus G of the waste is increased for cases with high interface shear stiffness. Although the influence on the tension at the anchorage is not very big (difference still up to 25 %), this modification of the model provides satisfying results for the displacement at the free end of the geomembrane (Figure 3.20). The difference for most of the results is less than 5 %. The reason for the difference of the tension is still the decrease of the shear stress at the top of the upper interface. It should be emphasized that the key for getting better results lies around the anchorage of the geomembrane. Due to the fact that most of the stress/strain is concentrated near this point it is very important to get stabile conditions for this area.

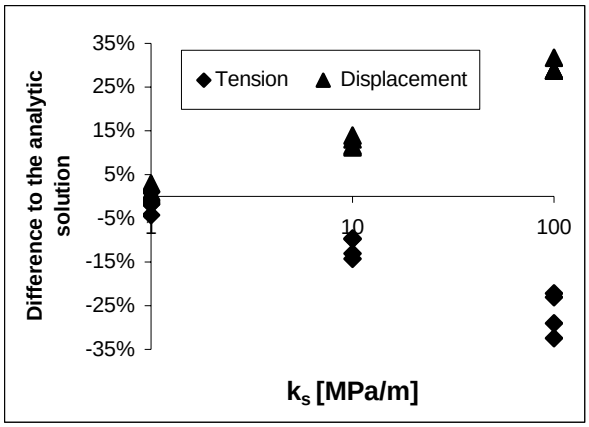

Fig. 3.18: Comparison FLAC – Analytic solution: Influence of the interface shear stiffness

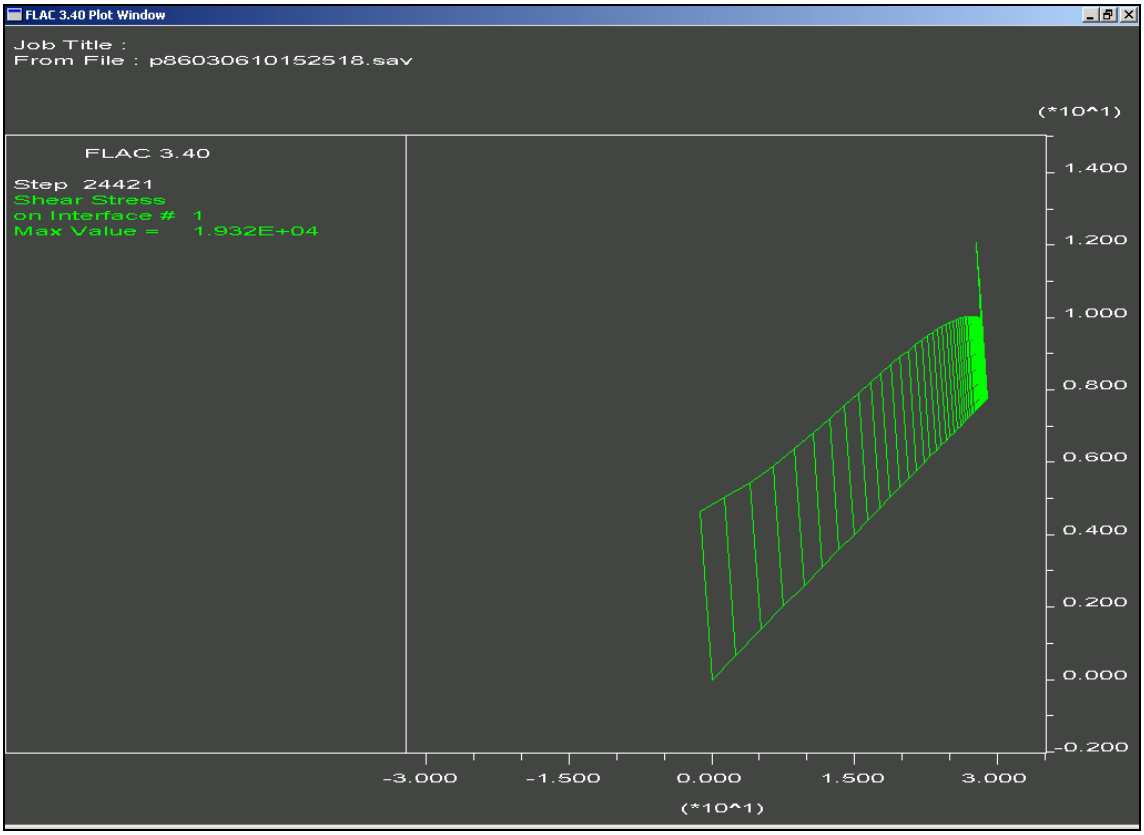

Fig. 3.19: Stiff interface (ks=100MPa/m): Shear stress distribution upper interface

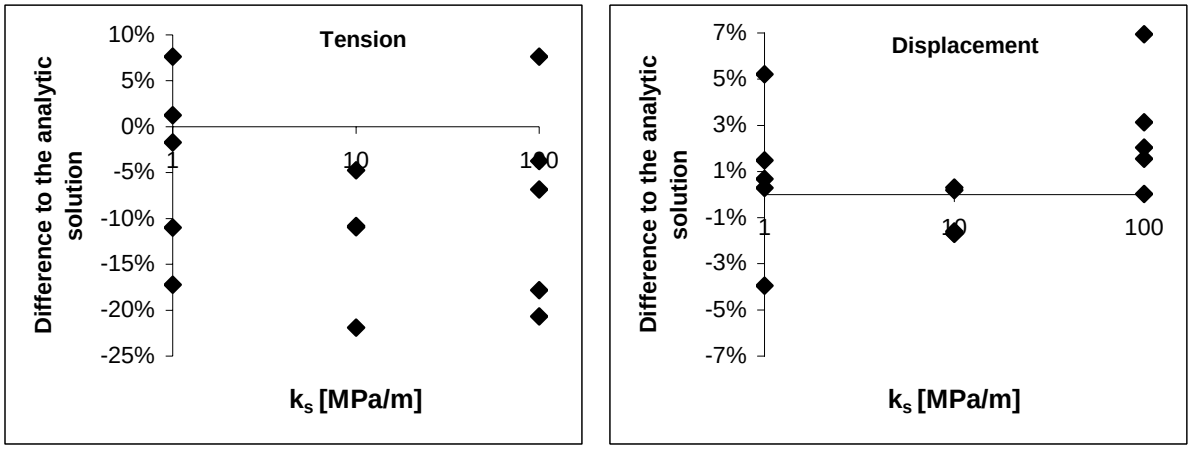

(a) (b)

Fig. 3.20: Comparison FLAC – Analytic solution: Influence of the interface shear stiffness

3.3.4 Example – lower interface in the elastic state

The presented example should on one hand highlight the difficulties still remaining with the numerical model, but on the other hand show that the results determined from the analytic solution and FLAC are, within a certain difference, comparable. Table 3.1 contains the input parameters for this example.

Waste			upper interface			Geomembrane			lower interface			clay		
ϑ	30	°	ϕ_u	33	°	t	0,0015	m	ϕ_l	25	°	G	10	MPa
β	30	°	c_u	0	MPa	E	180	MPa	c_l	1	MPa	D	1	m
L	30	m	η	1					η	1		k_s	10	MPa/m
H	6	m	p_u	0	Pa				p_l	0	Pa			
K_x	0		k_s	10	MPa/m				k_s	10	MPa/m			
γ	15000	N/m³	k_n	10000	MPa/m				k_n	10000	MPa/m			

Tab. 3.1: Example elastic interface behaviour – input parameters

	T_{max} [kn]	u [mm]	τ_u [kPa]
Analytic solution	6,40	3,90	38,97
FLAC	6,27	3,85	38,7 / 33,5 / 85,6 *
Difference [%]	**-2,1%**	**-1,2%**	-
T_{max}...tension at the anchorage			
u [mm]...displacement at the free end of the geomembrane			
τ_u...shear stress upper interface		* average / lowest / highest τ_u	

Tab. 3.2: Example elastic interface behaviour - results

Using high cohesion for the lower interface ensures that it will remain in the elastic state. For the upper interface the cohesion is zero and the friction angle is just a little bit higher than the slope angle to control the shear stresses at the top of the geomembrane.

One of the remaining problems is that it's not possible to get constant shear stresses for the upper interface as in the analytic solution. The shear stress decreases towards the top of the upper interface leading to lower tension in the geomembrane for many cases. For the presented example the shear stress is for most parts of the geomembrane close to the expected value (39 kPa) of the analytic solution (Figure 3.21). The decrease of the shear stress at the top of the upper interface is for this case not significant. This leads to similar results for the maximum tension in the geomembrane for the analytic and the numerical solution (Table 3.2). It should be highlighted again that this decrease is for some other cases the reason for a difference in tension up to 25%. Furthermore there is a peak for the last element of the interface (Figure 3.22), due to high normal stresses which allow a higher shear resistance before the element would start to slip.

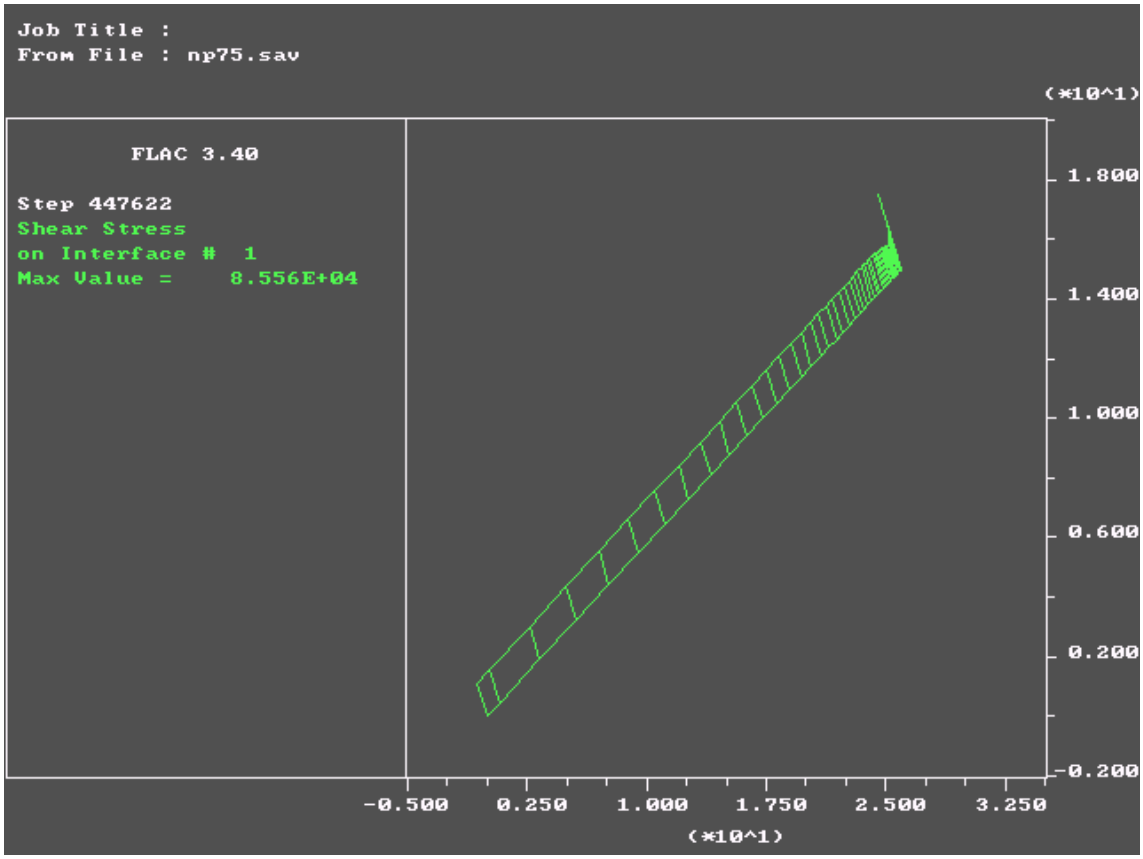

(a)

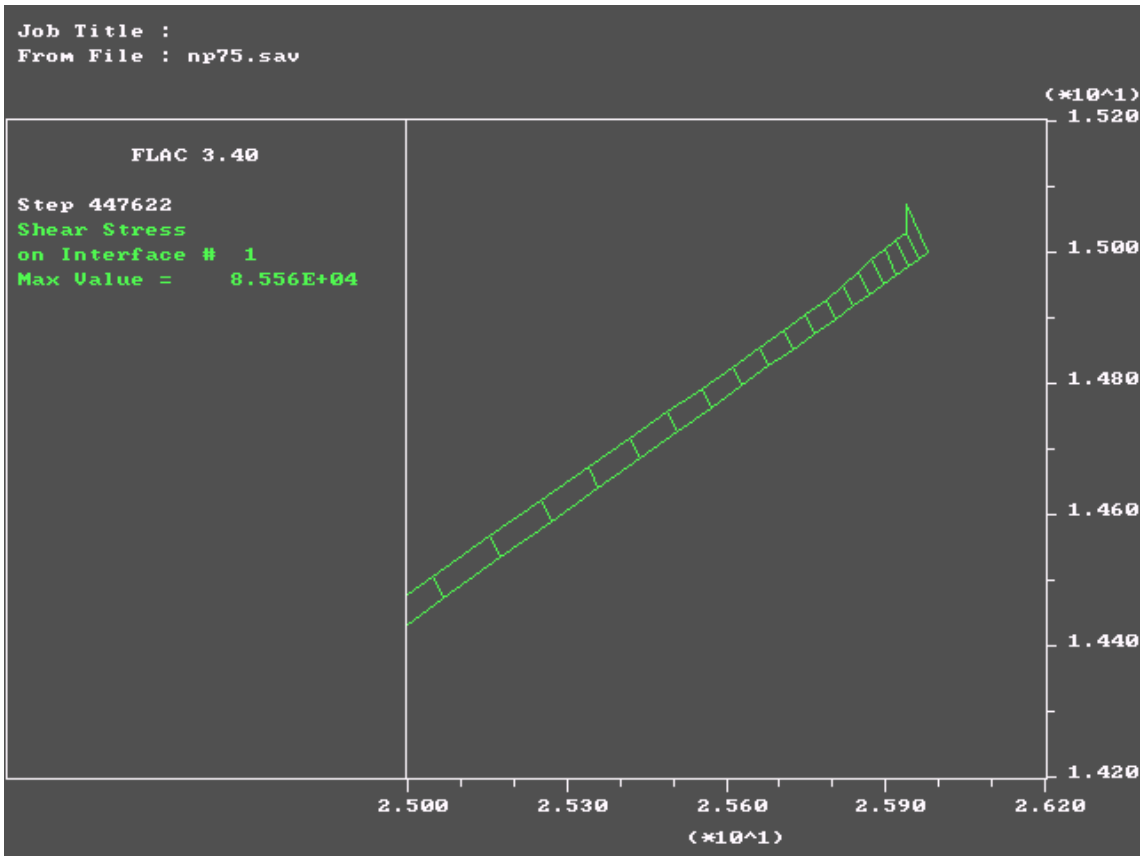

(b) zoom of the top part of (a)

Fig. 3.21: Example elastic interface behaviour – shear stress upper interface

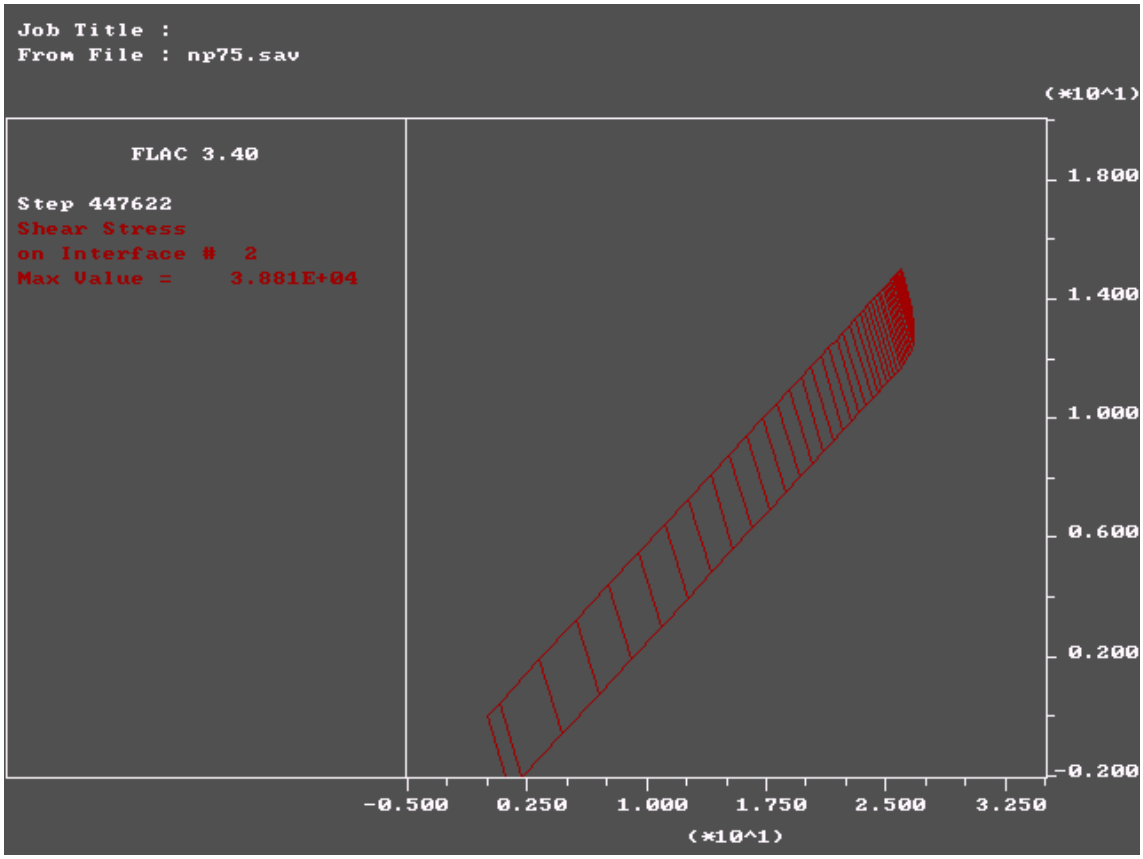

(a)

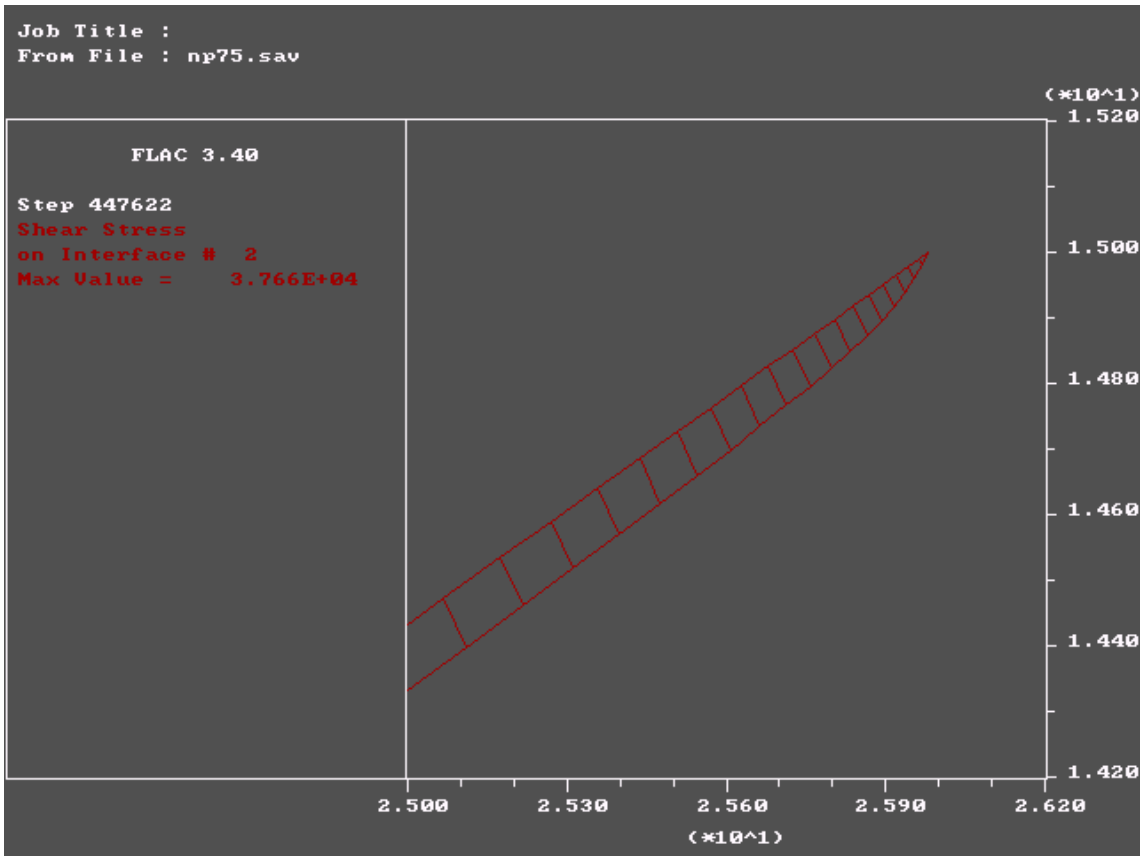

(b) zoom of the top part of (a)

Fig. 3.22: Example elastic interface behaviour – shear stress lower interface

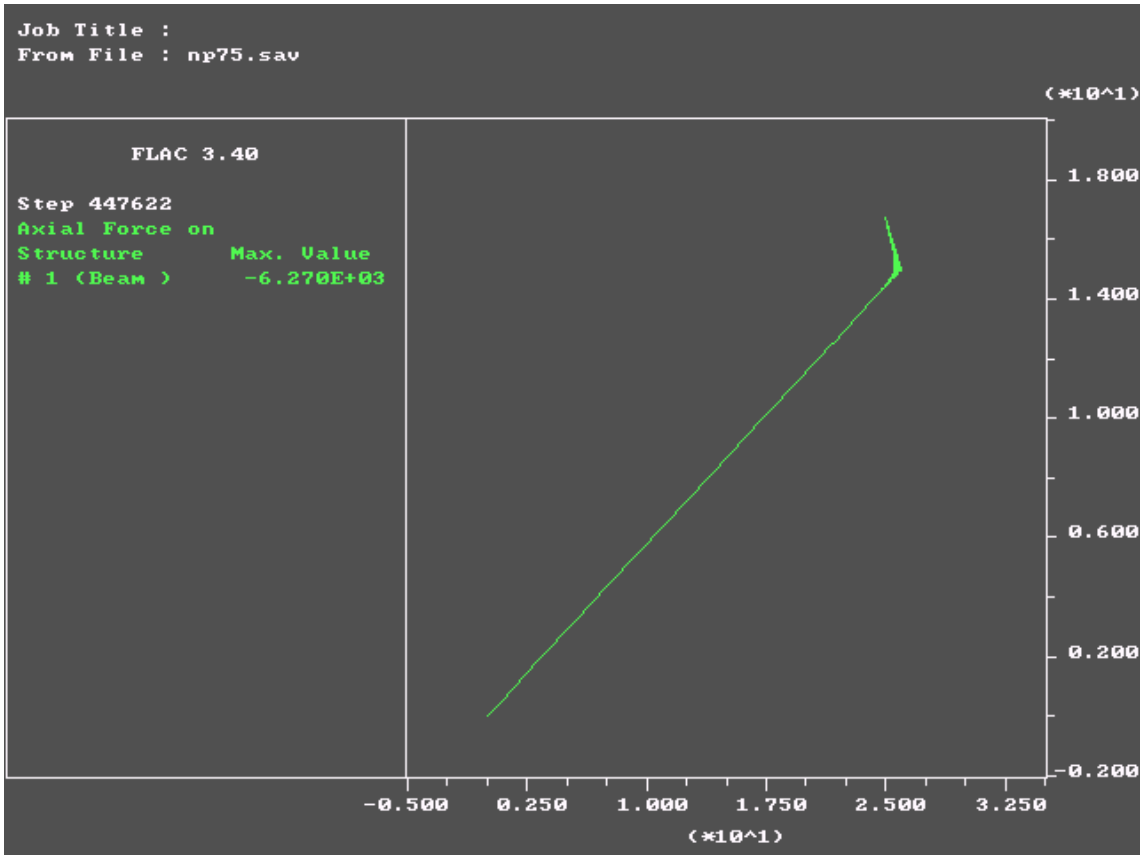

Fig. 3.23: Example elastic interface behaviour – tension along the geomembrane

The shear stress at the lower interface (Figure 3.22) is typical for all cases. The shear stress has for most parts of the interface similar values as for the upper interface and decreases at the top until it is zero at the anchorage of the geomembrane. This is the reason why most of the tension in the geomembrane is, matching with the analytic solution, built up close to anchorage (Figure 3.23).

For this example the results of both solutions are close to each other (Table 3.2). Talking about the displacement this will be the same for most elastic cases, whereas the tension at the anchorage is highly depended on the shear stress distribution on the top of the upper interface. It's not possible to make any assumptions about the influence of certain model parameters on this distribution. Future work could concentrate on getting stabile conditions for the area around the anchorage, which might lead to a better correspondence of the results between both solutions.

3.3.5 Lateral support of the waste body - K_x

On of the main aspect to use Kodikara's simplified analytic solution is to determine earth pressure coefficients K_x that represent field conditions. All work so far presented in this chapter is based on the assumption that there is no lateral support ($K_x = 0$) for the waste body. This is a kind of worst case scenarios. The other boundary for the K_x value is the case with full lateral support at the bottom of the waste body. For this purpose the model was adapted, putting rollers (fixed in x-direction) on the lower side of the waste body (Figure 3.24) which allow the waste to settle but not to move laterally. The results of this model can not be directly compared with the analytic solution, thus it is not possible to back calculate K_x values from the tension and the displacement determined from FLAC. This is due to the following reasons:

- K_x is constant for the analytic solution, whereas it varies along the slope for the numerical model (Figure 3.25). It is not possible to use an average K_x value determined from the numerical solution and compare with a result from the analytic solution using the same K_x. This would overestimate the effect of the lateral support, because as mentioned above most of the stress/strain is introduced into the geomembrane near the anchorage. Therefore the shear stress at the top of the slope, which is dependent on the K_x value at the top, will be the most important parameter for the tension at the anchorage. As shown in Figure 3.25 K_x near the anchorage is much smaller than the average K_x.
- There is no free deformation at the bottom of the geomembrane (Figure 3.26). In the analytic solution the displacement of the waste does not contribute to the results, consequently the geomembrane can deform just because of the applied stress and the interface characteristic of the lower interface. However for this model the geomembrane is hold back by the fixed waste body, thus influencing the deformation of the geomembrane. To get similar results in FLAC the geomembrane should be able to get some compression. In this model the plastic moment for the geomembrane is zero. If the geomembrane gets compression it starts to wrinkle leading to nearly no displacement for the last element of the geomembrane.

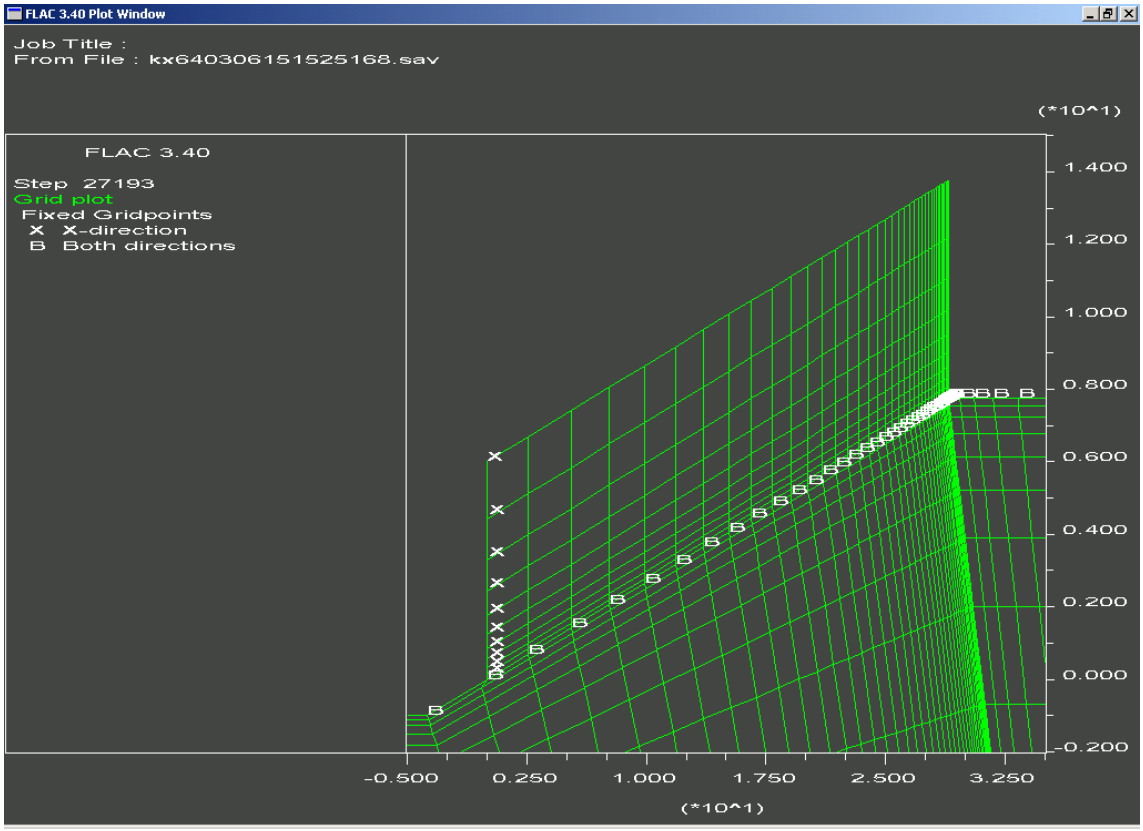

Fig. 3.24: Lateral supported waste – boundary conditions

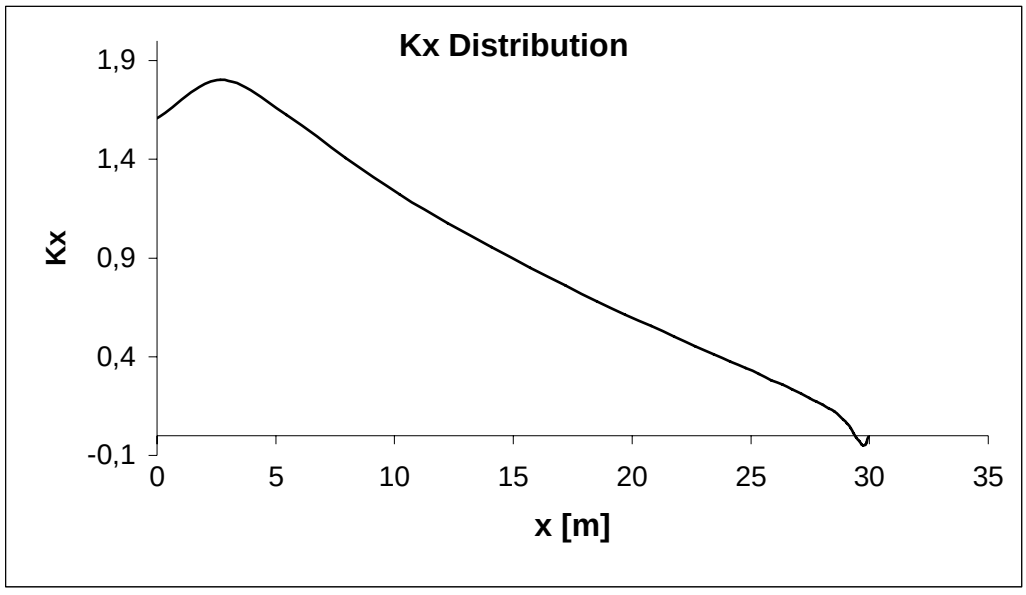

Fig. 3.25: Kx distribution along the slope
x…distance from the bottom of the slope

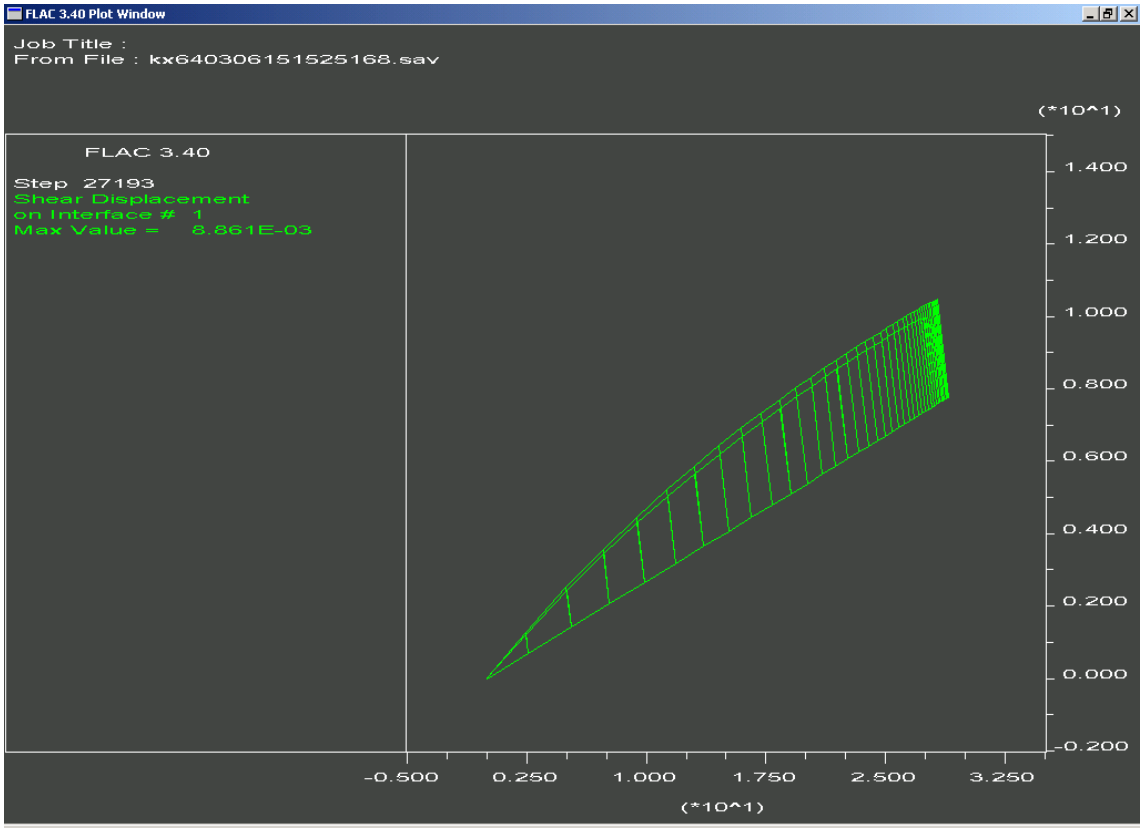

(a)

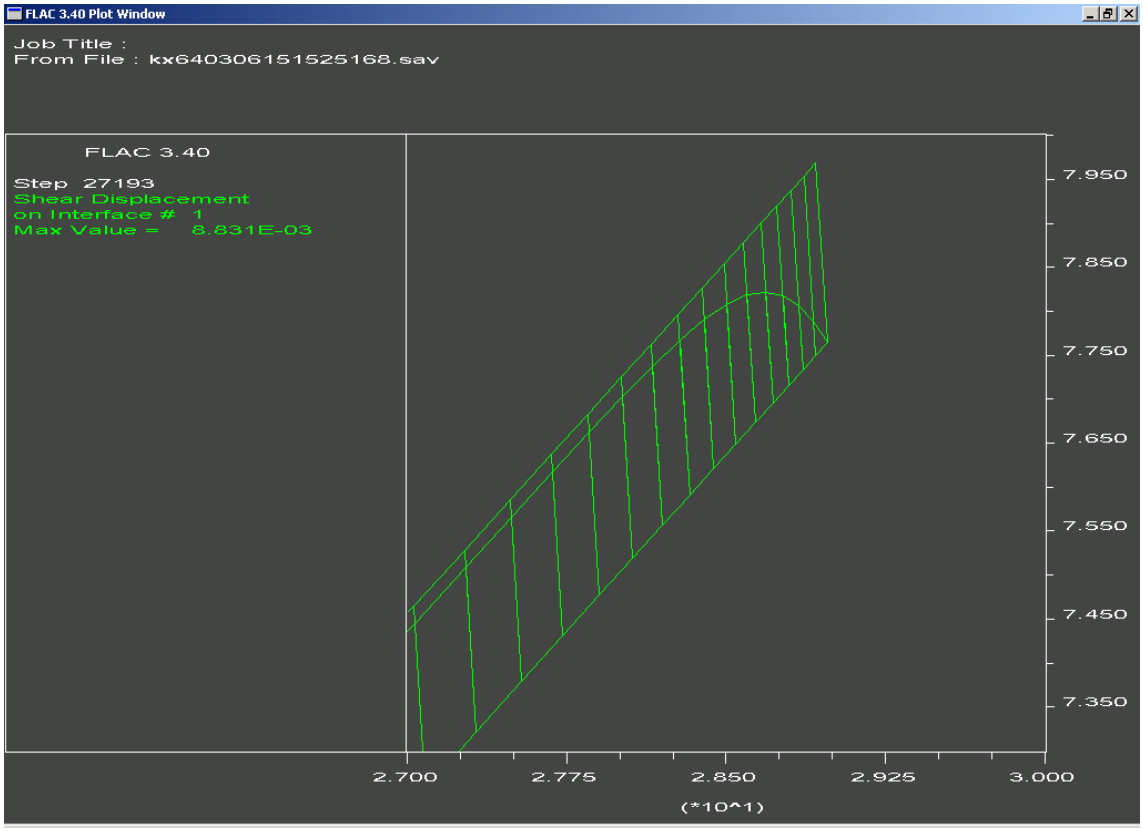

(b) zoom of the top part of (a)

Fig. 3.26: Lateral supported waste – shear displacement upper interface

To evaluate a $K_{x.}$ value for field conditions it might be more suitable to create a numerical model which also includes the bottom of a landfill. Further research could concentrate on finding a correlation between the K_x -distribution of the FLAC model and the K_x value of the analytic solution. Furthermore the analytic solution could be adapted, including a varying K_x along the slope.

3.4 Conclusion

The aim of modelling the analytic solution (Kodikara, 2000) for the tension developed at the anchorage of a geomembrane with FLAC was to analyze and compare the results. Using the analytic instead of the numeric solution to determine the tension at the anchorage of a geomembrane would help to save time and money during the design process.

Several assumptions (e.g.: rigid subsoil, high shear modulus of the waste, limiting the shear resistance of the upper interface, no lateral support of the waste body), that are far away from field conditions for some cases have been made to overcome difficulties during the modelling process. With these assumptions it has been possible to get comparable results between both solutions for the displacement at the bottom and, within a bigger range also for the tension at the top of the geomembrane. Furthermore, the presented model has shown that it is very difficult to model situations where most of the strain/stress develops around a particular point. This sensitivity towards a change of the model and a change of certain parameters should be taken into account for future adaptations of the numerical model.

Future work could concentrate on creating a less sensitive, more stabile FLAC model. A major improvement would a more reliable model with which enables to estimate the earth pressure coefficient (K_x) of the waste body. It might also be necessary to adapt the analytic solution for varying K_x values along the slope. Comparable results between both solutions could lead to a fast and efficient use of the analytic solution for design purposes.

4 Stability of steep cover systems

4.1 Introduction

The stability of a landfill cover is generally analyzed by the limit equilibrium method. This method has been used in geotechnical engineering over a long time, is broadly accepted, easy to use and expresses the stability of the slope in a simple way. The Factor of safety for this kind of analysis is defined as the quotient of the available shear strength and the shear stress required for equilibrium. Within the limit equilibrium method there are two main solutions for analyzing steep veneer slopes. The simplest way of analyzing a slope is to consider an infinite slope configuration (Figure 4.2). For such cases the stability of the systems is just based on soil/interface strength and eventually on an additional reinforcement which reduces the driving forces. This assumption is the most conservative one and can also be regarded as a special case (neglecting the toe buttressing effect) of the two wedge-finite slope analysis. In the two wedge-finite slope analysis the slope is divided into one active wedge which might slip down the slope and a passive wedge at the toe of the slope which acts as an additional support for the whole system (Figure4.1).

A main concern for both methods and generally spoken for the limit equilibrium method is that these solutions do not consider the stress-strain compatibility of the different materials involved in the stabilization of the slope. All materials will develop its design strength at different levels of displacement. For example the interface shear strength and the tension of high modulus reinforcement need little displacement to be developed whereas the toe buttressing effect will occur at lager deformations. It might also be possible that at a certain level of displacement one material has not developed its full design strength whereas another component might be closer to its residual strength than to its peak strength. Consequently all strengths for the different materials should be calculated for a certain displacement and it should never be the case that all force are super positioned without looking at the deformation required for these forces to develop.

Other instruments used during the design process are numerical models and design charts. Analyzing the slope stability with a computer program is more time consuming, hard to model and a good knowledge of the input parameters is required. Furthermore the interpretation of the results is not as easy and as for the limit

equilibrium method. Design charts might be used to get a rough idea about the influence of the different parameters on the stability of the whole system but can never replace detailed stability analysis. Often such charts are carried out for certain geometry and a range of parameters that might not be suitable for the case analyzed by the designer.

This section provides the analytical framework for the stability analysis for an infinite steep veneer cover slope. The influence of slope-parallel, horizontally placed and fiber reinforcement on the factor of safety is shown. Case histories are presented to show successful application and difficulties during the construction process.

4.2 Stability of unreinforced veneers

4.2.1 Introduction

This section will focus on a literature review of the work carried out so far on analyzing unreinforced (and also slope parallel reinforced) veneers. Slope-parallel reinforced (in this paper also referred to as “conventionally” reinforced) covers are included in this part because for most of the papers it is not appropriate to decouple the unreinforced from the reinforced solution. Nearly all papers include the terms for the reinforced part in the analytic solution either from the beginning or present it as an extension of the framework for the unreinforced veneer. The main emphasis is put on two papers presented by Giroud *et al.* (1995b) and Koerner and Soong (1998). The analytical framework presented in this paper will be an extension of the solutions for an infinite slope presented by Zornberg *et al.* (2001).

4.2.2 Literature Review

The limit equilibrium method has been used for slope stability analysis during several decades. The first papers drawing special attention on the stability of landfill side and cover slopes are, to the best of the author’s knowledge, the ones by Giroud and Beech (1989) as well as Koerner and Hwu (1991). More recent work from the same authors published as an extension of these early papers are the papers by Giroud *et al.* (1995 a, b) and Koerner and Soong (1998).

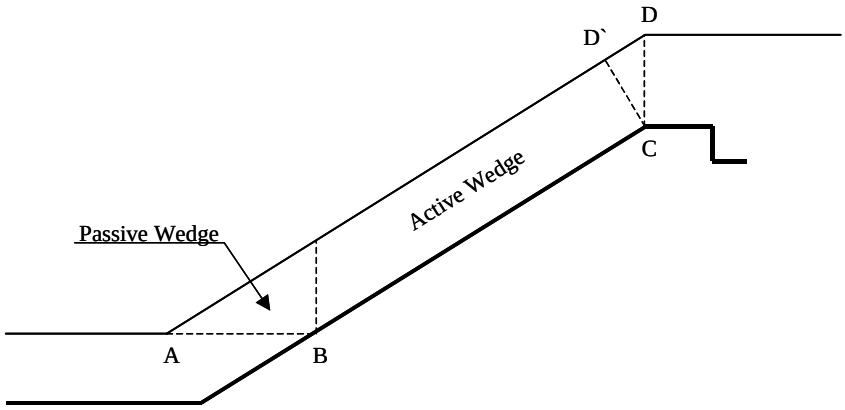

Fig. 4.1: Schematic representation of the geometry for a two wedge finite slope analysis
ABC = slip surface
CD = top border of the cover soil as defined in the analysis by Koerner and Soong (1998)
CD` = top border of the cover soil as defined in the analysis by Giroud *et al*. (1995 b)

The papers by Giroud *et al*. (1995 a, b) are companion papers where the basic one (1995b) contains the analytical framework for a finite slope stability analysis. The companion paper (1995a) determines solutions for the case where seepage is present along the slope. Solutions presented in these papers as well as in the one by Koerner and Soong (1998) are based on the two wedge finite slope analysis (Figure 4.1). However, the results especially from the view of a design engineer are different. The difference in the results is mainly based on the definition of the factor of safety and the fact that Giroud *et al*. (1995b) do not include a factor of safety at the horizontal failure surface (AB). Giroud *et al*. define the factor of safety "as the ratio between the resisting and the driving forces acting on the active wedge as projected on the slope direction". This definition is not consistent with the classical definition of the factor of safety "as the quotient of the available shear strength and the shear stress required for equilibrium", however it might lead to a powerful design instrument for steep veneer slopes. As shown in Table 4.1 the factor of safety for this solution is the sum of five separate terms and it easy for the designer to identify the different mechanisms that help to stabilize the slope, to quantify the relative contribution of each term/parameter to the factor of safety and to see the influence of certain parameters (e.g. slope angle, height, unit weight) on the factor of safety as a whole. Furthermore it is possible to separate the contribution of reliable parameters from the contribution of less reliable parameters. Talking about whether the change of a certain parameter decreases or increases the factor of safety it should be pointed out that an increasing veneer thickness might also increase the slope stability. This might be against the "feeling" of the designer and only relies on the buttressing effect (see

also Druschel and Underwood, 1993) of the soil at the toe of the slope. The designer should take special care about the estimation of this lateral support at the toe of the slope. Factors that can decreases the buttressing effect, include insufficient soil compaction, weakening of the soil due to saturation and the fact the actual deformation of the soil might be less than the deformation required to mobilize the full soil resistance. It should be stated again that designers should consider the contribution of each mechanism/parameter to the slope stability for a definite deformation. Summarizing the individual terms without paying attention on the stress-strain compatibility would result in an overestimation for the factor safety because the different strengths are mobilized at different levels of displacement.

$$FS = \frac{\tan\phi}{\tan\phi_m} = \frac{\tan\delta}{\tan\delta_m} = \frac{c}{c_m} = \frac{a}{a_m} \tag{4.1}$$

where ϕ = internal friction angle of the soil (soil-to-soil), δ = interface friction angle (soil-to-geomembrane), c = soil cohesion and a = adhesion along the soil-to-geomembrane interface.

As a conclusion it may be said that Giroud *et al* (1995b) use an arbitrary definition for the factor of safety and the assumption that the horizontal failing surface (AB) is on the edge of failure (FS = 1) to develop a highly practical equation for analyzing the stability of a finite veneer slope. Furthermore it is shown that the assumptions made by Giroud *et al*. (1995b) represent a good approximation of the more rigorous solution developed by Koerner and Hwu (1991). Koerner and Hwu (1991) do not give an explicit definition of the factor of safety, however, for the unreinforced slope they used the expressions shown in Equation (4.1). The index *m* in Equation (4.1) stands for mobilized values, in other words for the values required for equilibrium which is consistent with the classical definition of the factor of safety (Equation 4.2). For cases of slope-parallel reinforcement this definition is neglected and the factor of safety is calculate separately as the quotient of provided reinforcement strength and required reinforcement stress for equilibrium under the assumption that the factor of safety along all interfaces equals one. Engineers trying to adapt Giroud's solution for cases including forces from construction equipment, seepage and seismic forces should be aware that this might result in a bigger discrepancy between the results of this and other more rigorous (e.g.: Koerner and Soong, 1998) solutions.

Slope	Infinite slope		Additional terms for finite slope		
Mechanism	Interface shear		Toe buttressing		Geosynthetic
Parameter	Interface friction	Interface adhesion	Soil internal friction	Soil cohesion	Geosynthetic tension
Symbol	δ	a	ϕ	c	T
Factor of safety	$\frac{\tan\delta}{\tan\beta}$	$+\frac{a}{\gamma t \sin\beta}$	$+\frac{t}{h}\frac{\tan\phi/(2\sin\beta\cos^2\beta)}{1-\tan\beta\tan\phi}$	$+\frac{c}{\gamma h}\frac{1/(\sin\beta\cos\beta)}{1-\tan\beta\tan\phi}$	$+\frac{T}{\gamma h t}$
$\phi\nearrow$	$\Leftrightarrow$	$\Leftrightarrow$	$\nearrow$	$\nearrow$	$\Leftrightarrow$
$\beta\nearrow$	$\searrow$	$\searrow$	$\searrow$	$\searrow$	$\Leftrightarrow$
$h\nearrow$	$\Leftrightarrow$	$\Leftrightarrow$	$\searrow$	$\searrow$	$\searrow$
$\gamma\nearrow$	$\Leftrightarrow$	$\searrow$	$\Leftrightarrow$	$\searrow$	$\searrow$
$t\nearrow$	$\Leftrightarrow$	$\searrow$	$\nearrow$	$\Leftrightarrow$	$\searrow$

Tab. 4.1: Meaning of the terms of the factor of safety equation and influence of the parameters (adapted from Giroud *et al*., 1995 b)
β = slope angle, γ = unit weight of the soil above the slip surface, t = thickness of the soil layer above the slip surface, h = height of the slope

Koerner and Soong (1998) presented a solution for the two wedge finite slope analysis. They do not define the factor of safety explicit; however their analysis is consistent with the classical definition for the factor of safety. In contrast to Giroud *et al.* (1995 a, b) they do not neglect the factor of safety for the horizontal failure surface (AB). It is assumed that the same factor of safety is required along the horizontal and the inclined (BC) failure plane. The resulting factor of safety is the solution of a quadratic equation, which makes it hard for the design engineer to estimate the influence of certain parameters on the result. The paper also includes the analytical framework for other cases such as forces from construction equipment and seepage, seismic forces as well as the stabilization effects of toe berms, tapered slopes and slope reinforcements.

As a matter of completeness it should be said that there are other papers dealing with veneer stability which provide a general overview on different aspects during the design (e.g.: Alexiew, 1994; Kirschner,1995) and/or construction process (e.g.: Thiel and Stewart, 1993; Punyamurthula and Hawk, 1998) without giving a detailed analytic solution for the slope stability.

4.2.3 Analysis of unreinforced veneers

This section presents an analytical framework for the stability of unreinforced veneers based on the paper by Zornberg *et al.* (2001). An infinite slope configuration is considered for evaluation of stability.

Although different definitions for the factor of safety have been reported for the design of reinforced soil slopes, the definition used in this paper is relative to the shear strength of the soil:

$$FS = \frac{Available\ soil\ shear\ strength}{Soil\ shear\ stress\ required\ \ for\ equilibrium} \tag{4.2}$$

This definition is consistent with conventional limit equilibrium analysis, for which extensive experience has evolved for the analysis of unreinforced slopes. Current design practices for reinforced soil slopes often consider approaches that decouple the soil reinforcement interaction and do not strictly consider the factor of safety defined by Equation (4.2). Such analyses neglect the influence of reinforcement forces on the soil stresses along the potential failure surface and may result in factors of safety significantly different than those calculated using more rigorous approaches.

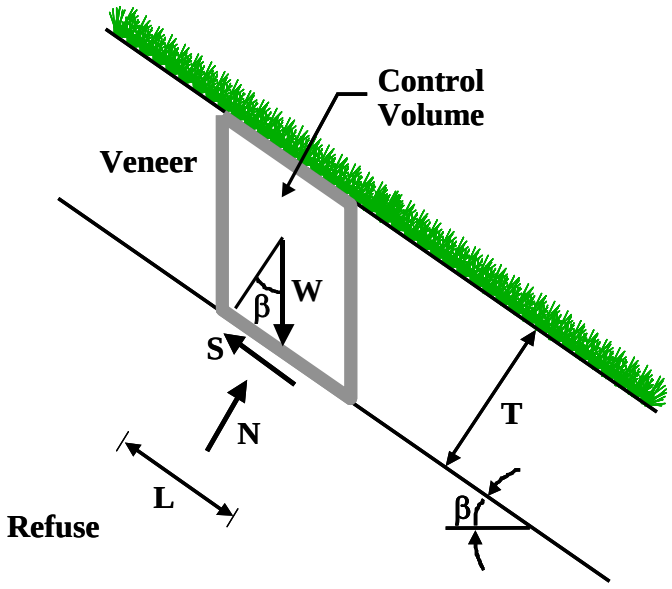

Fig. 4.2: Unreinforced veneer
(from Zornberg *et al*., 2001)

Considering the normal and shear forces acting in a control volume along the veneer slope (or infinite slope), and assuming a Mohr-Coulomb shear strength envelope, Equation (4.2) can be expressed as:

$$FS = \frac{c + (N/L)\tan\phi}{S/L} \tag{4.3}$$

where N = normal force acting on the control volume; S = shear force acting on the control volume; L = length of the control volume; c = soil cohesion; and ϕ = soil friction angle.

In the case of an unreinforced veneer (Figure 4.2), the shear and normal forces required for equilibrium of a control volume can be defined as a function of the weight of this control volume. That is:

$$S = W \sin\beta \tag{4.4}$$

$$N = W \cos\beta \tag{4.5}$$

$$W = \gamma L T \tag{4.6}$$

where W = weight of the control volume; β = slope inclination; T = veneer thickness; and γ = soil total unit weight.

From Equations (4.3), (4.4), (4.5), and (4.6), the classic expression for the factor of safety FS_u of an unreinforced veneer can be obtained:

$$FS_u = \frac{c}{\gamma T \sin\beta} + \frac{\tan\phi}{\tan\beta} \tag{4.7}$$

This factor of safety of the unreinforced slope FS_u will be used to demonstrate the influence of the different ways of slope reinforcement on the veneer stability.

4.3 Stability of slope parallel reinforced veneers

4.3.1 Introduction

Slope reinforcement is used in cases where the shear strength of the soil or the weakest interface is not high enough to provide the necessary resistance for the stability of the veneer. The most common method is to reinforce a steep veneer is to place a reinforcement layer (normally a geogrid) above the potential failure plane and anchor it at the crest of the slope. Other techniques such as horizontally placed reinforcement and fiber reinforcement are more recent developments or still at experimental stage.

This section provides the analytical framework for conventionally reinforced veneers, leading to an equation to calculate the required tensile stress of the reinforcement for a know slope geometry, known interface characteristic and a required target factor of safety. A Case history (Baltz *et al*., 1995) focuses on the possible adjustment of the design during the construction process and on special solutions (e.g.: anchorage around corners) which evolved during the project.

4.3.2 Analysis of slope-parallel reinforced veneers

In the case of a reinforced veneer (Figure 4.3, 4.5, 4.8), the shear and normal forces acting on the control volume are defined not only as a function of the weight of the control volume, but also as a function of the tensile forces that develop within the reinforcements. For analyzing slope-parallel reinforcement a uniformly distributed tensile force per unit length is assumed. In this case, the shear force is defined by:

$$S = W \sin\beta - t_p L \tag{4.8}$$

where t_p = slope-parallel reinforcement tensile stress, which is proportional to the allowable reinforcement tensile strength (T_a) and the slope length (L_T). This can be expressed as follows:

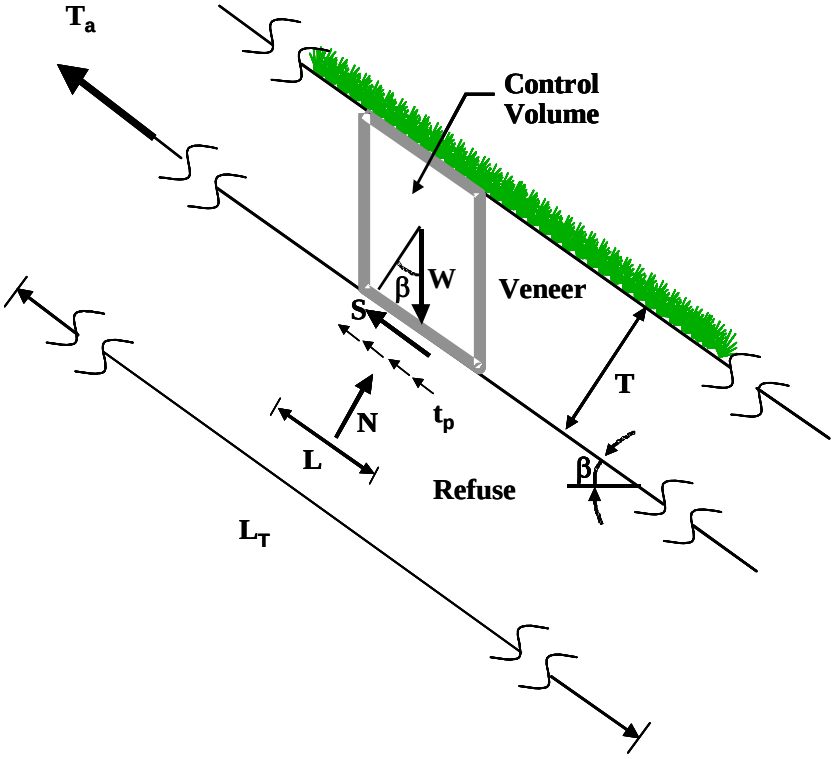

Fig. 4.3: Slope-parallel reinforced veneer

$$t_p = \frac{T_a}{L_T} \tag{4.9}$$

From Equations (4.3), (4.5), (4.6), and (4.8), the following expression can be obtained for the factor of safety $FS_{r,p}$ of a conventionally reinforced veneer:

$$FS_{r,p} = \frac{\dfrac{c}{\gamma\, T\, \sin\beta} + \dfrac{\tan\phi}{\tan\beta}}{1 - \dfrac{t_p}{\gamma\, T \sin\beta}} \tag{4.10}$$

The equation above can be simplified by defining the normalized distributed reinforcement tensile stress $t_p{}^n$ (dimensionless), as follows:

$$t_p{}^n = \frac{t_p}{\gamma\, T} \tag{4.11}$$

Using Equations (4.7) and (4.11) into Equation (4.10) leads to:

$$FS_{r,p} = \frac{FS_u}{1 - t_p{}^n \dfrac{1}{\sin\beta}} \tag{4.12}$$

Equation (4.12) provides a convenient expression for stability evaluation of reinforced veneer slopes. It should be noted that if the distributed reinforcement tensile stress *t* equals zero (i.e. in the case of unreinforced veneers), Equation (4.12) leads to $FS_{r,p} = FS_u$. When the soil cohesion *c* equals zero, Equation (4.10) can be simplified as follows:

$$FS_{r,p} = \frac{\tan\phi}{\tan\beta}\left(\frac{1}{1 - \dfrac{t_p{}^n}{\sin\beta}}\right) \tag{4.13}$$

Reinforcement requirements needed to achieve a target factor of safety FS_r of the reinforced veneer, expressed in terms of the normalized required distributed slope-parallel tensile stress $t_p{}^n{}_{req}$, which can be derived from Equation (4.12):

$$t_p{}^n{}_{req} = \frac{FS_r - FS_u}{FS_r}\sin\beta \tag{4.14}$$

Similarly, reinforcement requirements that are needed to achieve a target factor of safety FS_r , expressed in terms of the required tensile stress $t_{p\ req}$ can be obtained from Equations (4.7), (4.11) and (4.14) as follows:

$$t_{p\,req} = \left(FS_r - \frac{c}{\gamma\, T\, \sin\beta} - \frac{\tan\phi}{\tan\beta}\right)\frac{\gamma\, T \sin\beta}{FS_r} \tag{4.15}$$

Equation (4.15) can be used to assess the reinforcement requirements for a given soil shear strength and veneer configuration (slope inclination and veneer

thickness). For example, Figure 4.4 shows the reinforcement tensile stress required to achieve a factor of safety FS_r =1,5 in a veneer slope where the soil shear strength is characterized by a cohesion c = 5 kPa and a friction angle ϕ = 30°. The figure shows the various combinations of veneer thickness and veneer slope inclination that satisfy the design criterion.

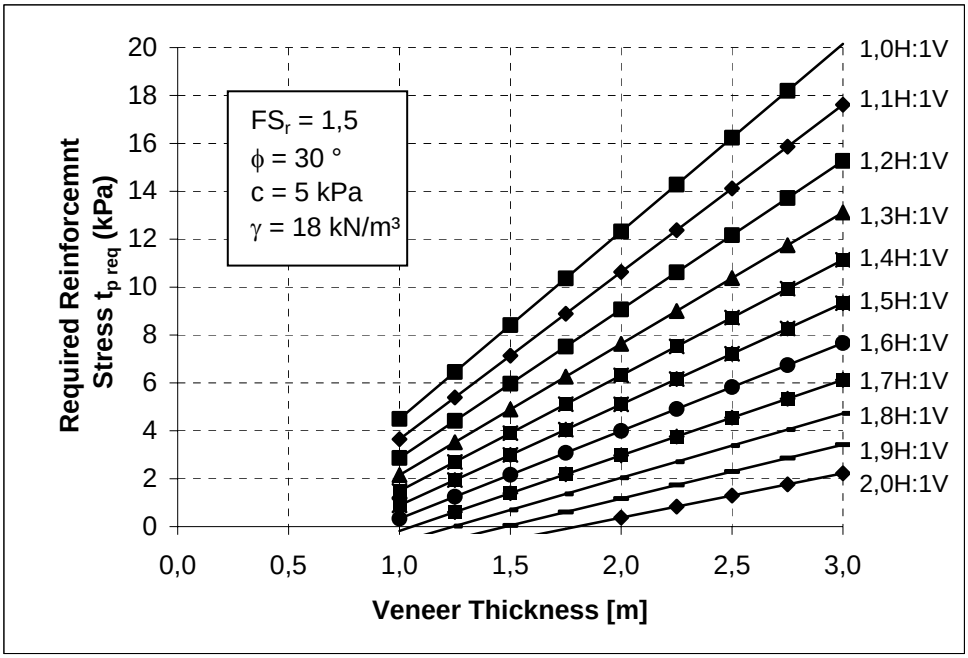

Fig. 4.4: Reinforcement requirements for a slope-parallel reinforced veneer

4.3.3 Case history: remediation of a superfund landfill

As part of remediation work of a superfund landfill site a reinforced cover was constructed. A general site description is given in Table 4.2. The first phase of the construction work included flattening the slopes to an maximum steepness of 3:1 (H:V). Stability analysis showed that the slopes were still too steep to reach the required factor of safety (1,5) without reinforcement. Placing a geogrid directly above the geomembrane provided this additional support to the cover system. The applicability of this solution (placing the geogrid directly on the geomembrane) was verified by the results of direct shear and pullout tests. Prior to the construction of the whole cover system a test strip was installed which allowed optimizations for the construction process of the chosen cover design (Table 4.3).

Site description			
General		**Reinforced veneer slope**	
Project:	Remediation of a superfund landfill site	Slope steepness:	3:1 (H:V)
Location:	New Jersey	Maximum length of the reinforced slope:	30 m
Landfill area:	11,7 ha	Installed geogrids:	29.300 m²

Tab. 4.2: Remediation of a superfund landfill – side description (adapted from Baltz *et al*., 1995)

The major challenge in the construction of the cap was the anchorage of the geogrid at the top of the slope. Because of the proximity of the geogrid to the geomembrane in the thin cover it was not possible to construct an anchor trench. Anchoring the geogrid directly, with a runout length, into the flat top plane of the cover system was considered as an appropriate solution. It should be noted that not geogrid pullout, but the block of soil above the geogrid sliding on the geomembrane was determined as the critical failure mode. Due to fact that the required runout length of the reinforcement was proportional to the slope length the final anchorage length of each panel was determined on site during the construction process. Another problem related to the anchorage arose because of the L-shaped geometry of the landfill. Around the corners of the slope the anchorage elements had to be placed above each other. To compensate for the decreasing resistance of each anchorage panel, because it was not fully encapsulated with soil, the length of each panel was extended with the bottom panel to be the longest. Concerns about how much resistance would develop between two geogrids were overcome by evaluating geogrid to geogrid interface characteristics. Finally detailed panel layouts were provided for each corner.

Final Cover Design (Slope)	
Topsoil:	0,15 m
Common fill:	0,46 m
Drainage layer	Geocomposite drainage net
Reinforcement layer:	PET geogrid
Barrier layer:	0,75 mm PVC geomembrane
Foundation layer:	0,6 m natural clay
Gas collection layer:	Geonet
Total thickness:	1,3 m

Tab. 4.3: Remediation of a superfund landfill – final cover design (adapted from Baltz *et al*., 1995)

Other cases histories about conventionally reinforced cover systems are presented in the papers by Alexiew and Sobolewski (1997), Fox (1993) and Martin and Simac (1995). Martin and Simac (1995) reported the construction of reinforced

cover on a 168 meter long slope. Because any discontinuity of the reinforcement could cause a failure of the system a special method was designed to connect the geogrid panels. Two adhesive impregnated non-woven geotextiles were placed under and above the geogrid overlap. Heating the geotextiles formed a good bond between the two layers and ensured a tight connection of the reinforcement.

4.4 Stability of horizontal reinforced veneers

4.4.1 Introduction

The design concept for this type of reinforcement is to support the slope with horizontally placed, uniaxial reinforcements which are anchored in a underlying strong mass of solid waste or soil. This method was developed to have an alternative for long, steep veneers for which a conventional slope parallel reinforcement might not be suitable. The reinforcement acts as an additional horizontal force, decreasing the driving forces acting on the slope. Zornberg *et al.* (2001) presented a limit equilibrium based analysis of the reinforced slope which can be used to design the reinforcement elements. They also showed a successful application of this new reinforcement technique. In southern California reinforced veneers were constructed as landfill covers on slopes as steep as 1,5 horizontal to 1 vertical and up to a maximum reinforced height of 55 meters. Reinforcing the slope with horizontally placed geogrids was considered to be an appropriate cover because this system could fulfill all design criteria (percolation control, resistance against erosion, static and seismic stability) and was cost efficient. This Section will concentrate on the analytic expressions derived to analyze the reinforced slope and the case history presented by Zornberg *et al.* (2001).

4.4.2 Analysis of horizontally reinforced veneer slopes

For the purpose of the analyses of a horizontally reinforced slope, the reinforcement tensile forces are assumed horizontal and represented by a distributed reinforcement tensile stress t_h, which corresponds to a uniformly distributed tensile force per unit *height*. For a given slope with layers of reinforcement t_h can be expressed through:

$$t_h = \frac{T_a}{s} \tag{4.16}$$

where T_a = allowable tensile strength of the reinforcement and s = vertical spacing between the layers (Figure 4.5).

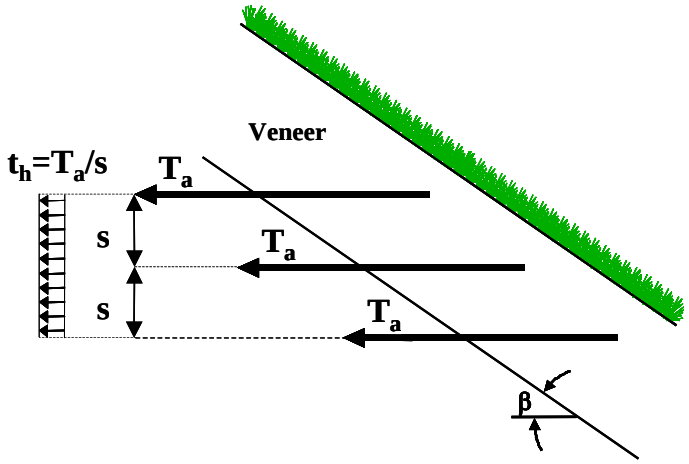

Fig. 4.5: Uniformly distributed tensile stress per unit height

In this case, the shear and normal forces needed for equilibrium of a control volume are defined by:

$$S = W \sin\beta - t_h H \cos\beta \tag{4.17}$$

$$N = W \cos\beta + t_h H \sin\beta \tag{4.18}$$

$$H = L \sin\beta \tag{4.19}$$

where H = vertical component of the length of the control volume (Figure4.6).

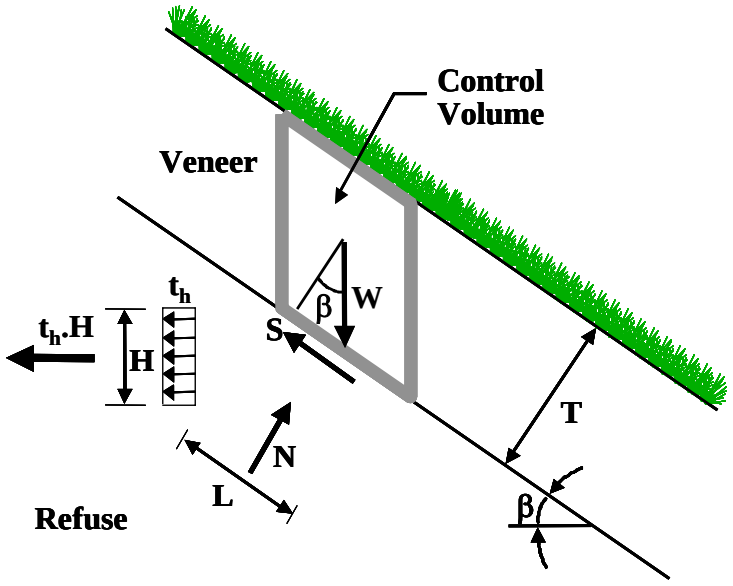

Fig. 4.6: Horizontally reinforced veneer
(adapted from Zornberg *et al*., 2001)

Using (4.3), (4.6), (4.17), (4.18), and (4.19), results in a factor of safety $FS_{r,h}$ of a horizontally reinforced veneer:

$$FS_{r,h} = \frac{\frac{c}{\gamma\, T \sin\beta} + \frac{\tan\phi}{\tan\beta} + \frac{t_h}{\gamma\, T} \sin\beta \tan\phi}{1 - \frac{t_h}{\gamma\, T}\cos\beta} \tag{4.20}$$

Using the normalized distributed reinforcement tensile stress t_h^n (dimensionless) defined by Equation (4.21):

$$t_h^{\,n} = \frac{t_h}{\gamma\, T} \tag{4.21}$$

and Equation (4.7) into Equation (4.20) leads to:

$$FS_{r,h} = \frac{FS_u + t_h^{\,n} \sin\beta \tan\phi}{1 - t_h^{\,n} \cos\beta} \tag{4.22}$$

Equation (4.22) can be simplified, for cases where the soil cohesion *c* equals zero, as follows:

$$FS_{r,h} = \frac{\tan\phi}{\tan\beta}\left(\frac{1 + t_h^{\,n} \tan\beta \sin\beta}{1 - t_h^{\,n} \cos\beta}\right) \tag{4.23}$$

Similar to the analytic framework shown in section 4.3.2 this leads, for a target factor of safety FS_r, to a normalized required distributed horizontal tensile stress $t_h^{\,n}{}_{req}$:

$$t_{h\,req}^{n} = \frac{FS_r - FS_u}{FS_r + \tan\beta \tan\phi} \frac{1}{\cos\beta} \tag{4.24}$$

The required tensile stress $t_{h\ req}$ can be obtained from Equations (4.7), (4.21) and (4.24) as follows:

$$t_{h\ req} = \frac{FS_r - \frac{c}{\gamma\, T \sin\beta} - \frac{\tan\phi}{\tan\beta}}{FS_r + \tan\beta \tan\phi} \frac{\gamma\, T}{\cos\beta} \tag{4.25}$$

Figure 4.7 shows possible combinations of slope inclination, veneer thickness and distributed tensile stress to achieve a target factor of safety FS_r = 1,5 for the given input parameters.

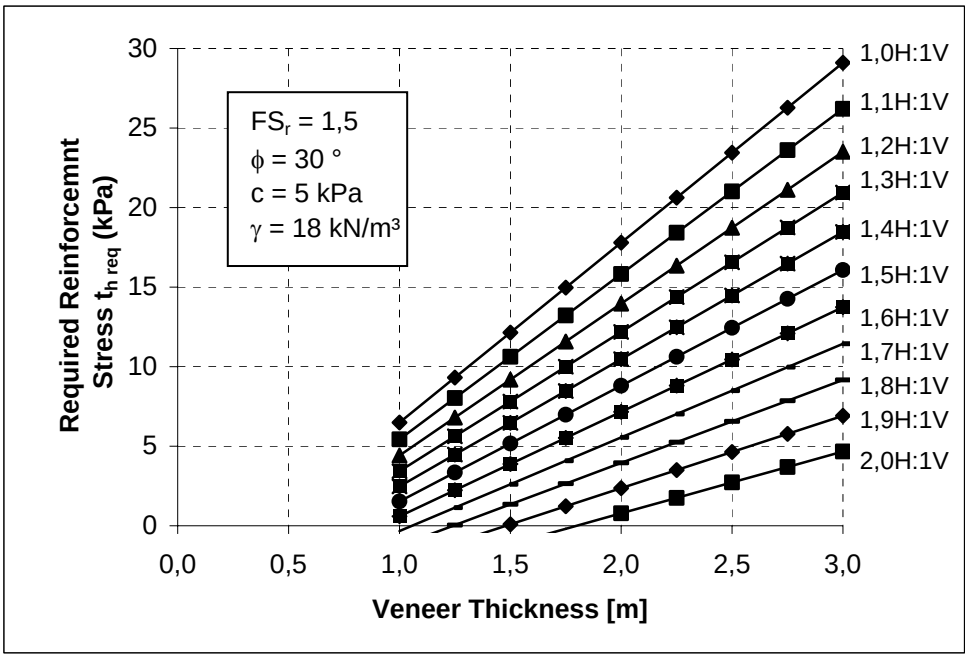

Fig. 4.7: Reinforcement requirements for a horizontally reinforced veneer (adapted from Zornberg *et al*., 2001)

4.4.3 Case history: geosynthetic-reinforced veneer slope for a hazardous landfill

A reinforced veneer was constructed as part of the final closure of the Operating Industries, Inc. (OII) landfill. This case history highlights the final closure of a hazardous landfill where the severe site constrains were overcome by designing and constructing an alternative final cover incorporating horizontal geosynthetic veneer reinforcement. An overview of the site description and the reinforced veneer slope is given in Table 4.4.

Operating Industries, Inc. (OII) Landfill (California)			
Site description		**Reinforced veneer slope**	
Waste composition:	Municipal, industrial, liquid and hazardous wastes	Location:	North slope
		Slope steepness:	Up to 1,5:1 (h:v)
Volume of stored waste:	30 million m³	Veneer thickness:	1,8 m
Area of Parcel	60 ha	Total volume of cover soil:	500.000 m³
Area of refuse prism	50 ha	Installed geogrids:	170.000 m²
Hight of refuse prism	35 – 65 m	Maxi. height of the reinforced slope:	55 m
Area of flat top deck	15 ha	Construction time:	1 year

Tab. 4.4: Operating Industries, Inc. (OII) Landfill – Site description (adapted from Zornberg *et al*., 2001)

After evaluating various alternatives an evapotranspirative constructed in a monolithic fashion (monocover), and incorporating geogrids reinforcement for veneer stability was selected as appropriate for the North Slope of the landfill. This design

concept made it possible to overcome several difficulties due to the steepness and the height of the slope and to fulfill all design requirements. The slope was to steep to construct any kind of layered cover system, particular a cover incorporating geosynthetic components (geomembranes or GCLs). Furthermore the height of the slope and the lack of space at the toe, made it unfeasible to change the geometry of the slope or to construct lateral support elements at the toe of the slope. The selected 1,8 meter thick evapotranspirative monocover (Table 4.5) had additional advantages over traditional layered cover systems, including superior long-term percolation performance in arid climates, ability to accommodate long-long term settlements, construct ability, and ease of long-term operations and maintenance.

Besides the static and seismic stability the cover had to be, in terms of percolation, hydraulically equivalent or better than a prescriptive cover and it was also necessary protect the slope against erosion. It was possible to demonstrate the hydraulically equivalence of the evapotranspirative cover to the prescriptive cover by modeling the percolation through both covers. Furthermore an extensive laboratory test program was carried out to characterize on-site and imported cover soils. All these aspects and results of the analytical framework for the slope stability discussed in section 4.4.2 led to the final design shown in Figure 4.8 and Table 4.5.

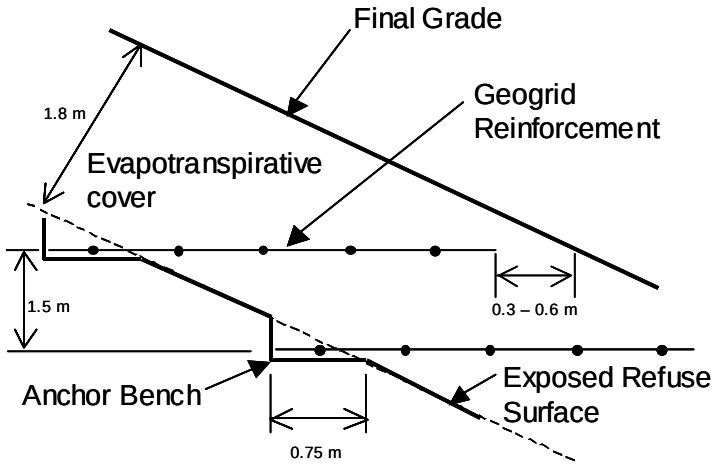

Fig. 4.8: Operating Industries, Inc. (OII) Landfill – Typical veneer reinforcement detail (from Zornberg *et al*., 2001)

The construction process started with stripping and screening of the existing non-engineered cover. The cover was then filled in horizontal lifts starting at the base of the landfill. Reaching the level where a horizontal reinforcement had to be placed the anchor bench was excavated and the pre-cut geogrids where placed with an 150 mm overlap (in the direction of the scraper traffic) on the rough surface of the

underlying fill, but not attached to it. This placement method was considered to be the least disruptive to the geogrids panels and to ensure a good bonding between the panels and the soil. It was possible to finish construction work with this technically new and economically feasible design concept within 12 months.

Final Design

Soil	
- Vegetation to promote evapotranspiration and provide erosion protection - 1,2 m-thick evapotranspirative soil layer to provide moisture retention, minimize downward migration of moisture and provide a viable zone for root growth - foundation layer consisting of soil and refuse of variable thickness Total thickness: 1,8 m	
Reinforcement	
Material:	Polypropylene uniaxial geogrids
Vertical Spacing:	1,5 m for slopes steeper than 1,8:1 3 m for slopes between 2:1 and 1,8:1
Horizontal distance to the final surface:	0,3-0,6 m to permit surface construction, operation and maintenance without the risk of exposing or snagging the geogrid
Minimum embedment depth:	0,75 m

Tab. 4.5: Operating Industries, Inc. (OII) Landfill – Final design
(adapted from Zornberg *et al*., 2001)

4.5 Stability of fiber-reinforced veneers

4.5.1 Introduction

In application involving slope stabilization, either fiber reinforcement or planar reinforcement can be used to increase the factor of safety. A promising potential application for the use of fiber-reinforcement to enhance veneer stability is the area of landfill engineering. Advantages of fiber-reinforcement over planer reinforcement especially for landfill covers include:

- Randomly distributed fibers maintain strength isotropy and do not support the development of potential planes of weakness that can develop parallel to planer reinforcement elements.
- No anchorage into the component material below the veneer (horizontally-placed reinforcement) or at the crest of the slope (slope-parallel reinforcement) is required.
- The tension developed by the fibers within the soil-fiber composite can often provide additional strength *at low confining pressures* as required for thin veneers.

- Beside the stabilising functions fibers mixed into cover soil may also mitigate the potential for crack development, provide erosion control and facilitate vegetation development.

Until recently fiber-reinforced soil has been characterized as a single homogenized material, the performance of which has been characterized by laboratory testing of composite fiber-reinforced soil specimen. This composite approach with its need of testing soil composite specimen has been probably the major drawback in the implementation of fiber-reinforcement in soil stabilization projects. To overcome this disadvantage a discrete approach which characterizes the fiber-reinforced soil as a two-component (fibers and soil) material was developed by Zornberg (2000). The methodology proposed for stability analysis of fiber-reinforced soil slopes is generic and treats the fibers as discrete reinforcing elements which contribute to stability by developing tensile stresses. The main conclusions derived from this paper, with regard to the design of veneer slopes, are:

- The reinforced mass is characterized by the mechanical properties of individual fibers and of the soil matrix instead of the mechanical properties of the fiber-reinforced composite material
- A critical confining pressure at which the govering mode of failure changes from fiber pullout to fiber breakage can be defined using the individual fiber and soil matrix properties.
- The fiber-induced distributed tension is a function of the fiber content, the fiber aspect ratio, and the interface shear strength of individual fibers if the governing mode of failure is by fiber pullout.
- The fiber-induced distributed tension is a function of the fiber content and the ultimate tensile strength of individual fibers if the governing mode of failure is by fiber breakage.
- The discrete framework can be implemented into an infinite slope limit equilibrium framework. Convenient expressions can be obtained to estimate directly the required fiber content to achieve a target factor of safety.

The design methodology for fiber-reinforced soil structures using a discrete approach is consistent with current design guidelines for the use of continuous planar reinforcements and with the actual soil improvement mechanisms. Consequently, with the advantages of this new discrete design approach and the advantages over

continuous planer reinforcement mentioned above, fiber-reinforced cover systems could become a economical and technically feasible alternative to “conventionally” reinforced veneer slopes.

4.5.2 Analysis of fiber-reinforced veneer slopes

The analytical framework presented in this section is based on the paper by Zornberg (2000) and is consistent with the solutions presented in this chapter for the stability of an infinite slope. Further information about the discrete approach for fiber-reinforced soil including detailed explanation of the variables used to calculate the fiber-induced distributed tension can also be obtained from Zornberg (2000).

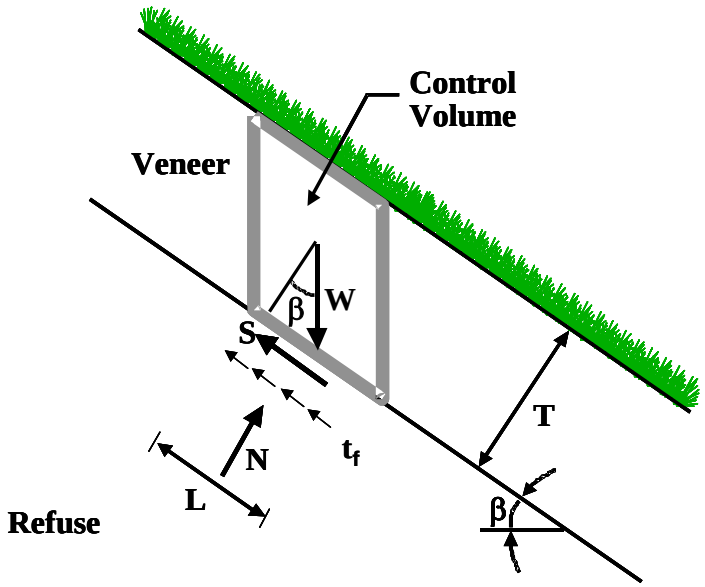

Fig. 4.9: Fiber-reinforced veneer

Figure 4.9 shows a schematic view of a fiber-reinforced infinite soil veneer. The empirical coefficient α that accounts for the effect of the direction of t_f is included in the analytical framework for completeness, even though α is equal to unity if the orientation of the fiber-induced distributed tension t_f is parallel to the failure surface as assumed herein.

As briefly discussed in the introduction of this section, the behavior of the fiber-reinforced soil mass depends on whether the failure mode is governed by fibers pullout or by fibers breakage. The governing mode behavior of the fiber-reinforced soil mass depends on the magnitude of the critical normal stress, $\sigma_{n,crit}$, which should be compared to the magnitude of the normal stress σ_n at the base of the veneer.

If $\sigma_n < \sigma_{n,crit}$, the dominant mode of failure is the fibers pullout. This will be the case for all cover system applications. Using the analytical framework presented by Zornberg (2000) the fiber-induced distributed tension t_f is defined by:

$$t_f = \eta \chi c_{i,c} c + \eta \chi c_{i,\phi} \tan\phi \sigma_n \quad (426)$$

where $c_{i,c}$ and $c_{i,\phi}$ are the interaction coefficients for the cohesive and frictional components of the interface shear strength; η = aspect ratio of the individual fibers, χ = volumetric fiber content and

$$\sigma_n = \frac{N}{L} \quad (4.27)$$

the normal stress at the base of the veneer Using the Equations (4.5),(4.6),(4.26) and (4.27) leads to:

$$t_f = \eta \chi c_{i,c} c + \eta \chi c_{i,\phi} \tan\phi \gamma T \cos\beta \quad (4.28)$$

Similarly, if $\sigma_n > \sigma_{n,crit}$, the dominant mode of failure is fibers breakage. Even though this will not be the governing mode of failure for cover slopes the solution for this case is presented for completeness. The fiber-induced distributed tension t_f is defined by:

$$t_t = \sigma_{f,ult} \cdot \chi \quad (4.29)$$

where $\sigma_{f,ult}$ = ultimate tensile strength of the individual fiber.

Using

$$S = W \sin\beta - \alpha t_f L \quad (4.30)$$

for the shear force needed for equilibrium of a control volume and Equations (4.5) and (4.6) into (4.3) leads to:

$$FS_{r,f} = \frac{\frac{c}{\gamma T \sin\beta} + \frac{\tan\phi}{\tan\beta}}{1 - \frac{\alpha t_f}{\gamma T \sin\beta}} \quad (4.31)$$

Defining the normalized distributed reinforcement tensile stress t_f^n (dimensionless) of a fiber-reinforced slope as follows:

$$t_f^n = \frac{t_f}{\gamma T} \quad (4.32)$$

and using Equations (4.7) and (4.32) into Equation (4.31) leads to:

$$FS_{r,f} = \frac{FS_u}{1 - \alpha\, t_f^{\,n}\, \dfrac{1}{\sin\beta}} \tag{4.33}$$

The fiber-induced normalized distributed tension $t_f^n{}_{req}$ required in a generic infinite slope with a given soil shear strength in order to achieve the target factor of safety FS_r can be obtained using Equation (4.33) as follows:

$$t_f^{\,n}{}_{req} = \frac{FS_r - FS_u}{\alpha\, FS_r} \sin\beta \tag{4.34}$$

The required tensile stress $t_{f\,req}$ can be obtained from Equations (4.7), (4.32) and (4.34) as follows:

$$t_{f\,req} = \left(FS_r - \frac{c}{\gamma\, T\, \sin\beta} - \frac{\tan\phi}{\tan\beta} \right) \frac{\gamma\, T \sin\beta}{\alpha\, FS_r} \tag{4.35}$$

If $\sigma_n < \sigma_{n,crit}$ by using Equations (4.28) and (4.35) a convenient expression can be obtained to define the fiber content, $\chi_{req,1}$, required to satisfy a target factor of safety FS_r by:

$$\chi_{req,1} = \frac{FS_r - \left(\dfrac{c}{\gamma T \sin\beta} + \dfrac{\tan\phi}{\tan\beta} \right)}{\alpha \cdot FS_r \cdot \eta \left(c_{i,c} \dfrac{c}{\gamma T \sin\beta} + c_{i,\phi} \dfrac{\tan\phi}{\tan\beta} \right)} \tag{4.36}$$

It can be seen that less reinforcement is required if longer and thinner fibers (aspect ratio η) are used and the soil-fiber interface friction (interaction coefficients $c_{i,c}$, $c_{i,\phi}$) is high.

For the case of $\sigma_n > \sigma_{n,crit}$ the required fiber content, $\chi_{req,2}$, to stabilize a fiber-reinforced slope is given by:

$$\chi_{req,2} = \frac{\gamma T \sin\beta}{\alpha \cdot FS_r \cdot \sigma_{f,ult}} \left(FS_r - \frac{c}{\gamma T \sin\beta} - \frac{\tan\phi}{\tan\beta} \right) \tag{4.37}$$

Figures 4.10 and 4.11 show the influence of the veneer thickness and the aspect ratio of the fibers on the required (volumetric) fiber contents for cases where $\sigma_n < \sigma_{n,crit}$. It can be observed that the required fiber content tends to an asymptotic value for high veneer thicknesses. In fact, from inspection of Equation (4.36), the required fiber content is independent of the veneer thickness if the soil veneer has zero cohesion (or it is assumed to be zero). Talking about the influence of the aspect ratio it can be seen that that the required fiber content decreases for fibers with

higher aspect ratios. As can be inferred from inspection of Equation (4.36), the required fiber content is indirect proportional to the aspect ratio of the fibers.

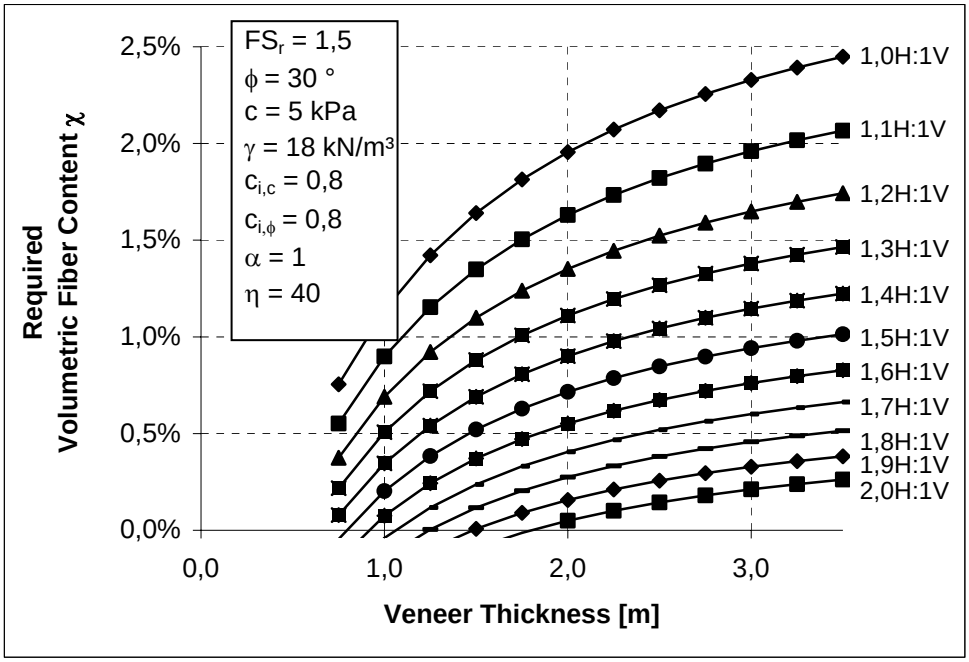

Fig. 4.10: Reinforcement Requirements for a fiber-reinforced slope as a function of the veneer thickness

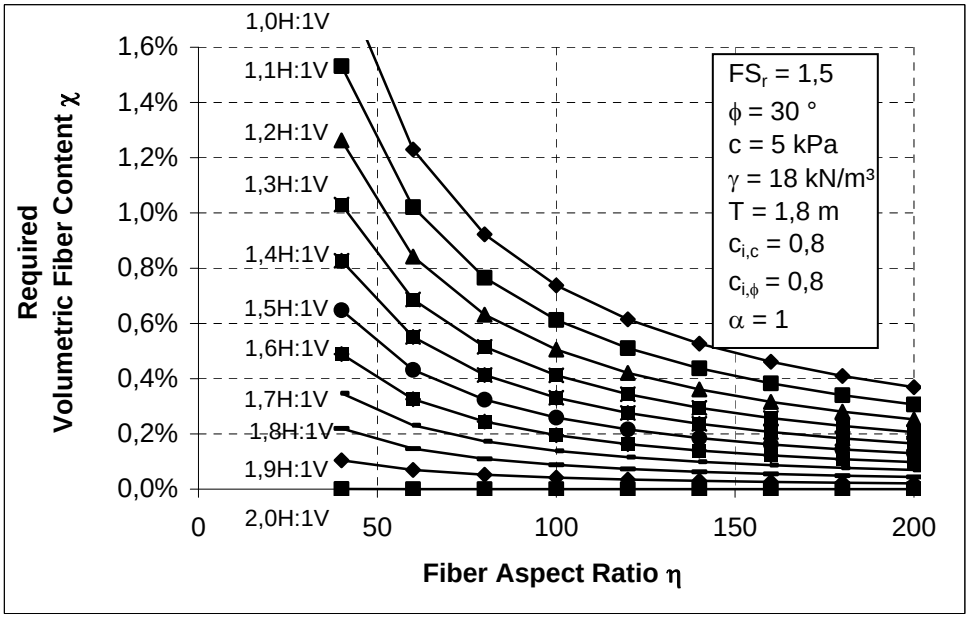

Fig. 4.11: Reinforcement Requirements for a fiber-reinforced slope as a function of the fiber aspect ratio η

4.6 Geosynthetic based design concepts for additional slope stability

The reinforcement methods presented above help to stabilize a slope as a whole. In many cases it's applicable to consider other design concepts to support this

structural reinforcement or even substitute it. Many Case histories have shown successful applications of additional veneer support to overcome obstacles due to the special situation of these projects.

Cargill and Olen (1998) presented a case history of the Town of Babylon Landfill in New York. Geogrid reinforced soil slope modules were constructed at the bottom of the steeper slopes. This module based system was considered the most applicable solution because it made it possible to overcome restriction on waste regarding, which would be necessary to construct a conventional final cover. Each module consisted of a uniaxial HDPE geogrid as primary reinforcement and a biaxial HDPE geogrid as a secondary reinforcement. The secondary reinforcement was used to wrap the slope face for erosion protection and to provide support to a zone of topsoil within a seeded erosion control mat until vegetation could be established. The spacing of the primary reinforcement (0,46 m up to 1,37 m) was depended on the steepness of the modules(1H:2V, 1H:1,5V or 1H:1V), whereas the secondary reinforcement was placed in layers of 0,46 m to provide a continuous face of the slope. Each module was 6,1 m high and a top bench width of 6,1 m was chosen to have enough space for a drainage swale and for construction and maintenance equipment. With the flexible arrangement of the modules it was possible to construct a slope geometry which came close to the one of the existing slope leading to a minimum of required excavation and additional backfill behind the reinforced soil structures. Approximately 4300 m of these modules were established providing the required support to the lower parts of the cover system. The elevation at the most critical slope was 36 meters above the surface of the surrounding terrain.

Another concept is to ad a toe buttress at the bottom of the slope. Compared to the toe buttress effect only developing due to the passive wedge of the veneer slope these reinforced soil structures can be considered as more reliable structural support elements. In most cases these structures have the additional benefit of flattening the cover slopes above the toe buttress. Zornberg and Kavazanjian Jr. (1998) report a case where a 460 meter long and 4,6 meter high toe buttress was constructed to support slopes which were up to 37 meters high and as steep as 1,3H:1V. Due to the fact that the front of the reinforced slope was founded on concrete piles and the back part was above the existing waste body the main focus of this paper was put on the differential settlements of the structure and its effects on the strain development within the reinforcement. Another case history was presented

by Daly and McKelvey III (1999). Twelve pits containing highly acid organic compounds and oil-based drilling mud had to be covered and surrounded by a vertical cut-off wall. The required maximum steepness for cover stability and space limitation made it, in some parts of the site, impossible to key the cover system directly into the vertical barrier. A soldier pile wall was constructed at the toe of the slope to create the required space for the construction equipment needed to install the cut-off wall. After the installation of the cut-off wall the geomembrane panels of the cover system were placed over the soldier pile wall and keyed into the vertical barrier. The construction was completed with a geogrid reinforced soil structure, acting as a lateral support at the toe of the slope.

Cover System Design	
Protection Layer:	0,6 m Vegetative Cover Soil
Drainage Layer:	Geocomposite
Barrier Layer:	1 mm Geomembrane
Barrier Layer:	GCL
Barrier Layer:	0,5 mm Geomembrane
Gas Collection Layer	0,15 m Sand
Reinforced Foundation Layer:	0,15 m HDPE Reinforced Geocells Geotextile (for construction purpose only)
Unreinforced Foundation Layer:	0,15 m Sand

Tab. 4.6: Geocell reinforced cover system over a drilling mud filled pit (adapted from Daly and McKelvey, 1999)

This case history also involved the use of geocells to increase the stability of final cover systems. Over pits with a high percentage of drilling mud a light-weight cover system (Table 4.6) had to be constructed to minimize the settlements and to address possible bearing capacity problems. Reinforcing the foundation layer with three-dimensional geocells provided the needed support for the cover system. The main advantage of geocells is that they work on confinement and not on friction as conventional planer reinforcement does. Consequently special attention should be drawn to the compaction of the soil within the cells to guarantee sufficient confinement of the soil mass. This lateral confinement helps to increase the slope stability in two ways. First the shear strength of the cellular reinforced soil layer is increased due to additional lateral pressures. This can be expressed as apparent cohesion in the Mohr-Coulomb failure envelope (Figure 4.12; Bathurst and Karpurapu, 1993). Second the bearing capacity of the whole system is increased because of the following three mechanisms (see also Figure 4.13):

- The load transferred to the underlying soil mass is reduced because, depending on the relative soil-geocell displacement along the walls of the geocell, shear stresses which act against the loading will develop.
- The geocell reinforcement transfers the loading to deeper depths, thus the system is behaving like embedded foundations, which have higher bearing capacities than surfaces foundations.
- The three dimensional geocell mattress will act similar to a beam or hammock, helping to distribute the load and transferring parts of the load to the sides of the reinforcement (Dash *et al*., 2001)

Another reason why geocells were considered as appropriate solution to stabilize the cover of the drilling mud filled pits was that reinforcement effects would develop without initial displacements as needed for planar reinforcement. These displacements would not been available because of the thin cover system design.

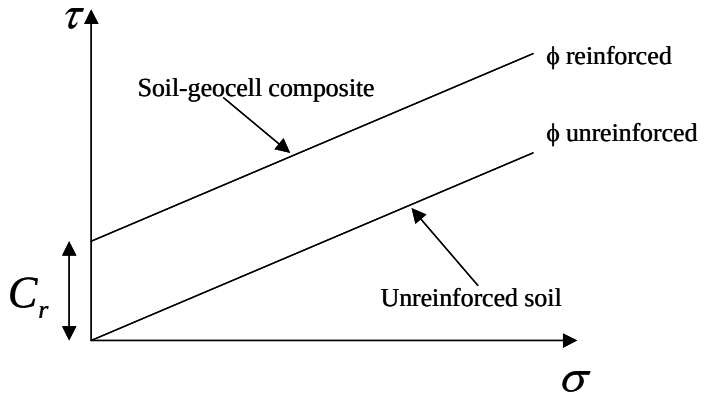

Fig. 4.12: Mohr-Coulomb failure envelope for unreinforced soil and soil-geocell composite (adapted from Bathurst and Karpurapu,1993)
C_r = apparent cohesion

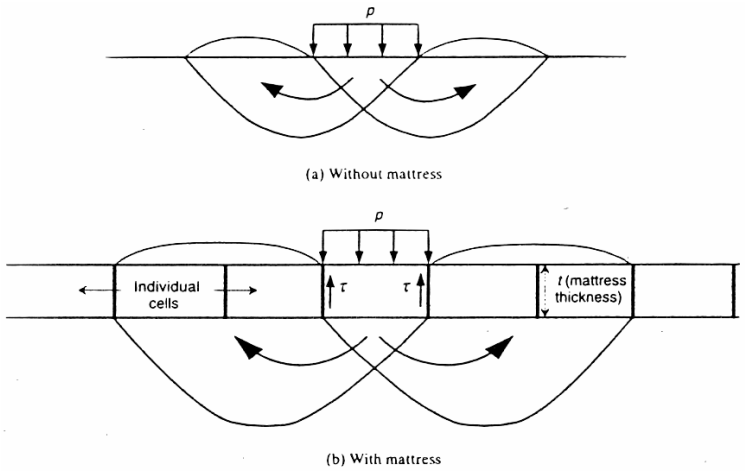

Fig. 4.13:Influence of geocell reinforcement on the bearing capacity (from Koerner,1998)

4.7 Conclusions

A framework is provided for the design of steep landfill cover slopes. The analytical solutions derived herein are based on the infinite slope analysis with a consistent definition of the factor of safety as "*as the quotient of the available shear strength and the shear stress required for equilibrium*". Solutions are presented for the case of unreinforced, slope-parallel, horizontally and fiber-reinforced veneers.

Factor of Safety						
Definition				Influence on the factor of safety compared to FS_u		
				t^n↗	β↗	ϕ↗
Unreinforced veneer:	$FS_u = \frac{c}{\gamma\, T\, \sin\beta} + \frac{\tan\phi}{\tan\beta}$					
Slope-parallel reinforced veneer:	$FS_{r,p} = \frac{FS_u}{1 - t_p{}^n \frac{1}{\sin\beta}}$	with	$t_p{}^n = \frac{t_p}{\gamma\, T}$	↗	↘	↔
Horizontally reinforced veneer:	$FS_{r,h} = \frac{FS_u + t_h{}^n \sin\beta \tan\phi}{1 - t_h{}^n \cos\beta}$	with	$t_h{}^n = \frac{t_h}{\gamma\, T}$	↗	?	↗
Fiber-reinforced veneer:	$FS_{r,f} = \frac{FS_u}{1 - \alpha\, t_f{}^n \frac{1}{\sin\beta}}$	with	$t_f^n = \frac{t_f}{\gamma\, T}$	↗	↘	↔

Tab. 4.7: Influence of slope-parallel, horizontally placed and fiber-reinforcement on the factor of safety of a infinite veneer slope
t_p = distributed tensile stress per unit length of a slope-parallel reinforced veneer
t_h = distributed tensile stress per unit ***height*** of a horizontally reinforced veneer
t_f = distributed tensile stress per unit length of a fiber-reinforced veneer
↗ ...increasing, ↔…no influence, ↘…decreasing, ?…either increasing or decreasing

Table 4.7 shows, for each case, expressions for the factor of safety and the influence of some parameters on the factor of safety compared to the unreinforced slope. It can be seen that additional reinforcement leads to a higher factor of safety. For slope-parallel reinforced and fiber-reinforced veneers increasing slope inclination leads to a decreasing factor of safety. This can be explained because for steeper slopes a relatively bigger part of the soil weight acts along the failure plane, thus increasing the driving forces. Consequently for steeper slopes the same amount of provided reinforcement contributes relatively less to stabilize the slope. It is worth noting that for horizontally placed reinforcement the factor of safety increases with higher soil friction because parts of the reinforcement stress act perpendicular to the failure plan, thus providing more shear strength.

Analytical expressions provide the reinforcement requirements (Table 4.8) for veneer slopes as a function of soil shear strength and the veneer configuration (thickness and slope inclination).

Reinforcement Requirements	
Slope-parallel reinforced veneer:	$t_{p\,req} = \left(FS_r - \frac{c}{\gamma\, T\, \sin\beta} - \frac{\tan\phi}{\tan\beta} \right) \frac{\gamma\, T \sin\beta}{FS_r}$
Horizontally reinforced veneer:	$t_{h\,req} = \frac{FS_r - \frac{c}{\gamma\, T\, \sin\beta} - \frac{\tan\phi}{\tan\beta}}{FS_r + \tan\beta\, \tan\phi} \frac{\gamma\, T}{\cos\beta}$
Fiber-reinforced veneer:	$t_{f\,req} = \left(FS_r - \frac{c}{\gamma\, T\, \sin\beta} - \frac{\tan\phi}{\tan\beta} \right) \frac{\gamma\, T \sin\beta}{\alpha\, FS_r}$

Tab. 4.8: Reinforcement requirements for slope-parallel, horizontally and fiber-reinforced veneer slopes
FS_r = given target factor of safety
$t_{p\,req}$ = required distributed tensile stress per unit length of a slope-parallel reinforced veneer
$t_{h\,req}$ = required distributed tensile stress per unit ***height*** of a horizontally reinforced veneer
t_f = distributed tensile stress per unit length of a fiber-reinforced veneer ($\sigma_n < \sigma_{n,crit}$)

Provided tensile stress	
Slope-parallel reinforced veneer:	$t_p = \frac{T_a}{L_t}$
Horizontally reinforced veneer:	$t_h = \frac{T_a}{s}$
Fiber-reinforced veneer:	$t_f = \eta\, \chi \left(c_{i,c}\, c + c_{i,\phi}\, \tan\phi\, \gamma\, T \cos\beta \right)$

Tab. 4.9: Provided tensile stress
t_p = distributed tensile stress per unit length of a slope-parallel reinforced veneer
t_h = distributed tensile stress per unit ***height*** of a horizontally reinforced veneer

Table 4.9 shows how to determine the provided tensile stress per unit length/height for slope-parallel, horizontally and fiber-reinforced veneers. For both, slope-parallel, horizontally reinforced veneers the provided tensile stress increases with a higher allowable reinforcement tensile strength (T_a). It should be pointed out that one of the main advantages of horizontally placed reinforcement over slope-parallel reinforcement is that the provided tensile stress is independent of the slope length (L_T). In the case of horizontally placed reinforcement the provided tensile stress decreases as vertical spacing between the reinforcement layers increases, whereas for slope-parallel reinforcement the provided tensile stress decreases if the veneer becomes longer. As to fiber-reinforced veneers, the provided tensile stress increases with longer and thinner fibers (fiber aspect ratio η), with higher soil-fiber

interface shear strength(interaction coefficients $c_{i,c}$, $c_{i,\phi}$) as well as higher soil shear strength (c, ϕ), with a higher fiber contents(χ) and with higher normal stress at the base of the veneer ($\gamma T\cos\beta$).

Furthermore, case histories draw the attention on successful applications and highlight problems that had to be solved during the design and construction process. Advantages and disadvantages of the different design concepts for the reinforcement of steep veneers are shown in Table 4.10. Finally other design concepts for additional slope stability are presented by means of case histories. Geosynthetics were successfully used in reinforced soil structures at the bottom of the slope, in a module-based cover system and a light-weight cover system.

Reinforced Landfill Covers		
	Advantages	Disadvantages
Unreinforced veneer:	• Easiest way to construct a cover • No additional reinforcement required • Cheap • No stress-strain compatibility problems between soil and reinforcement	• Only suitable for flat slopes
Slope-parallel reinforced veneer:	• Well established technique • A lot of experience • Easy construction • Fast panel placement	• Anchorage at the top of the slope required • High stresses in the reinforcement • Good connections between the panels are needed to transfer the stresses to the anchorage
Horizontally reinforced veneer:	• Stresses in the reinforcement panels are independent of the slope length • Local failure of one panel might not lead to failure of the whole slope	• Anchorage into the underlying mass required • Layer by layer construction (slow) • New technique – lack of field experience • Only suitable for evapotranspirative covers
Fiber-reinforced veneer:	• No anchorage required • Strength isotropy • Provide strength at low confinement • Additional benefits such as: reducing the potential for crack development, provide erosion control and facilitate vegetation development	• Still in the experimental phase • No field applications • Possible problems during construction (e.g. mixing of the fibers into the soil)

Tab. 4.10: Reinforced Landfill Covers: Advantages and disadvantages of different design concepts

References

Alexiew, D.(1994). „Bemessung geotextiler Beweherungselemente für Dichtungsysteme auf geneigten Flächen." *10. Fachtagung "Die sichere Deponie"*, Würzburg , pp. 197-212

Alexiew, D., Sobolewski, J. (1997). „Effiziente Oberflächenabdichtungen – zwei Praxisbeispiele für steile Deponieoberflächen." *Proc. 1. Österreichische Geotechniktagung,*, Vienna , pp. 317-336

ASTM D 4439 (2001). „Standard Terminology for Geosynthetics." West Conshohocken, Pennsylvania, USA

Baltz, J. F., Zamojski, L., Reinknecht, D. (1995). „Design and Construction of a Geogrid-Reinforced Veneer Landfill Cap." *Proc. Geosynthetics '95 Conference*, Nashville, USA, pp. 759-770

Barker, P., Esnault, A., Braithwaite, P. (1997). "Containment Barrier at Pride Park, Derby, England." *Proc. International Containment Technology Conference*, St. Petersburg, Florida, pp. 95-103

Bathurst, R.J., Karpurapu, R. (1993). „Large-Scale Triaxial Compression Testing of Geocell-Reinforced Granular Soil." *Geotechnical Testing Journal (Journ.),*Vol. 16, No. 3, ASTM, Philadelphia, Pennsylvania, USA, pp. 296-303

Bouazza, A., Kavazanjian, E. (2001). Construction on Former Landfills. *Proceedings 2nd ANZ Conference on Environmental Geotechnics,* Newcastle, pp. 467-482

Bouazza, A., Parker, R. (1997). Applications of Containment Technologies for Contamination Remediation/control: Status and Experiences. *Proc. International Containment Technology Conference*, St. Petersburg, Florida, pp. 33-42

Bouazza, A., Zornberg, J.G., Adam, D. (2002). "Geosynthetics in Waste Containment Facilities: Recent Advances," *Proc. 7th IGS Conference*, Nice, France, pp.445-506

Brandl, H. (1990). "Doppelte Umschließung von Deponien mittels des Dichtwand-Kammersystems." *5. Nürnberger Deponieseminar - Geotechnische Probleme beim Bau von Abfalldeponien*, Heft 54 der Veröffentlichungen des Grundbauinstitutes der Landesgewerbeanstalt Bayern, pp. 165-189

Brandl, H. (1994). "Vertical Barriers for Municipal and Hazardous Waste Containment." *Developments in Geotechnical Engineering*, Balasubramaniam et al. (eds), Bangkok, A.A.Balkema, pp. 301-334

Brandl, H. (1998). "Dichtwände im Grund-, Wasser- und Deponiebau." *Österreichischer Betonverein – Schriftenreihe Heft 29*, Vienna, pp. 33-48

Brandl, H. (2002). "Geotechnik bei Altlasten und neuen Deponien." *Vorlesungsunterlagen Institut für Grundbau und Bodenmechanik*, TU-Wien

Brandl, H., Adam, D. (2000). "Special Applications of Geosynthetics in Geotechnical Engineering." *Proc. 2nd European Geosynthetics Conference*, Bologna, pp. 27-64

Brauns, J. (1978): „Wirksamkeit unvollkommener Abdichtungswände unter Staubauwerken.", *Institut für Bodenmechanik und Felsbau*, Heft 80, Universität Fridericana Karlsruhe

Cargill, K.W., Olen, K.L. (1998). „Landfill Closure Using Reinforced Soil Slopes." *Proc. 6th IGS Conference*, Atlanta, Georgia, USA, pp. 481-486

Cortilever, N.C. (1999): „Landfill ‘Schoteroog’ by Means of a Cement-Bentonite –Liner Composite Wall”, paper available from http://www.geotechnics.nl/papers/papers.html (23.04.2002)

Dachler, R. (1936). *Grundwasserströmungen*, Julius Springer Verlag, Vienna

Daly, K.R., McKelvey III, J.A. (1999). „Overcoming the Obstacles: Installation of a Geosynthetic Cover System Over Hazardous Waste Pits ." *Proc. Geosynthetics '99 Conference*, Boston, Massachusetts, USA, pp. 1097-1109

Daniel, D.E., Koerner, R.M.(2000). „On the Use of Geomembranes in Vertical Barriers.” *Proc. GeoDenver 2000, Advances in Transportation and Geoenvironmental Systems Using Geosynthetics*, J.G. Zornberg and B.R. Christopher (eds), GSP No. 103, ASCE, Reston, VA, pp. 81-93

Dash, S.K., Krishnaswamy, N.R., Rajagopal, K. (2001). „Bearing Capacity of Strip Footings Supported on Geocell-Reinforced Sand.” *Geotextiles and Geomembranes (Journ.)*, Vol. 19, No. 4, Elsevier Publ. Co., pp. 235-256

Druschel, S. J., Underwood, E. R. (1993). „Design of lining and Cover System Sideslopes." *Proc. Geosynthetics '93 Conference*, Vancouver, Canada, pp. 1341-1355

Fosse, G.J., Vonderembse, G., (2001). “Contaminant Transport through Composite Geomembrane-Soil-Bentonite Cut-Off Walls.” *Proceedings 2nd International Conference Containment Technology*, Orlando, CD-Rom

Fox, G. (1993). „Geogrid Provides Design Solutions at Midway Landfill.” *Proc. Geosynthetics '93 Conference*, Vancouver, Canada, IFAI Publ., pp. 1229-1242.

Giroud, J.P., Bachus, R.C., Bonarpate R: (1995a). „Influence of Water Flow on the Stability of Geosynthetic-Soil Layered Systems on Slopes.” *Geosynthetics International (Journ.)*, Vol. 2, No. 6, pp. 1149-1180

Giroud, J.P., Beech, J.F. (1989). „Stability of Soil Layers on Geosynthetic Lining Systems.” *Proc. Geosynthetics '89 Conference*, San Diego, USA, pp. 35-46

Giroud, J.P., Williams, N.D., Pelte, T:, Beech, J.F. (1995b). „Stability of Geosynthetic-Soil Layered Systems on Slopes.” *Geosynthetics International (Journ.)*, Vol. 2, No. 6, pp. 1115-1148

Gundle Lining Systems, Inc. (1993). “Laboratory Test Results of Gundwall Locking Section with Hydrotite Leakage Potential Testing.” GoeSyntec Consultants, Project No. GL3398, Houston, Texas (in Koerner and Guglielmetti, 1995),

Hermanns Stengele, R. (1999). “Umweltgeotechnische und wirtschaftliche Aspekte beim Einsatz von reaktiven Wänden bei der Sicherung von Altlasten.” *2. Österreichische Geotechniktagung*, ÖIAV (eds), Vienna, pp. 249-264

International Geosynthetics Society (IGS), (2000). „Recommended Descriptions of Geosynthetics Functions, Geosynthetics Terminology, Mathematical and Graphical Symbols.” Easley, South Carolina, USA

Inyang, H.I (1995). “Performance Monitoring and Evaluation.” *Assessment of Barrier Technologies: A Comprehensive Treatment for Environmental Remedial Application*, R.R. Rumer and J.K. Mitchell (eds), NTIS Publ. No. PB96-180583, pp. 355-400

Itasca Consulting Group, Inc. (1998). „FLAC – Fast Lagrangian Analysis of Continua – Theory and Background.” Minneapolis, Minnesota, USA

Technical Committee 5 (TC 5) – Task Force 1, "Chapter 1: Terminology, Definitions and Units." *Design Basics and Performance Criteria*, unpublished report

Jefferis, S.A., Norris, G.H., Thomas, A.O. (1997). "Contaminant Barriers from Passive Containment to Reactive Treatment Zones." *Proc. 14th ICSMFE*, Hamburg, A.A.Balkema, pp. 1955-1960

Kirschner, R. (1995). „Bemessung von Geogittern für die Bewehrung von Deponiebdichtungssystemen auf Böschungen." Bauingeniuer (Journ.), Nr. 70, Springer-Verlag, pp. 183-187

Kodikara, J. (1996). „Prediction of Tension in Geomembranes placed on Landfill Slopes." *Environmental Geotechnics*, M. Kamon (eds),Vol. 1, A.A.Balkema, pp. 557-562

Kodikara, J. (2000). „Analysis of Tension Development in Geomembranes placed on Landfill Slopes." *Geotextiles and Geomembranes (Journ.)*, Vol. 18, pp. 47-61

Koerner, R.M. (1998). *Designing with Geosynthetics*, 4th Edition, Prentice Hall Inc., Upper Saddle River, NJ, 761 pgs

Koerner, R.M., Guglielmetti, J. (1995). "Vertical Barriers: Geomembranes.", *Assessment of Barrier Technologies: A Comprehensive Treatment for Environmental Remedial Application*, R.R. Rumer and J.K. Mitchell (eds), NTIS Publ. No. PB96-180583, pp. 95-118

Koerner, R. M., Hwu, B.-L. (1991). „Stability and Tension Considerations Regarding Cover Soils on Geomembrane Lined Slopes." *Geotextiles and Geomembranes (Journ.)*, Vol. 10, No. 4, Elsevier Publ. Co., pp. 335-356

Koerner, R.M., Soong, T.-Y. (1998). „Analysis and Design of Veneer Cover Soils." *Proc. 6th IGS Conference*, Atlanta, Georgia, USA, pp. 1-23

Krishna Prasad, K. V. S., Madhav, M. R., Kodikara, J., Bouazza, M. (2001). „Tension in Geosynthetic Liner based on Hyperbolic Interface Response.", *Landmarks in Earth Reinforcement*, Ochiai, H. et al. (eds), Kyushu, A.A.Balkema, pp. 231-234

Manassero, M., Benson, C.H., Bouazza, A. (2000), "Solid Waste Containment Systems.", *Proc. GeoEng2000* , Melbourne, Australia, pp. 520-642

Manassero, M., Van Impe, W.F., Bouazza, A. (1997). „Waste Disposal and Containment." *Environmental Geotechnics*, M. Kamon (eds),Vol. 3, A.A.Balkemapp. pp. 1425 – 1474

Manassero, M., Viola, C. (1992). "Innovative Aspects of Lecheate Containment with Composite Slurry Walls: A Case History.", *Slurry Walls: Design, Construction and Quality Control, ASTM STP 1129*, David B. Paul, Richard R. Davidson and Nicholas J. Cavalli (eds), American Society for Testing and Materials, Philadelphia, pp. 181-193

Martin, J. S., Simac, M. R. (1995). „The Design and Construction of 168 Meter-Long Geogrid Reinforced Slopes at the Auburn, NY, Landfill Close." *Proc. Geosynthetics '95 Conference*, Nashville, USA, pp. 771-784

Mitchell, J.K., Rumer, R.R. (1997). "Waste Containment Barriers: Evaluation of the Technology.", *Proc. In Situ Remediation of the Geoenvironment*, J.C.Evans (eds), GSP No. 71, ASCE, Reston, VA, pp. 1-25

Mitchell, J. K., Seed, R. B., Seed, H. B., (1990). „Kettleman Hills Waste Landfill Slope Failure. I.; Liner System Properties." *Journal of Geotechnical Engineering*, ASCE, No. 4, April 1990, pp. 647-668

Previtt, K.D., Matthews, S.C., Hodges, R.A. (1996). *Barriers, Liners and Cover Systems for Containment and Control of Land Contamination*, Construction Industry Research and Information Association, Special Publication Nr. 124, London, 278 pgs

Punyamurthula, S., Hawk, D. (1998). „Issues with Slope Stability of Landfill Cover Systems." *Proc. GRI-12 Conference*, GII Publ., Folsom, PA, pp. 259-268

Rumer, R.R, Mitchell, J.K. (1995) (eds). "Assessment of Barrier Technologies: A Comprehensive Treatment for Environmental Remedial Applications.", *International Containment Technology Workshop*, Baltimore, Maryland, NTIS Publ. No. PB96-180583, 437 pgs

Rumer, R.R, Ryan, M.E. (1995) (eds). *Barrier Containment Technologies for Environmental Remediation and Applications*, John Wiley & Sons, NY, 170 pgs

Soudain, M. (1997). "Iron Construction", *Ground Engineering*, July

Tachavises, C., Benson, C.H. (1997a). "Flow Rates through Earthen, Geomembrane and Composite Cut-Off Walls.", *Proc. International Containment Technology* , St. Petersburg, Florida, pp. 945-953

Tachavises, C., Benson, C.H. (1997b). "Hydraulic Importance of Defects in Vertical Groundwater Cut-Off Walls.", *Proc. In Situ Remediation of the Geoenvironment*, J.C.Evans (eds), GSP No. 71, ASCE, Reston, VA, pp. 168-180

Tammemagi, H. (1999). "The Waste Crisis." Oxford University Press.

Thiel, R.S., Stewart, M.G. (1993). „Geosynthetic Landfill Cover Design Methodology and Construction Experience in the Pacific Northwest." *Proc. Geosynthetics '93 Conference*, Vancouver, Canada, pp. 1131-1144

Thomas, R.W., Koerner, R.M. (1996). „Advances in HDPE Barrier Walls." *Geotextiles and Geomembranes (Journ.)*, Vol. 14, Nos. 7/8, pp. 393-408

Zornberg, J.G. (2000). „Development of a Discrete Design Methodology for Fiber-Reinforced Soil." *Geotechnical Research Report*, Department of Civil, Environmental and Architectural Engineering, University of Colorado at Boulder, July 2000

Zornberg, J.G., Christopher, B.R. (1999). „Geosynthetics. Chapter 27." *The Handbook of Groundwater Engineering*, Jacques W. Delleur (Editor-in-Chief), CRC Press, Inc., Boca Raton, Florida.

Zornberg, J.G., Kavazanjian Jr., E. (1998). „Evaluation of a Geogrid-Reinforced Slope Subjected to Differential Settlements." *Proc. 6th IGS Conference*, Atlanta, Georgia, USA, pp. 469-474

Zornberg, J.G., Somasundaram, S, LaFountain,.L.(2001). „Design of Geosynthetic-Reinforced Veneer Slopes." *Landmarks in Earth Reinforcement*, Ochiai, H. et al. (eds), Kyushu,, A.A.Balkema, pp. 305-310

List of Figures

List of Tables